THE QUESTION OF RELATIONSHIP BETWEEN LOW AND HIGH GRADE METAMORPHIC ROCKS IN THE FRENCH MOUNTAIN, AREA, OF THE CAPE BRETON HIGHLANDS, NOVA SCOTIA

by

DEBORAH M. CONROD

Submitted in partial fulfillment of the
requirements for a Bachelor of Science (Honours) Degree

at

Dalhousie University
Halifax, Nova Scotia
March 1984

DALHOUSIE UNIVERSITY
Department of Geology
Halifax, N.S. Canada B3H 3J5 Telephone (902) 424-2358 Telex: 019-21863

DALHOUSIE UNIVERSITY, DEPARTMENT OF GEOLOGY

B.Sc. HONOURS THESIS

Author: Deborah M. Conrod

Title: The Question of Relationship Between Low and High Grade Metamorphic Rocks in the French Mountain Area of the Cape Breton Highlands, Nova Scotia.

Signature of author

Date: April 2, 1984

Distribution License

DalSpace requires agreement to this non-exclusive distribution license before your item can appear on DalSpace.

NON-EXCLUSIVE DISTRIBUTION LICENSE

You (the author(s) or copyright owner) grant to Dalhousie University the non-exclusive right to reproduce and distribute your submission worldwide in any medium.

You agree that Dalhousie University may, without changing the content, reformat the submission for the purpose of preservation.

You also agree that Dalhousie University may keep more than one copy of this submission for purposes of security, back-up and preservation.

You agree that the submission is your original work, and that you have the right to grant the rights contained in this license. You also agree that your submission does not, to the best of your knowledge, infringe upon anyone's copyright.

If the submission contains material for which you do not hold copyright, you agree that you have obtained the unrestricted permission of the copyright owner to grant Dalhousie University the rights required by this license, and that such third-party owned material is clearly identified and acknowledged within the text or content of the submission.

If the submission is based upon work that has been sponsored or supported by an agency or organization other than Dalhousie University, you assert that you have fulfilled any right of review or other obligations required by such contract or agreement.

Dalhousie University will clearly identify your name(s) as the author(s) or owner(s) of the submission, and will not make any alteration to the content of the files that you have submitted.

If you have questions regarding this license please contact the repository manager at dalspace@dal.ca.

Grant the distribution license by signing and dating below.

_____ _____

Name of signatory Date

French Mountain, Cape Breton Highlands
Nova Scotia

TABLE OF CONTENTS

LIST OF FIGURES

LIST OF TABLES

ABSTRACT

French Mountain in the Cape Breton Highlands of Nova Scotia is underlain by two broad metamorphic complexes: a metasedimentary complex and a composite gneiss complex. The metasedimentary complex, located on the southwestern slopes of the mountain, consist of interlayered phyllite, semi-pelite and psammite. The gneiss, located on the top of the mountain, consists of mainly a biotite-quartz-feldspar gneiss interlayered with minor amphibolite gneiss and feldspar augen gneiss. Over a kilometer of land devoid of outcrop separates the two complexes. Other mappable lithologies within the area include various granitoid bodies, amphibolite, diorite and granitic dykes.

The metasedimentary complex shows a progressive metamorphic sequence indicated by the presence of the key metamorphic index minerals; chlorite, biotite, garnet and staurolite. Mineral-fabric relations indicate that the metamorphism began during the early stages of the deformation which produced the pervasive schistosity, and continued until the later stages or even after deformation had ceased. The gneiss locally contains kyanite which developed before the deformation that produced the schistosity within the gneiss.

The orientation of structural elements differs considerably between the two complexes. The gneiss has undergone at least three phases of deformation while the metasedimentary complex has undergone at least two phases. Both complexes contain a pervasive schistosity, minor folds,

crenulations and rare kink folds and the metasedimentary complex also contains a biotite mineral lineation and a poorly developed second crenulation. It is unknown whether the schistosity within the gneiss was developed during the same "event" that produced the schistosity within the metasedimentary rocks, and thus it is unknown whether the kyanite within the gneiss belongs to the progressive sequence found within the metasedimentary complex. Schistosity within the metasedimentary complex strikes northeast-southwest in the west, dipping moderately to the northwest, and swings northwest-southeast in the east dipping moderately to the northeast, defining a large fold which folds the metasedimentary complex. Schistosity within the gneiss strikes consistently north-south dipping steeply to the east. No unconformity was observed between the two complexes, however the distinctly different orientations of the structural elements suggest that a structural break of some sort exists. The steeper dip of the gneiss suggests that the gneiss may have been thrust from east to west over the metasedimentary complex.

It is unresolved whether the gneisses are basement rock to the metasedimentary complex or whether the two complexes represent one protolithic package with the gneiss a higher metamorphic grade equivalent of the metasedimentary rocks.

ACKNOWLEDGEMENTS

My sincere thanks go to Dr. R. A. Jamieson for suggesting this project and for her advise and discussions during its progress; to Mr. G. Brown for the preparation of thin and polished sections, to Mr. R. M. MacKay for his guidance at the electron microprobe; to Pierre Doucet for his assistance during the fieldwork; and to Mrs. Dianne Crouse for her typing of the thesis. I dedicate this work to my parents for their love and support.

CHAPTER 1

INTRODUCTION

1 INTRODUCTION

The Cape Breton Highlands, located in the eastern Canadian Appalachian Belt, is principally underlain by variously metamorphosed plutonic, sedimentary and volcanic rocks (Figure 1.1).

Much of the geology of the Highlands is, at present poorly understood. Even in recent compilations much of the Highlands is classified as undifferentiated gneiss (e.g. Keppie, 1979). The poor exposure, structural complexity, scarcity of radiometric dates and lack of fossil control have made regional correlation difficult. These factors are partially responsible for the poor understanding; however arbitrary assignment of the metasedimentary rocks to the George River Group and the metavolcanic rocks to the Fourchu Group has led to much confusion in the literature. The arbitrary assignment of the metasedimentary rocks to the George River Group and metavolcanic rocks to the Fourchu Group has made studies of the relations between the metavolcanic and metasedimentary rocks and relations between the low and high grade rocks difficult and confusing.

Much of the central Higlands is underlain by gneiss which is bounded on the north, south and west by low to medium grade metavolcanics and metasediments. These metavolcanics and metasediments have been variously equated with the Fourchu Group (Weibe, 1972 and Neale and Kennedy, 1975), the George River Group (Milligan, 1970; Chatterjee, 1980) or they have been considered separately (Macdonald

Figure 1.1. The General Geology of the Cape Breton Highlands (Jamieson, in press), showing that much of the Cape Breton Highlands is underlain by undifferentiated gneiss and metavolcanic and metasedimentary units, and showing the scarcity of radiometric dates presently known for the Highlands area. (All dates are given in millions of years.)

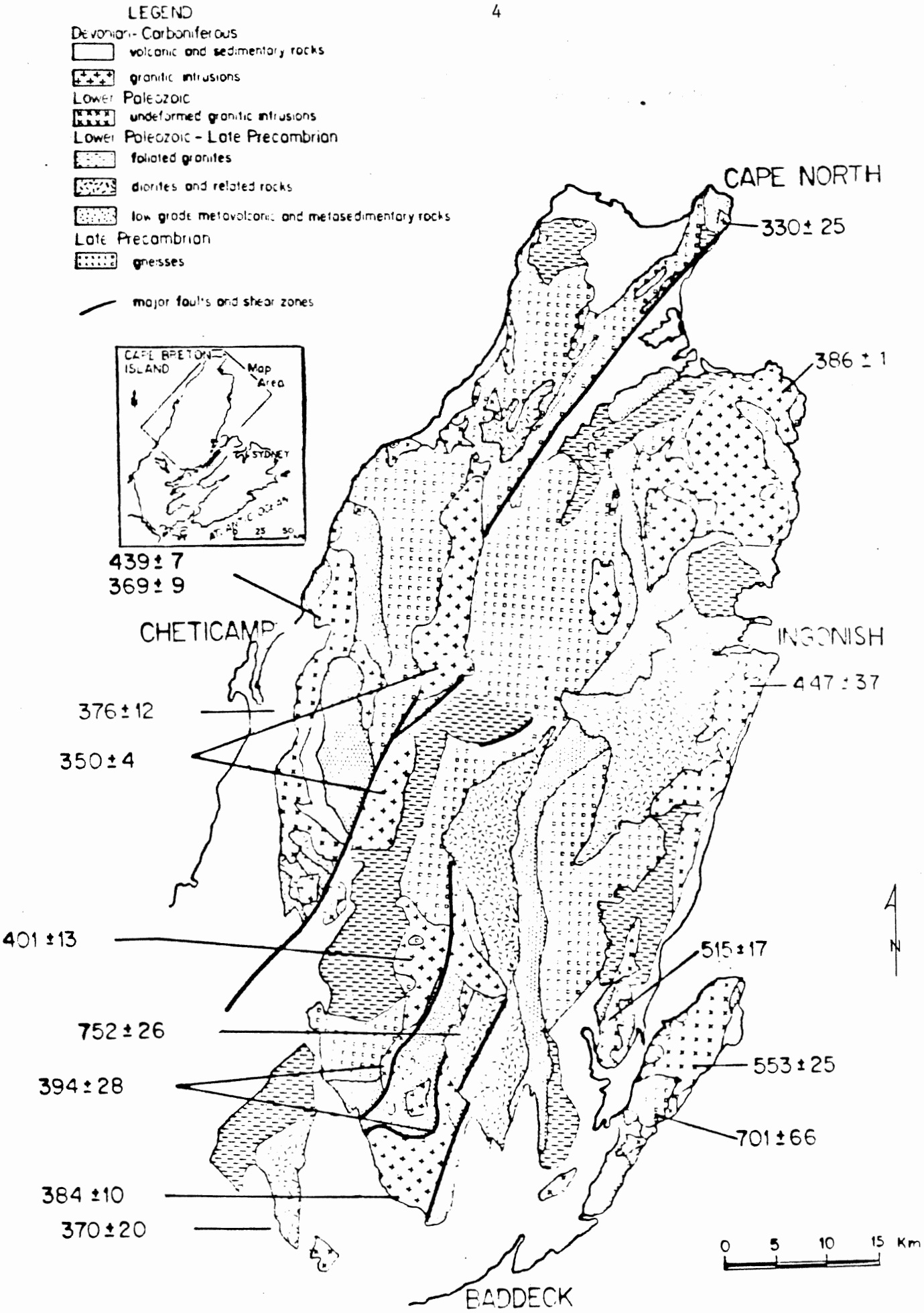
LEGEND
Devonian - Carboniferous
volcanic and sedimentary rocks
granitic intrusions
Lower Paleozoic
undeformed granitic intrusions
Lower Paleozoic - Late Precambrian
foliated granites
diorites and related rocks
low grade metavolcanic and metasedimentary rocks
Late Precambrian
gneisses
major faults and shear zones
CAPE BRETON ISLAND
Map Area
SYDNEY
CAPE NORTH
330 ± 25
386 ± 1
439 ± 7
369 ± 9
CHETICAMP
INGONISH
447 ± 37
376 ± 12
350 ± 4
401 ± 13
515 ± 17
752 ± 26
553 ± 25
394 ± 28
701 ± 66
384 ± 10
370 ± 20
N
0 5 10 15 Km
BADDECK

and Smith, 1980; Jamieson, 1981; Currie, 1982; Jamieson and Doucet, 1983).

Presently there are two conflicting proposals for the relationship between low and high grade metasedimentary assemblages. Weibe (1972), Neale and Kennedy (1975) and Currie (in press) support the proposal that the gneiss represents crystalline basement to the low and medium grade metasedimentary rocks. Recent detailed studies of well exposed sections have failed to find convincing evidence of an unconformity (Jamieson, in press). An alternate proposal for the relation between the low and high grade metamorphic assemblages is given by Craw (in press) who proposes that the low to high grade metasedimentary and metavolcanic rocks were originally a continuous sequence that was tectonically shortened by stacking along high strain zones.

Much of the gneiss of the western Highlands is affected by a pervasive lower amphibolite facies retrograde metamorphism. This metamorphism which is apparently Acadian in age (Doucet, 1983) may be related to the stacking event (Jamieson, in press).

The question of whether the paragneisses are high grade equivalents of the low grade metasedimentary rocks has been undertaken in different parts of the Highlands. Macdonald and Smith (1980) examined low to medium grade metasedimentary and metavolcanic rocks (Money Point Group) and medium to high grade paragneisses (Cape North Group) in the Cape North area of Cape Breton and concluded that the two Groups were

essentially conformable with no evidence of any erosional or tectonic break between them. Macdonald and Smith (1980) documented a rapid increase in metamorphic grade from east to west through the Groups. Neale and Kennedy (1975) had examined the Money Point Group and Cape North Group previous to Macdonald and Smith (1980) and proposed that an unconformable contact separated the two Groups.

Craw (in press) examined the low to high grade metamorphic rocks in the Cheticamp River area, and delineated three metamorphic belts running in a north-south direction, with an increase in metamorphic grade from west to east. He concluded that the sequence represents a stacked assemblage due to east to west thrusting resulting in the low grade rocks at the bottom of the sequence and the high grade rocks at the top. He concluded that the three belts represent one or more "slices" of a single protolithic package.

Currie (1975, and in press) examined metasedimentary and metavolcanic rocks in the Cheticamp region (Figure 1.2) (which includes the French Mountain area). He assigned regional names to his metamorphic assemblages. The high grade assemblage (Pleasant Bay Complex) consisting of biotite, amphibolite, and granodiorite gneisses with minor marble and anorthite, is cut by an unfoliated but highly fractured granodiorite (Corney Brook Complex). This granodiorite has yielded a Cambrian age (Barr, pers. comm.). Currie (in press) proposes that the Pleasant Bay Complex is unconformably overlain by a metasedimentary and metavolcanic sequence (Jumping Brook Complex). A uranium-lead age

date obtained from zircons within a rhyolite dyke interpreted to feed the Jumping Brook Metavolcanics yielded an age of 439 ± 7 million years. A potassium-argon age obtained for this dyke yielded an age of 363 ± 9 million years (Currie, in press). Although this age represents an age of intrusion, the linking of the dyke to the basal volcanic rocks is tenuous (Jamieson, in press), thus a convincing age for the metasedimentary rocks remains to be obtained.

This study examines the relation between the lower grade metasedimentary rocks and the higher grade gneisses in the French Mountain area including a detailed petrological study of the rocks in the area, in an effort to determine whether an unconformable or gradational boundary exists between the two Complexes.

Previous work done in the area was undertaken by Currie (in press) who classified the lower grade metasedimentary rocks into the Jumping Brook Complex and the higher grade gneisses into the Pleasant Bay Complex (refer to Figure 1.2 for lithologic subdivisions of each unit).

Currie (in press) claims that the contact between the Jumping Brook Complex and the Pleasant Bay Complex is exposed along the north wall of the Jumping Brook canyon and that the Jumping Brook Complex is inverted and dips gently under the granitoid gneiss.

The objectives of this study were to map the specific area in question (French Mountain), to determine lithological units, and through a combination of detailed petrological study, field relations,

Figure 1.2. Map of the French Mountain Area produced by Currie (in press).

LEGEND

CARBONIFEROUS(?) AND OLDER

19 Cataclastic rocks; breccia, mylonite and blastomylonite, flaser gneiss

PENNSYLVANIAN

RIVERSDALE GROUP

18 Grey to grey-green muscovitic sandstone with rare coaly beds

PENNSYLVANIAN AND MISSISSIPPIAN

CANSO GROUP

17 Grey to buff flaggy sandstone with red shale interbeds

MISSISSIPPIAN

WINDSOR GROUP

16 Buff to grey limestone and dolostone, gypsum; rocks commonly contorted

MISSISSIPPIAN AND DEVONIAN

HORTON GROUP (14-15)

15 White to pink arkose, conglomerate, granite wash (15a); Flaggy grey sandstone with coaly beds (15b)

14 FISSET BROOK FORMATION. Black vesicular basaltic flows, tuff and pyroclastics (14a); Flow banded rhyolite, ignimbrite, quartz porphyry (14b)

DEVONIAN AND/OR SILURIAN

13 CHETICAMP GRANITE: Massive, medium-grained red biotite granite

12 MARGAREE GRANITE: Coarse pink biotite granite with potash feldspar megacrysts. 12a - rhyolite and quartz-feldspar porphyry

11 Leucocratic white to pink muscovite granite and pegmatite, commonly lineated and garnetiferous (may be older than 12).

10 Fine-grained, gneissic muscovite-biotite granite, locally grading to lit par lit gneiss or migmatite

CAMBRO-ORDOVICIAN (?)

TROUT BROOK COMPLEX (6-9)

9 Gabbroic and amphibolitic dykes and stocks

8 Mainly homogeneous grey-green gritty greywacke and correlative schists. Locally includes up to 20 percent of units 6 and 7.

7 Mainly pelitic gneiss and schist, commonly interbedded with 6 and 8

6 Basaltic flows and volcanic clastic rocks and correlative greenschists. Minor schistose rhyolite. Commonly interbedded with 7 and 8.

HADRYNIAN

CORNEY BROOK PLUTON

5 Pink hornblende-biotite granodiorite. Locally massive, but commonly shattered and strongly chloritized. Rarely megacrystic or schistose.

HELIKIAN (?)

PLEASANT BAY COMPLEX (1-4)

4 Generally granitoid gneiss, commonly composite. Mainly white to buff biotite granodiorite augen gneiss with lits and schliers of units 1-3, and lits, veins and patches of units 11-12.

3 Gneissic to schistose biotite amphibolite gneiss with lits of 2, 4, 12.

2 Biotite gneiss and schist, locally pelitic, grading to 3, 4 and 12.

1 White brecciated anorthosite variably altered and chloritized

Outcrop, area of outcrop

Strike and dip of bedding, tops unknown, tops known, overturned

Strike and dip of gneissosity or schistosity, inclined, vertical

Strike and dip of shearing, inclined, dip unknown

Lineation with plunge

Small fold showing sense of movement, plunge inclined, plunge unknown

Synclinal axis, upright, overturned; anticlinal axis, upright

Fault, shear zone; sense of movement uncertain

Reverse or thrust fault, teeth in hanging block

Geological boundary, approximate, assumed

Metamorphic mineral characteristics of metapelites: a-diaspore, a-and, b-biotite, b-andalusite, c-cordierite, c-andalusite, d-garnet, e-staurolite, f-kyanite

Geology by E.R.W. Neale 1964-66, A.S. Wallace 1964, N.L. Currie 1967-70
Geological compilation by N.L. Currie 1979

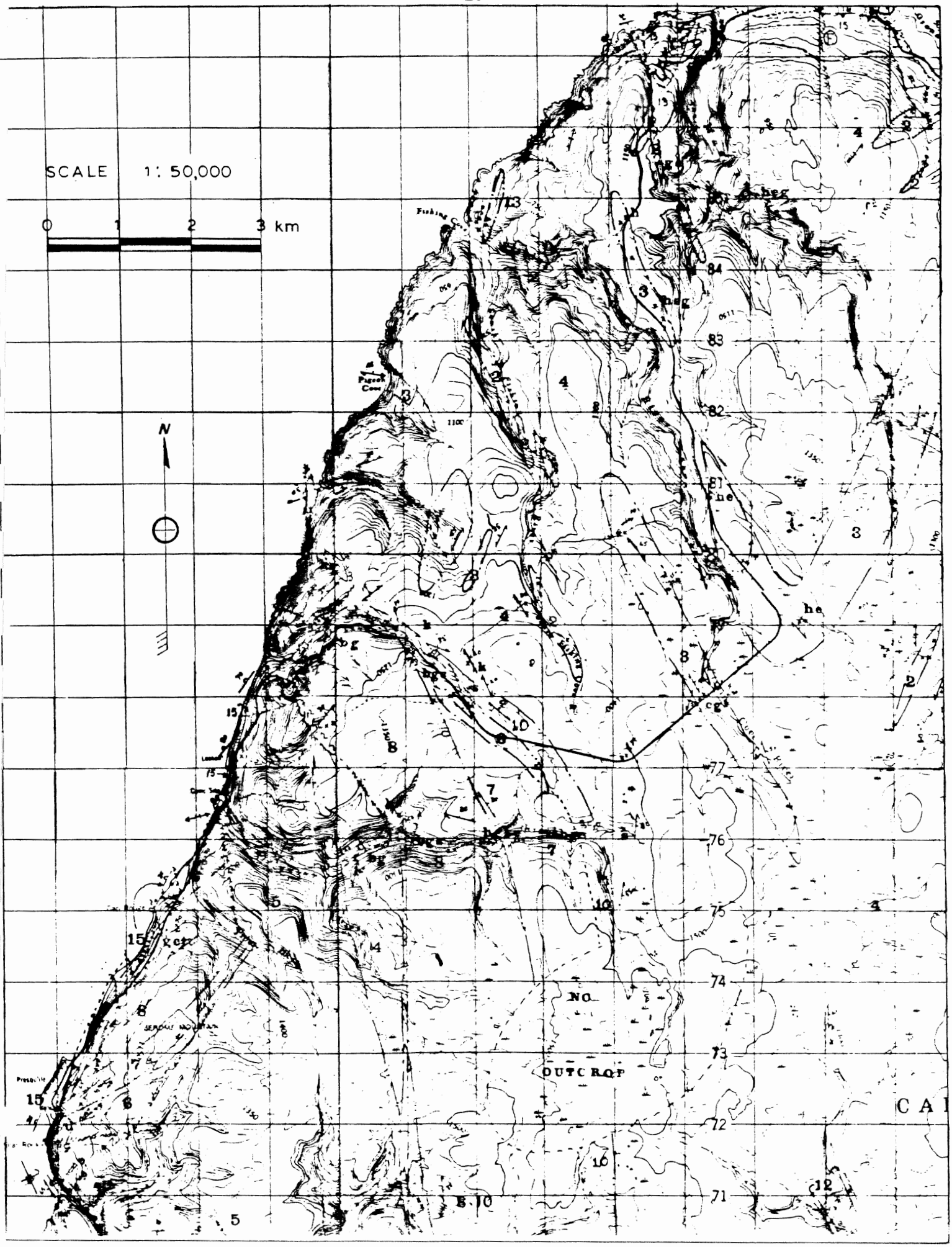
SCALE 1: 50,000
0 1 2 3 km
N
OUTCROP
NO

structural considerations and a limited geochemical study, try to determine the relationship between the two units.

Sixteen days were spent mapping, during the summer of 1982, however all other studies were carried out during the winter of 1983/84. During the field mapping lithologies were defined and structural features documented. Mapping was carried out via note taking and through the use of 1:10,000 orthoplots. Because the top of French Mountain is flat and essentially devoid of outcrop and because of the limited time in which to do the mapping, the mapping was restricted to the Cabot Trail, the Jumping Brook and its canyon walls, the informally named Fire-Tower Road and the Skyline Trail. Approximately 190 samples, encompassing all rock types identified, were collected from the area. Fifty-two thin sections from selected samples were studied petrographically and seven polished sections were selected for microprobe analysis of the various mineral phases. Detailed study of mineral phases, textures and relations between phases and fabrics was undertaken. A geological map and sample location map were constructed for the area at a scale of 1:10,000 and can be found in the back pocket of this paper.

CHAPTER 2

LITHOLOGIES, FIELD RELATIONS AND STRUCTURE

2.1 INTRODUCTION

The rocks of the French Mountain area have been classified into two broad complexes: a metasedimentary complex and a gneiss complex. The question of relationship between these two complexes depends on the correct correlation of units within each complex. Correlation between lithological units and the field relation between the two complexes is hindered by the poor outcrop on the top of French Mountain. A biotite-quartz-feldspar gneiss is the dominant lithology found at the top of French Mountain. A metasedimentary complex showing progressive metamorphism toward the gneiss, is the dominant lithology on the southwestern slopes of the mountain. Because of the lack of outcrop in the area, mapping was limited to the Cabot Trail and Jumping Brook, where outcrop is very good; to the Fire Tower Road where outcrop is moderate but sporadic; and to the Skyline Trail where outcrop is limited to the western most parts of the trail, near the coast of the Gulf of St. Lawrence. Mapping commenced 20.1 kilometers north of the village of Cheticamp along the Cabot Trail and continued to 7.2 kilometers before the village of Pleasant Bay. The metasedimentary complex, referred to as the Jumping Brook Complex by Currie (1982, in press), has been subdivided, in this study, into two subunits, each consisting of alternating horizons of phyllite, psammite and semi-pelite. The gneiss complex referred to as the Pleasant Bay Complex by Currie (in press), is considered in this study to be a composite gneiss consisting primarily of a biotite-quartz-feldspar gneiss, with minor proportions of an amphibolite and potassic feldspar augen gneiss. No exposure of

Figure 2.1 (a and b). Outcrop in the French Mountain Area of Cape Breton. a) looking west-southwest towards Cheticamp and b) looking east towards French Mountain.

the contact between these two complexes was observed in the field, and over a kilometer separates the last outcrop of the metasedimentary complex and the first outcrop of the gneiss complex.

Other mappable units in the French Mountain area include amphibolite, diorite, and a granitoid unit which may correspond to the Corney Brook Pluton (Currie, in press) but is referred to as Granitoid Unit "A" in this study; the informally named Jumping Brook granitoid unit; and various granitic dykes that cross-cut or run parallel to the main fabric of the rocks.

2.2 METASEDIMENTARY COMPLEX

2.2.1 Metasedimentary Unit 1

The rocks of Unit 1 outcrop in the southwestern part of the mapped area, along the Cabot Trail and in the upper and middle parts of the Jumping Brook. They are best exposed along the southern side of the Cabot Trail as indicated in Figure 2.2. Unit 1 has been reported to overlie the Corney Brook Pluton (Currie, in press) which has been dated at 530 ± 44 million years (Cormier, 1972). In this study, the contact between Unit 1 and Granitoid Unit A, assumed to be part of the Corney Brook Pluton through correlation with the map produced by Currie (in press), is a fault and therefore the relative ages between these two units could not be deduced. The fault truncates the northwesterly dipping fabric of Unit 1, and if Unit A is in fact part of the Corney Brook Pluton, which does not have a foliation, then it is assumed that

Figure 2.2. Outcrop of Unit 1 of the Metasedimentary Complex along the Cabot Trail where foliated interlayered phyllite, psammite and semi-pelite dip to the northwest.

the pluton post dates the Metasedimentary Complex.

Unit 1 consists of alternating horizons of phyllite, psammite, and semi-pelite. Because of the intimate interlayering, and inter-gradation between these subunits they have been mapped as one unit. The thickness of each subunit varies from less than a meter to meters thick, and few primary structures such as graded bedding were preserved.

The phyllite is fine grained and has a silvery-grey colour. The growth of porphyroblastic garnet is preferentially concentrated in the phyllite. The phyllite also contains a biotite mineral lineation which generally trends north-northeast to south-southwest with a very shallow to almost horizontal plunge to the north-northeast. Because of the shallow plunge its direction is sometimes difficult to determine.

The psammite of unit 1 is medium grained, black, and rather massive. Often it contains porphyroclasts of quartz and feldspar (Figure 2.4), approximately 1 to 8 millimeters in size. These porphyroclasts are ellipsoidal with their long axis parallel to the main fabric of the rock. Locally the psammite can become very coarse grained and light beige (Figure 2.5). Grain size gradations were noted in one location near the top of the north wall of the Jumping Brook canyon (outcrop in the upper right-hand corner of Figure 1.1b), however "way-up" indications were inconsistent. This inconsistency is believed to be due to local minor isoclinal folding (Figure 2.5).

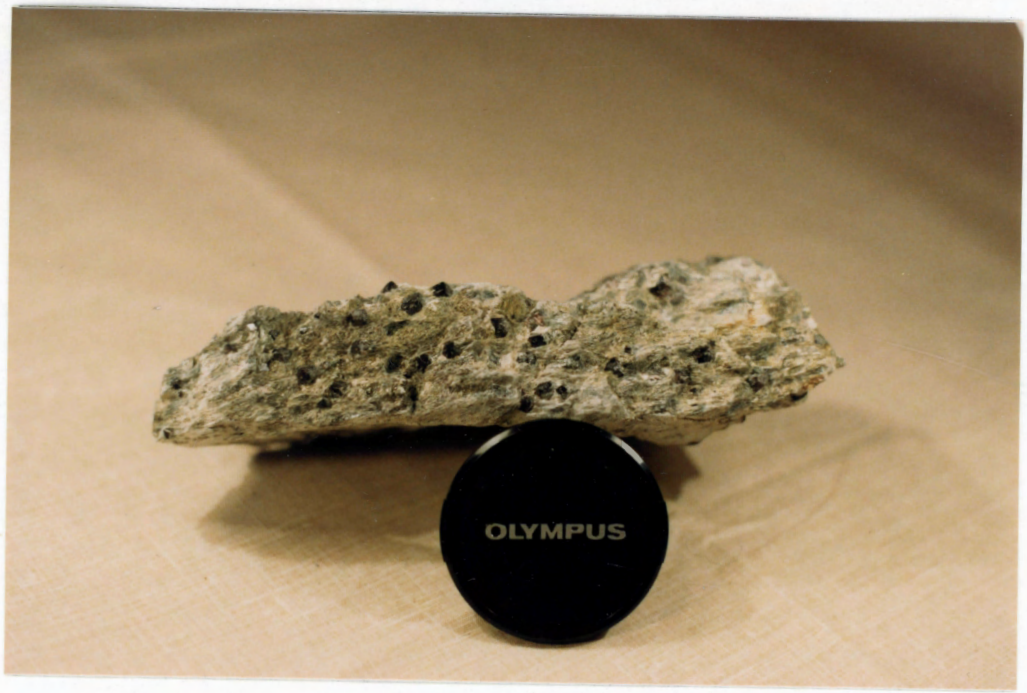

Figure 2.3. Porphyroblastic garnets in the phyllite of Metasedimentary Unit 1.

Figure 2.4. Porphyroclasts of quartz and feldspar in the psammite of Meta sedimentary Unit 2.

Figure 2.5. Grain size gradations in Metasedimentary Unit 1. Pen points in direction of decreasing size.

Figure 2.6. Fault along the Cabot Trail, displacing the foliation of Metasedimentary Unit 1.

The semi-pelitic rocks of unit 1 are rocks intermediate between the psammite and the phyllite. They are often a dull grey in color and do not have the silvery sheen characteristic of the phyllite. They often contain garnets but not in as great quantities as the phyllite.

A pervasive foliation defined by the alignment of biotite, muscovite and chlorite is well developed throughout the unit. Because this fabric is defined as a schistosity, it is best developed in the phyllite and rather poorly developed in the psammite. In the western most part of the unit the foliation strikes northeast-southwest and dips moderately to the northwest. The foliation however, swings east-west and dips moderately to the north in the eastern most part of this unit. This unit is interpreted in this study, to occupy the western most extent of a large northward plunging antiform (Map 1), which according to Currie (in press) refolds an earlier isoclinal fold whose nose can be observed along the Cabot Trail, north of Grande Falaise, south of the mapped area. Thus, the Jumping Brook Complex according to Currie has been folded at least twice.

The mafic mineral lineation is best seen in the phyllite layers. This lineation as discussed above is a biotite mineral lineation which is most readily observed on the foliation planes in the phyllite. Although somewhat variable, this lineation generally trends north-northeast to south southwest with shallow plunges to the north-northeast. A plot of the mineral lineations is given in Figure 2.16 on page 33 and on Map 1. Mineral lineations do not plunge down the dip of the foliation.

Quartz and feldspar porphyroclasts in the psammitic layers are generally elongated parallel to the pervasive foliation defined by the micaceous minerals. This feature is, in most cases, evident only in slabbed samples.

Well developed crenulations cross the foliation of the phyllitic and semi-pelitic horizons. These crenulations strike from northwest-southeast to southwest-northeast with shallow to moderate plunges to the northwest or southeast. Crenulations bend around pods or horizons rich in porphyroblastic garnet. This bending may account for the rather high variability in crenulation orientation. Examination of one hand sample shows that there are in fact two crenulation directions. The existence of two crenulations was not realized in the field and this could also be a factor in the variability, alghouth the crenulation measurements taken from the field are believed to be from the same crenulation set. The two crenulations can be distinguished by their different wave lengths, and amplitudes. The predominent crenulation has a wavelength of 1 millimeter and an amplitude of 1/2 millimeter.

Minor folds with wavelengths approximately ten centimeters and amplitudes approximately six to eight centimeters are common throughout the phyllitic and semi-pelitic horizons. These folds are commonly open, however tight to near isoclinal folding was noted in one location. Fold hinges are rounded rather than angular and fold axis plunge moderately to the north-northeast. This trend is shown on an equal area plot (Figure 2.17).

Rare kink folds occur with amplitudes and wavelengths approximately 1 centimeter, however, no orientation of these kinks was obtained. Phyllites to the south of the mapped area, along the Cheticamp River are intensely kinked (Craw, in press).

Folds on a scale of approximately 10 meters in wavelength are also common throughout Unit 1. These folds are characterized by large open curving limbs.

Normal faults and faults with unknown trends displace the foliation along the Cabot Trail (Figure 2.6).

2.2.2 Metasedimentary Unit 2

Unit 2 is distinguished from Unit 1 by its light beige color and compositional banding on the centimeter scale. Unit 2 also consists of interlayered phyllite, semi-pelite and psammite, and is best exposed in the upper part of the Jumping Brook and along the upper western slopes of the French Mountain along the Cabot Trail. The thickness of the compositional banding is variable but commonly on the order of two to ten centimeters (refer to Figure 2.7 and 2.8). This compositional banding could be a reflection of differences in the sediment type during deposition or due to metamorphic segregation. Because of the fine grain size of Unit 2, the banding is not considered to be gneissic banding.

Unit 2 is in gradational contact with Unit 1 over a distance of 185 m along the Cabot Trail. Metamorphic minerals such as biotite, garnet and staurolite are preferentially concentrated in the phyllitic horizons.

Figure 2.7. Compositional banding parallel to the foliation in the phyllite of Metasedimentary Unit 2.

Figure 2.8. Compositional banding parallel to the pervasive foliation in the staurolite-bearing phyllite of Metasedimentary Unit 2.

In the western-most part of this unit porphyroblastic biotite occurs in the phyllitic horizons (Figure 2.9). Toward the eastern most part of the Unit, porphyroblastic staurolite occurs in the phyllite. Although this rock, containing the staurolite, has been described as a granite gneiss (Currie, in press), it is considered a phyllite, in this study because of its find grained nature, (Figure 2.10 and 2.11).

The psammite of Unit 2 is distinguished from Unit 1 by the presence of randomly oriented hornblende scattered throughout the rock, but preferentially concentrated around the boundaries of narrow epidote, zoisite and feldspar veins that randomly penetrate the rock (Figure 2.12). Although this phenomenon occurs very locally within the psammite of Unit 1 it is a rather prominent feature of Unit 2. Hornblende growth is most extensive in minor phyllitic horizons within the psammite. These veins possibly formed from solutions, rich in elements that reacted with minerals of the phyllitic layers to produce the hornblende. Discussion of possible reactions involved are given in the Petrology Chapter. The veins are approximately 1 centimeter in width and do not appear to follow structural fabrics within the rock, such as foliation planes, but moved randomly through the rock. This hornblende-rich psammite appears to grade into the coarse grained amphibolite, over a distance of approximately 685 meters along the Cabot Trail.

No primary sedimentary features, other than the compositional layering which may represent original depositional layering, were observed in Unit 2.

Figure 2.9. Porphyroblastic biotite within the phyllite of Metasedimentary Unit 2.

Figure 2.10. Porphyroblastic staurolite in the phyllite of Metasedimentary Unit 2.

Figure 2.11. Porphyroblastic staurolite, garnet and biotite in the phyllite of Metasedimentary Unit 2.

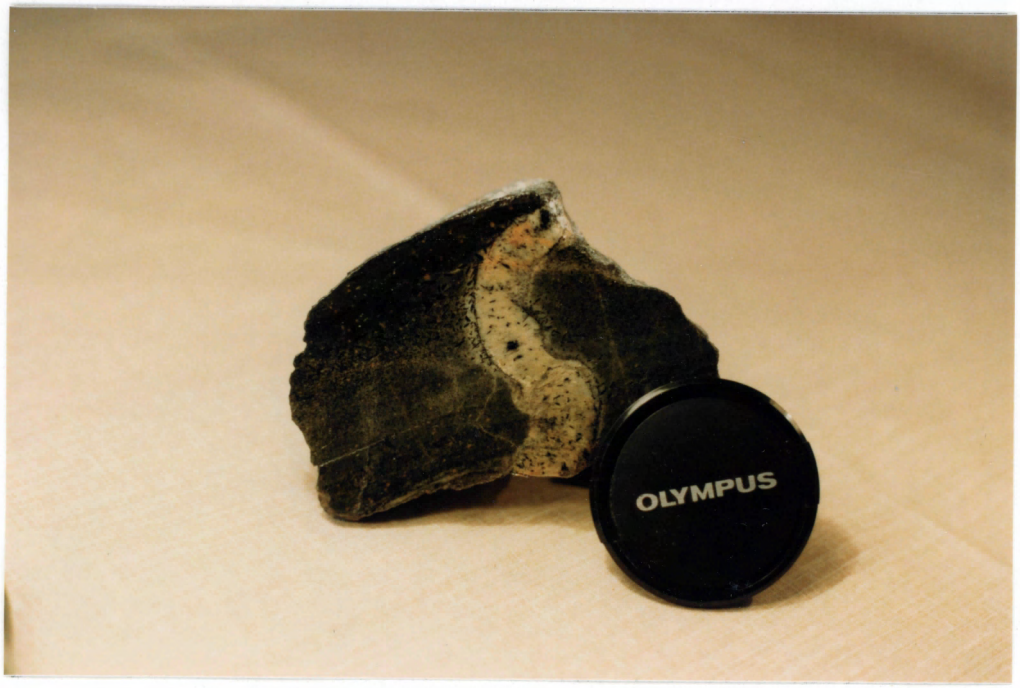

Figure 2.12. Feldspar, zoisite and epidote vein in psammite of Metasedimentary Unit 2, cross-cutting the foliation of the rock.

In one locality, coarse grained amphibolite outcrops within Unit 2. This is believed to be a relatively narrow dyke intruding the unit, although exact contact relations could not be determined in the field.

Unit 2 contains a pervasive foliation defined by the parallel alignment of biotite, muscovite and to a lesser extent chlorite. This schistosity is parallel to the compositional banding characteristic of this unit. The foliation strikes east-west, dipping moderately to the north in the western most part of the unit and swings around to strike northwest-southeast, dipping moderately to the northeast in the eastern most part of the unit, (Map 1). The swinging of the foliation from east-west in the eastern part of the unit, is interpreted in this study to mark the eastern limb of a large anticline plunging moderately to the northeast which folds both Unit 1 and Unit 2. An equal-area plot of poles to this pervasive foliation within Units 1 and 2 is given in Figure 2.13. The contoured plot of the poles to this foliation is given in Figure 2.14. The odd contour pattern, with the "island" in the northwest quadrant of the diagram is believed to be due to a local small-scale fold within Unit 2, since only two data points are held within that contour line.

Crenulations with shallow northward plunges occur in the phyllitic and semi-pelitic horizons of Unit 2. These crenulations cross the foliation and have amplitudes and wavelengths similar to those of Unit 1. The crenulations are not as numerous in Unit 2 as in Unit 1 which is probably a reflection of the decrease of phyllitic layers and increase in psammitic layers in Unit 2. An equal area plot of crenulation axis for

both Units 1 and 2 combined is given in Figure 2.15. From the plot, one can see the high concentration of data values indicating shallow plunges to the north.

Small symmetrical folds similar to those of Unit 1 are present in Unit 2 but not as numerous. This lack of minor folds in Unit 2 may also be a reflection of the decrease in the phyllitic layers which are less competent to the deformation stresses than the psammite. Generally these folds plunge moderately to the northeast, however a few plunge shallowly to the southwest. An equal area plot of minor fold axis within both Units 1 and 2 is given in Figure 2.17.

Rare kink folds, having amplitudes and wavelengths of approximately 1 centimeter were noted within Unit 2. No mineral lineations were evident in this Unit.

Examination of the equal-area plots of all these structural elements shows that the pervasive foliation, minor folds, crenulations and minor lineations may all be related in that the pervasive foliation was folded on a north-northeast trending axis.

The contact between the Metasedimentary Complex and the Jumping Brook Granitiod does not outcrop. A shear zone running diagonally down the north wall of the Jumping Brook canyon causes the granitoid to become highly sheared to protomylonite. Distinction between the sheared granitoid and Unit 1 is difficult as both are grey in color, fine grained and schistose. The presence of garnets within the Unit 1 has served to

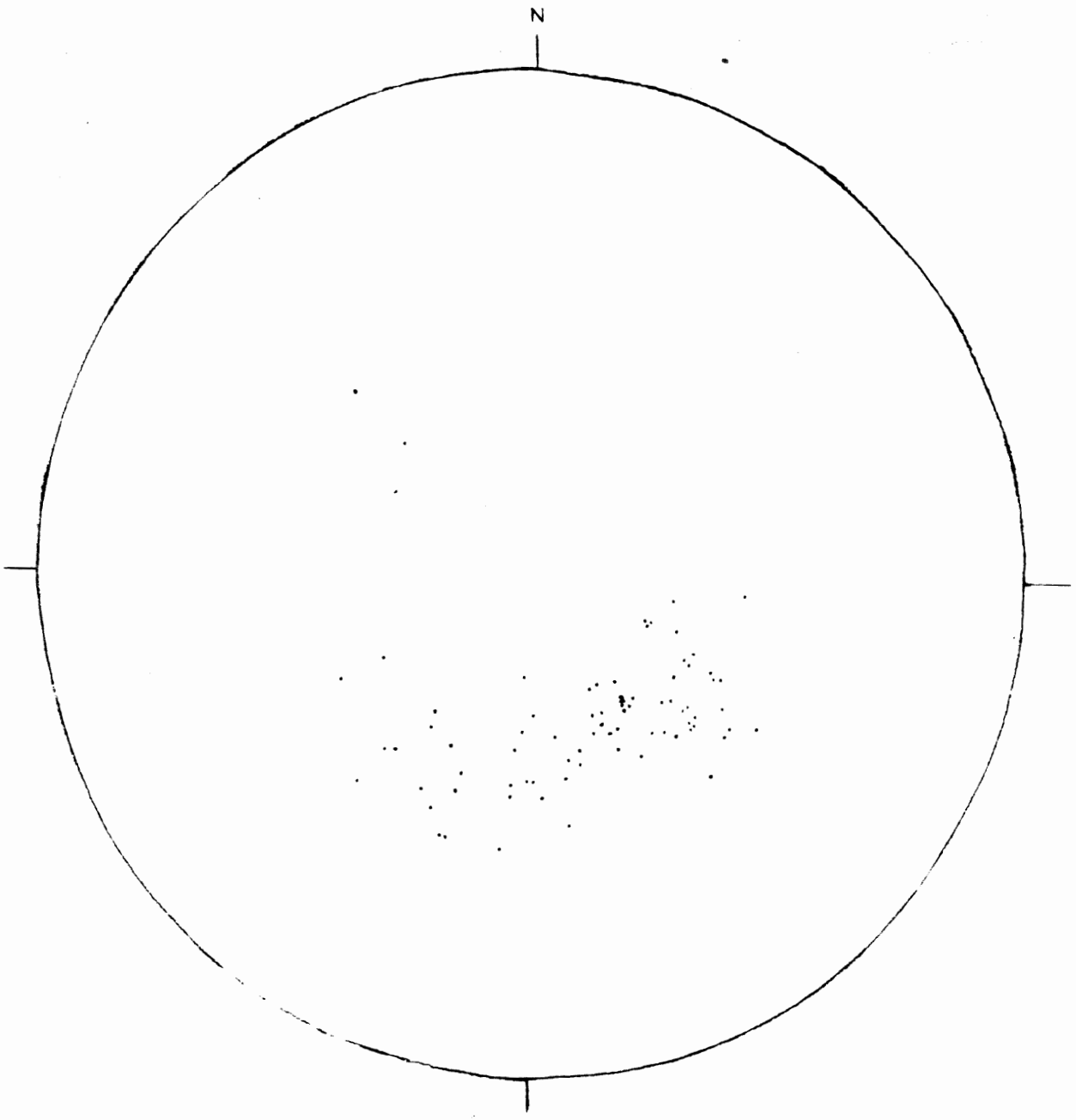

Figure 2.13. Equal-area plot of poles to the pervasive foliation within the Metasedimentary Complex.

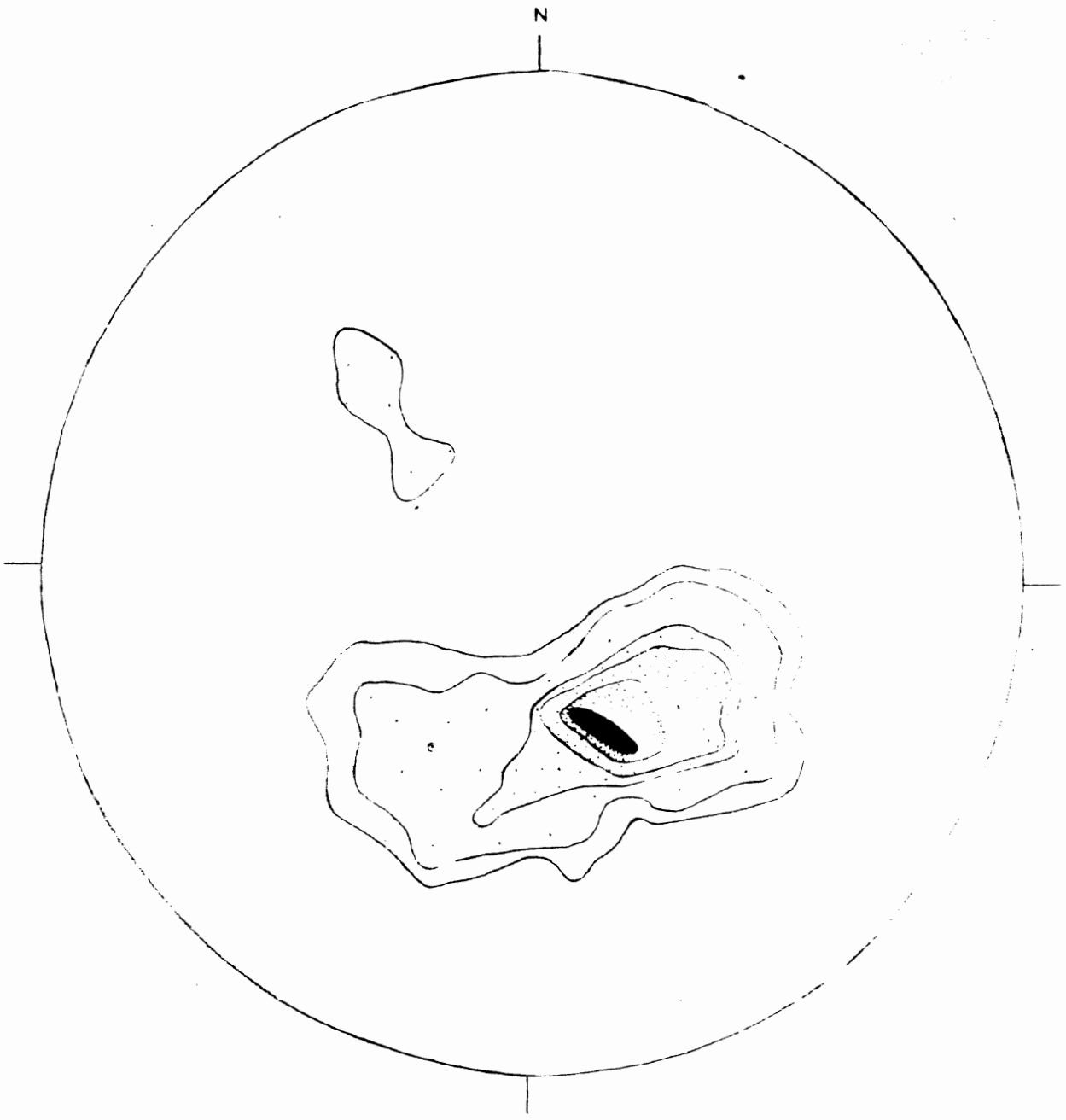

contours = 0.4 , 1 , 3 , 4 , 6 , 7 percent per 1 percent area

maximum value = 72 percent per 1 percent area

number of values = 76

Figure 2.14. Contoured equal-area plot of poles to the pervasive foliation within Metasedimentary Complex.

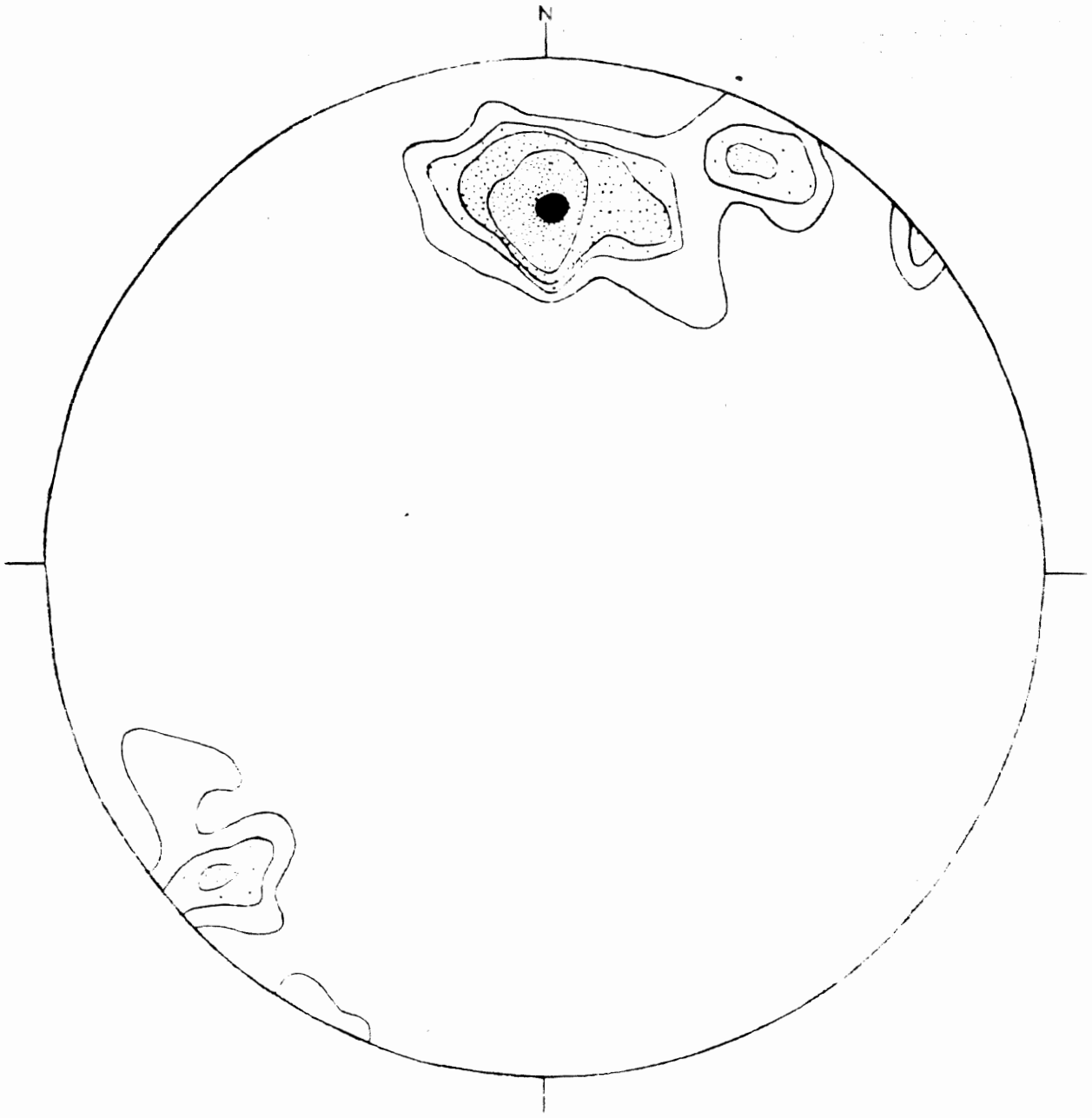

Figure 2.15. Contoured equal-area plot of crenulation axes of the Metasedimentary Complex.

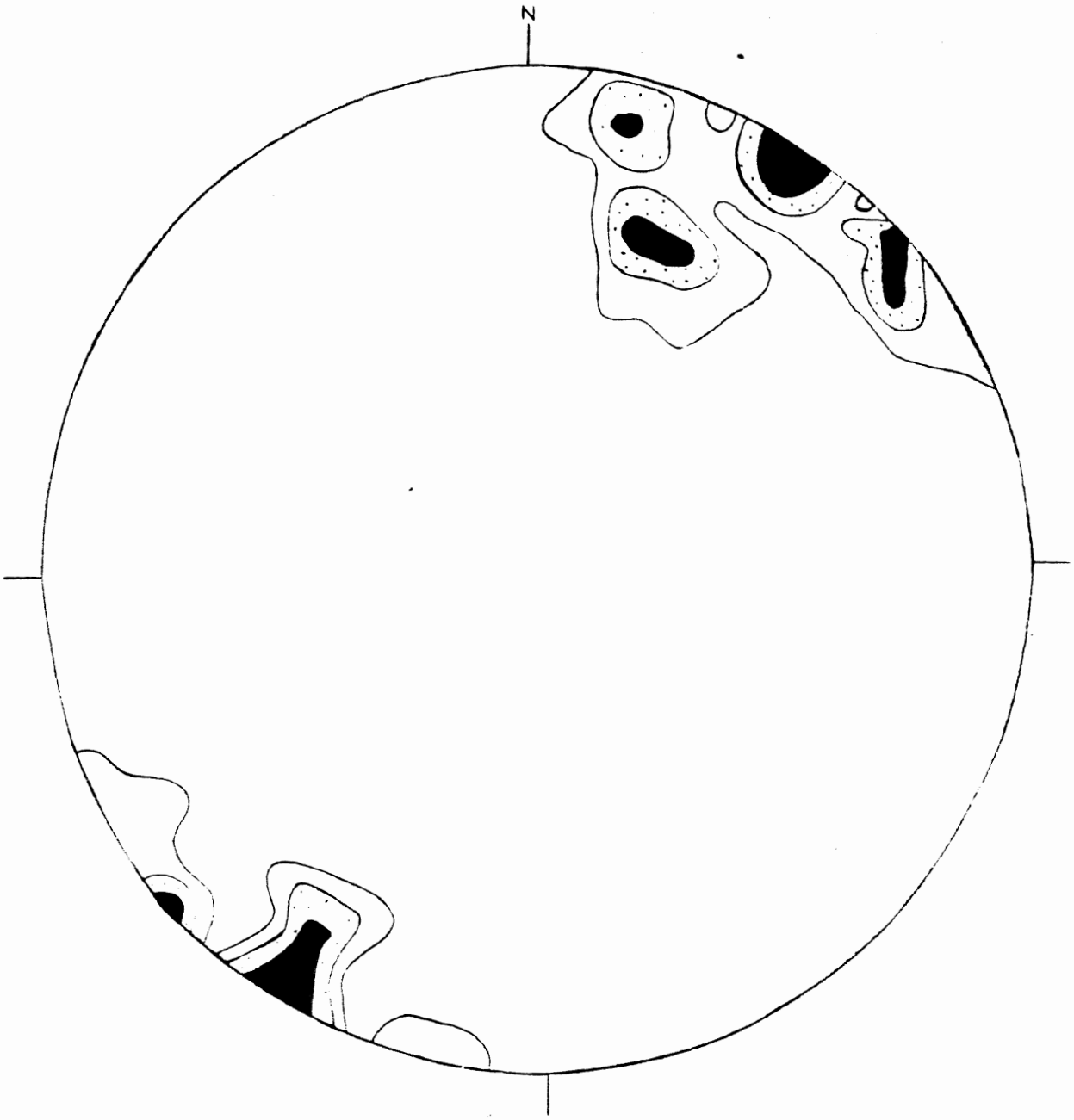

Figure 2.16. Equal-area plot of biotite mineral lineations within Unit 1 of the Metasedimentary Complex.

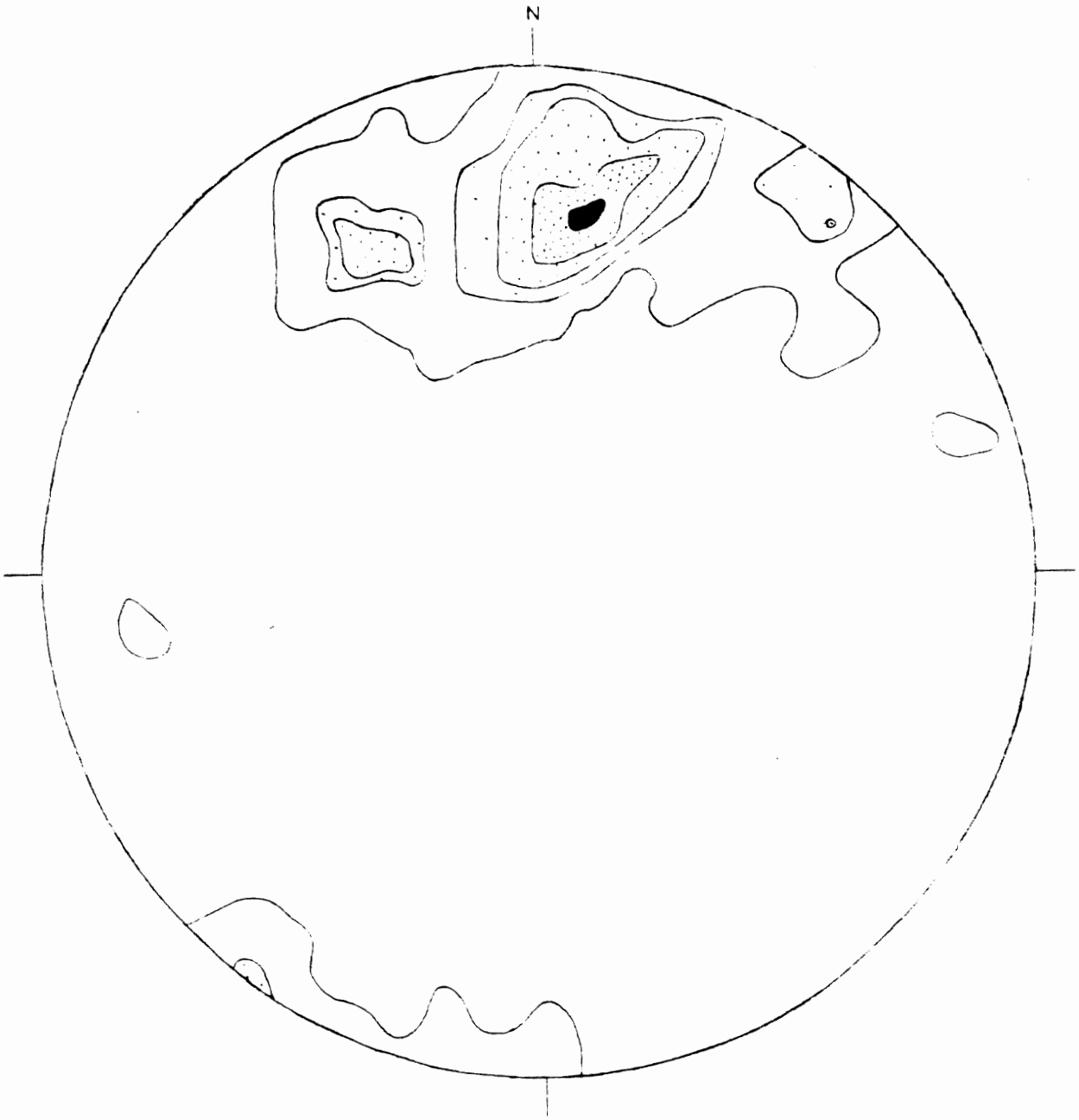

contours = 0.5, 1.5, 2, 3, 5 percent per 1 percent area

maximum value = 5.3 percent per 1 percent area

number of values = 97

Figure 2.17. Contoured equal-area plot of minor fold axes in the Metasedimentary Complex.

distinguish between the two lithologies in this study. Unit 2 of the Metasedimentary complex grades into the amphibolitic unit located at the top of French Mountain along the Cabot Trail.

2.3 AMPHIBOLITE

Unit 2 of the Metasedimentary Complex grades into the coarse grained amphibolite that is located at the top of French Mountain, along the Cabot Trail. The gradation appears as an increase in the amount of hornblende within the hornblende-rich psammite of Unit 2, toward the amphibolite.

Much of the amphibolite is massive, although toward the easternmost part of the exposure the amphibolite becomes rather schistose due to increasing amounts of biotite. Local patches of felsic material, approximately 5 centimeters in size are common throughout the unit. Distinction between the diorite and amphibolite in the field was based upon color index and the fact that the diorite showed little effects of metamorphism. Diorite contains approximately 50 percent mafic minerals while the amphibolite contains over 90 percent mafic minerals. The principal mafic mineral in both lithologies is hornblende and thus the amphibolite may be a metamorphosed diorite. Near the top of the Mountain, a granitic dyke a few meters wide intrudes the amphibolite and contains xenoliths of the amphibolite. No foliation measurements were recorded because of poor exposure and slumping in the immediate area.

2.4 DIORITE

Diorite was found in two localities within the mapped area: (1) on the top of French Mountain, east of the amphibolite along the Cabot Trail, near French Lake and (2) on the most western extent of the Skyline Trail near to the coast.

Diorite near French Lake is coarse grained, and locally foliated. Local patches of purple on the feldspar is believed to be fluorite although this was not confirmed in thin section study (Figure 2.18). Fluorite has been documented in the general area (Currie, in press, p. 18).

Diorite at the end of Skyline Trail lies structurally above Granitoid Unit A. The contact between the two lithologies does not outcrop but the highly altered and broken up nature of Unit A suggest that the contact may be a fault like the one between Unit 1 and Unit A. This diorite is medium grained and undeformed and contains xenoliths of fine-grained amphibolite.

The contact between the Diorite and the Jumping Brook Granitoid is not exposed and only a 10 centimeter wide contact zone between the Diorite and "A" shows that metasomatic reactions may have taken place between the two lithologies, resulting in a granitic looking rock with large hornblende crystals. Mafic minerals within the Diorite tend to occur in aggregates.

Figure 2.18. Diorite near to French Lake showing coarse grained nature, no fabric and purple mineral (possibly fluorite) near the top of the sample.

2.5 GRANITOID UNIT A

Granitoid Unit A which probably corresponds to the Corney Brook Pluton (Currie, in press) is located in the southwestern most part of the mapped area along the Cabot Trail and along the western most extent of the Jumping Brook Canyon wall. This pluton although documented to be undeformed (Currie, in press) shows a foliation near to the contact with Unit 1 of the Metasedimentary Complex. This feature could be a result of the fault motion as the foliations are highly variable in the area. The eastern edge of the pluton is highly brecciated and slickensides occur in various directions. The general foliation defined by the alignment of the mafic minerals, strikes approximately north-northeast to south-southwest. Within the contact zone between Unit 1 and Unit A the granitoid becomes a greenish grey fine grained cataclastic rock.

2.6 JUMPING BROOK GRANITOID

The informally named Jumping Brook granitoid is located on the northern wall of the Jumping Brook canyon along the middle and lower parts of the Jumping Brook (Figure 2.19). It is a light colored, medium grained granite which is undeformed at the top of the canyon wall and progressively becomes more sheared toward the bottom of the wall where it is barely distinguishable from the semi-pelite of the Metasedimentary Complex, and (Figure 2.20) although scree and boulders cover much of the lower wall, the progressive shearing in the granite is very evident. Foliation within the sheared granite strikes approximately east-west dipping moderately to the north. This foliation locally can be quite variable.

Figure 2.19. Outcrop of the Jamping Brook Granitoid along the north wall of the Jumping Brook Canyon and showing scree slopes along the lower part of the wall.

Figure 2.20. The progressive shearing of the Jumping Brook Granitoid (a) undeformed, (b) development of fabric, (c) sheared, (d) highly sheared and folded.

From (a) to (d) there is a progressive decrease in grain size, and progressive development of a fabric defined by the parallel elongation of grains.

(a)

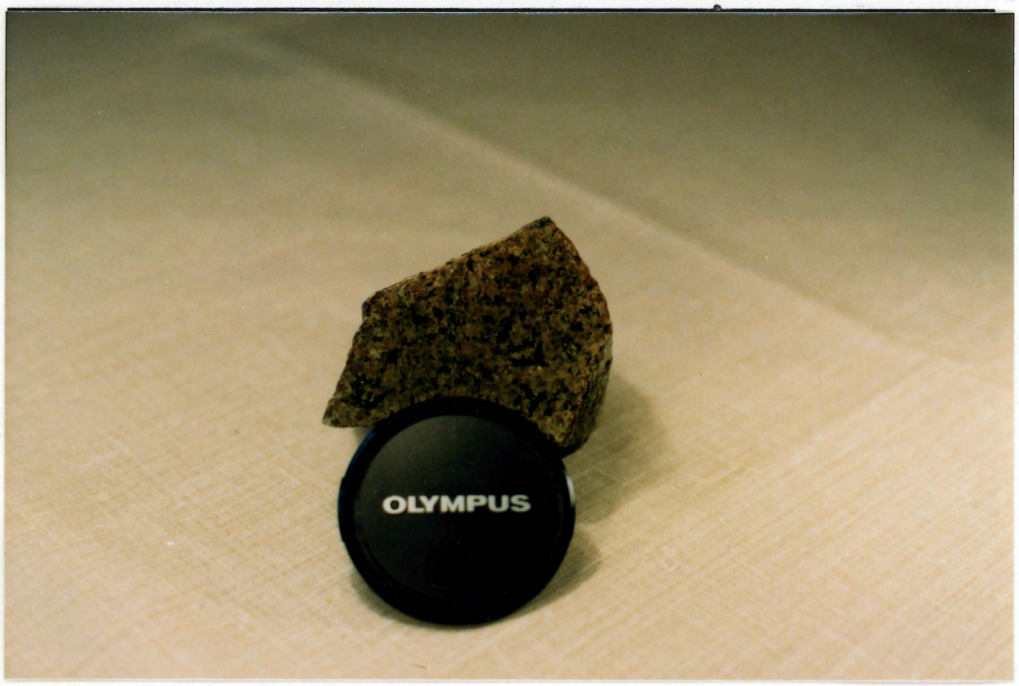

(b)

(c)

(d)

2.7 COMPOSITE GNEISS

2.7.1 Biotite-Quartz-Feldspar Gneiss

The biotite-quartz-feldspar gneiss is first observed 1.5 kilometers along the Fire Tower Road northwest from the Skyline Trail, and 1.2 kilometers west from French Lake, along the Cabot Trail. Direct contacts with the amphibolite, diorite, Jumping Brook Granitoid or Metasedimentary Complex are not observed. Much of the gneiss is associated with granitic and pegmatite dykes which cross-cut or run parallel to a well defined foliation in the gneiss. In many cases it is difficult to assess whether the granitic and pegmatite dykes are leucosomes resulting from anatexis of the gneiss, or injected into the gneiss from an external source. Some leucosomes are rimmed by melanosomes which have been documented as representing residual material during anatexis (Mehnert, 1968) (Figure 2.21), others have no melanosome (Figure 2.22), while others are wrapped around by the foliation of the gneiss.

The biotite-quartz-feldspar gneiss is highly varied in proportions of biotite, muscovite, quartz and feldspar, but because of intimate interlayering of mica-rich horizons with quartz-feldspar-rich horizons the gneiss was mapped under one unit (Figure 2.23 a, b).

Gneissic banding within the unit varies from 1 centimeter to 10 centimeters thick. Garnets are common throughout the unit but preferentially occur in the micaceous layers. Kyanite was recorded in one location in this study at the junction of the Fire Tower Road and a

road leading east to the fire tower. Cordierite was not observed in this study, however it has been recorded at the junction of the Fishing Cove River and the Cabot Trail (Currie, in press). Locally the gneiss becomes fine grained similar to the Metasedimentary Complex, although this may be due to local shearing.

A pervasive and very consistent foliation occurs in the gneiss. This foliation, defined by the parallel alignment of muscovite and biotite, strikes north-south and dips steeply to the east. An equal area plot of this foliation is given in Figure 2.24. Poorly preserved crenulations were noted in few gneiss hand samples but not during the field mapping and thus no orientation was obtained. Rare kink folds, small symmetrical, open folds and tight to isoclinal folds were observed within the gneiss. Only one measurement from the kinks was obtained and the kink axis plunged shallowly to the west. The small symmetrical folds have amplitudes and wavelengths of approximately 10 centimeters. These fold axes plunge shallowly to the south-southeast. The orientations of the isoclinal folds were not obtained. Two moderately sized folds, with wavelengths of 2 to 3 meters were recorded in the northern part of the mapped area. Their fold axes plunge shallowly to the north.

An early phase of deformation in the gneiss was recorded near the intersection of Fishing Cove River and the Cabot Trail. A ptygmatically folded granitic vein approximately 1 centimeter in width is wrapped around by the present pervasive foliation (Figure 2.29).

Figure 2.21. Leucosome in biotite-quartz-feldspar gneiss with melanosome, located on the northern extent of the Fire Tower Road.

Figure 2.22. Leucosome in biotite-quartz-feldspathic gneiss without melanosome, along the Fire Tower Road.

(a)

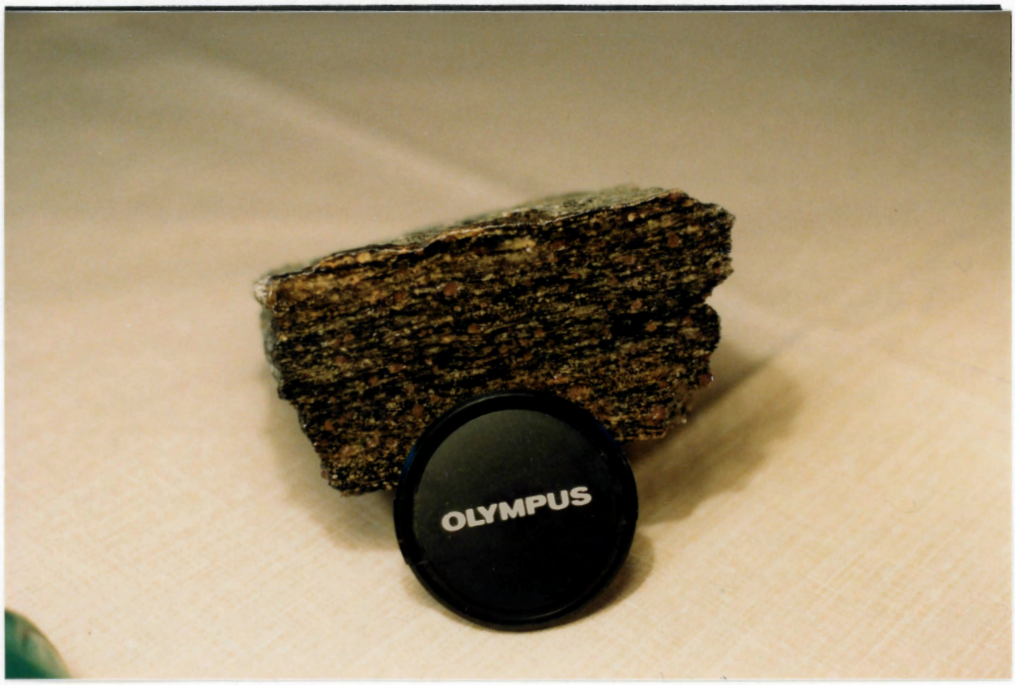

(b)

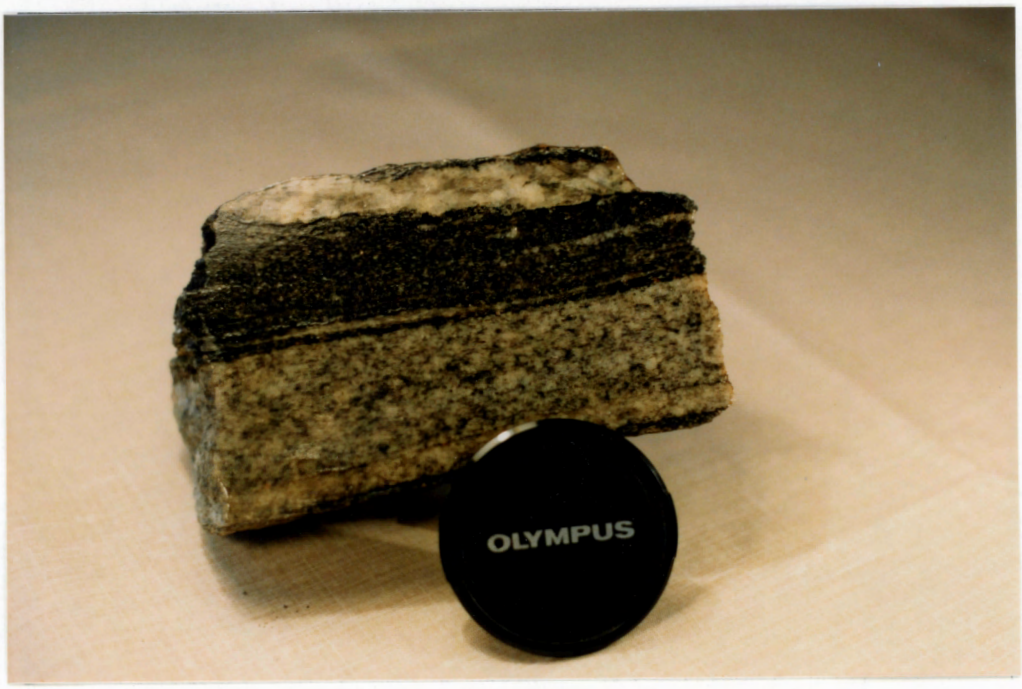

Figure 2.23. Biotite-Quartz-Feldspar gneiss (a) with garnets (b) with gneissic segregation.
The coarser grain size and well developed segregation distinguishes the gneiss from Unit 2 of the Metasedimentary Complex.

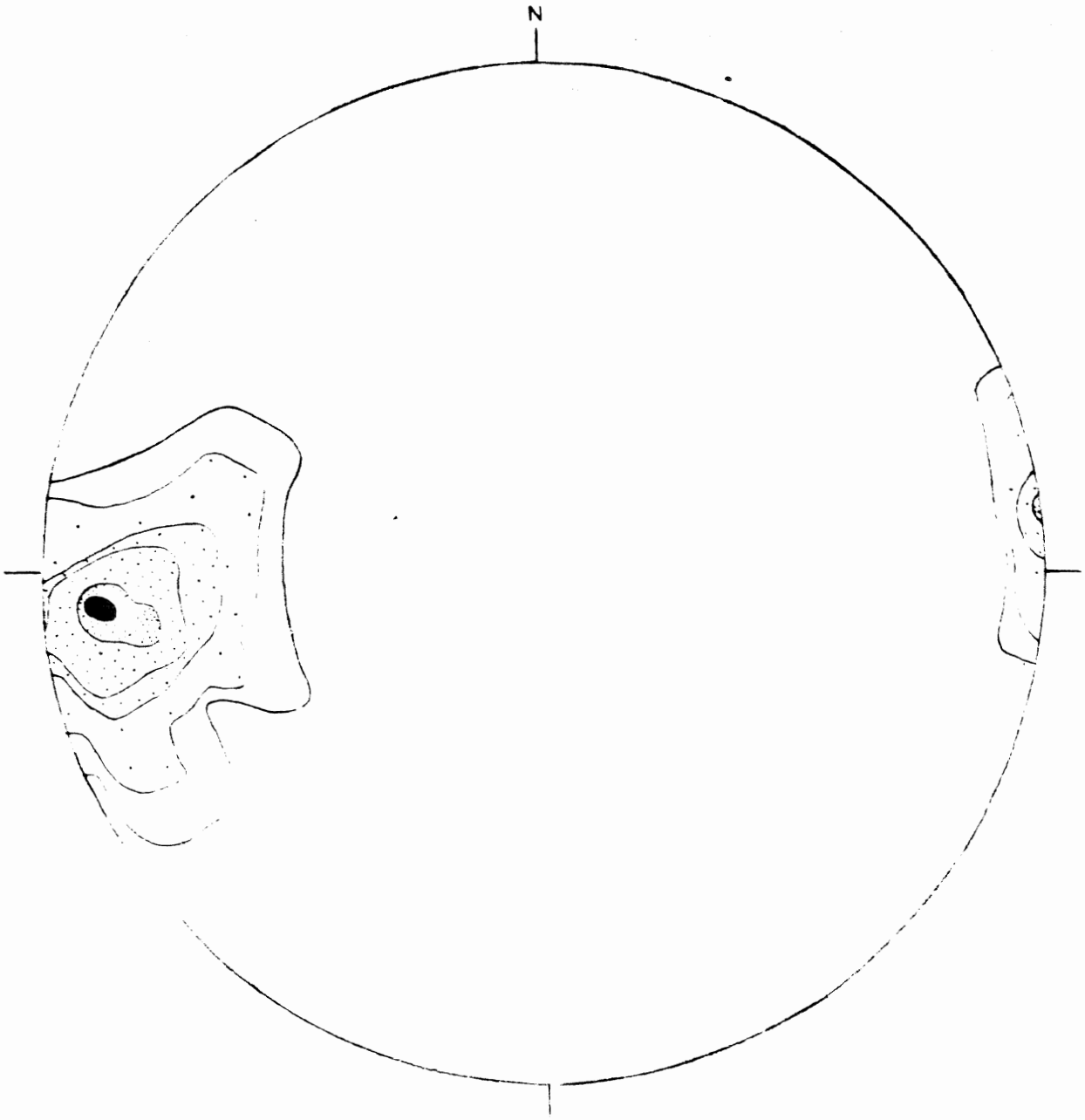

contours = 0.5,1.5,3,5,9,10.5 percent per 1 percent area

maximum value = 11 percent per 1 percent area

number of values = 67

Figure 2.24. Equal area plot of poles to the pervasive foliation within the biotite-quartz-feldspar gneiss.

2.7.2 Amphibolite Gneiss

Amphibolite gneiss was recorded in two locations within the mapped area: 1) at the junction of the Fishing Cove River and the Cabot Trail and 2) near the northeastern end of the Fire Tower Road.

Boundaries between the amphibolite gneiss and biotite-quartz-feldspar gneiss are gradational with the biotite content within the amphibolite gneiss increasing in percentage toward the contact. Foliation within the amphibolite gneiss is defined by the parallel alignment of hornblende. Gneissic layering is generally 1 to 3 centimeters in width, (Figure 2.25) and is parallel to the foliation which is also parallel to the foliation of the biotite quartz-feldspar gneiss. Pyrite is quite abundant in some horizons.

2.7.3 Feldspar Augen Gneiss

White and orange feldspar augen gneiss occurs in the northeastern part of the mapped area along the Fire Tower Road and the Cabot Trail. The orange potassic feldspar augen gneiss may represent deformed pegmatite. Figure 2.26 a, b show examples of the augen gneiss. The relation of the potassic feldspar augen gneiss to the biotite-quartz-feldspar gneiss or the amphibolite gneiss was not observed. The white feldspar-augen gneiss is found within the muscovite-rich quartz-feldspar gneiss and has a foliation parallel to the quartz-feldspar gneiss.

Figure 2.29. Ptygmatically folded granitic vein wrapped around by the pervasive foliation of the biotite-quartz-feldspar gneiss.

Figure 2.25. Amphibolite gneiss with gneissic banding.

(a)

(b)

Figure 2.26. (a) White feldspar-augen gneiss (b) potassic feldspar-augen gneiss showing core and mantle texture. Both showing features of protomylonite.

2.8 PEGMATITE AND GRANITE DYKES WITHIN THE GNEISS COMPLEX

Many granitoid dykes are found within the gneiss complex and although they are too numerous to indicate on the geological map, they were noted in the field and their relationship to the gneiss was recorded. Most dykes are from less than a meter to a few meters wide and either cross-cut the foliation of the gneiss or run parallel to it. Dykes vary from being undeformed to having a fairly well developed foliation. Some dykes clearly intrude the gneiss and contain xenoliths of the gneiss (Figure 2.27). Pegmatite varies from being very coarse grained to very fine grained. Locally it may occur as pods which are wrapped around by the foliation of the gneiss. Because the mineral proportions vary greatly from "dyke" to "dyke", all dykes were classified into one group termed undifferentiated granitic dykes as a detailed study of them is beyond the scope of this study. A discussion on the origin of the pegmatite and migmatite is found in the Metamorphism Chapter.

2.9 DISCUSSION

A summary of the lithologic units and their field relations is given in Table 2.1. The lack of data in Table 2.1 is a reflection of the poor exposure on the top of French Mountain.

Cross-sections through the Composite Gneiss Complex and the

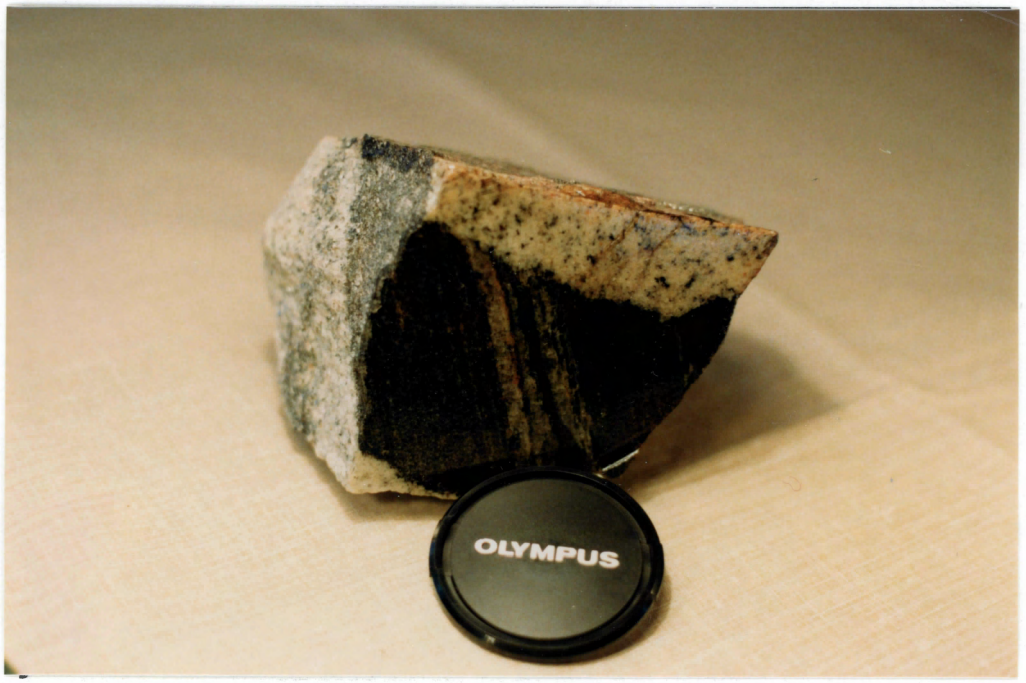

Figure 2.27. Biotite-quartz-feldspar xenolith in a granitoid dyke. The xenolith still contains the pervasive foliation and gneissic segregation.

Table 2.1. Summary Table of Field Relations between Major Lithological Units, without Genetic Inferences, in the French Mountain Area.

	Unit A	Unit 1	Unit 2	Amph.	J.B. Granitoid	S.T. Diorite	B-Q-F Gneiss	Amph. Gneiss	K-sp Augen Gneiss	Granitoid dykes in Gneiss
Unit A		fault contact	n.r. separated by Unit 1	n.r. separated by Units 1 and 2	n.r. no xenoliths	presently J.B. Diorite above Unit A but no xenoliths	n.r.	n.r.	n.r.	n.r.
Unit 1			gradational over a distance of 185 m. along Cabot Trail	n.r. separated by Unit 2	shear zone, fault assumed	n.r. separated by Unit A	n.r.	n.r.	n.r.	n.r.
Unit 2				gradational over a distance of 685 m. along Cabot Trail	n.r.	n.r.	n.r.	n.r.	n.r.	n.r.
Amph.					n.r.	diorite contains xenoliths fig. basic rock (?)	n.r.	n.r.	n.r.	n.r.
J.B. Granitoid						n.r. no xenoliths	n.r.	n.r.	n.r.	n.r.

Table 2.1 (continued)

	Unit A	Unit 1	Unit 2	Amph.	J.B. Granitoid	S.T. Diorite	B-Q-F Gneiss	Amph. Gneiss	K-sp. Augen Gneiss	Granitoid dykes in Gneiss
S.T. Diorite							n.r.	n.r.	n.r.	n.r.
B-Q-F Gneiss								gradational	gradational	intrusive to anatectic
Amphib. Gneiss									n.r.	intrusive
K-sp. Augen Gneiss										n.r.
Granitoid dykes in the Gneiss										

LEGEND: Unit A = Granitoid Complex
Unit 1, 2 = Metasedimentary Complex
Amph. = Amphibolite
J.B. Granitoid = Jumping Brook Granitoid
S.T. Diorite = Diorite outcropping at western end of Skyline Trail

B-Q-F Gneiss = Biotite-Quartz-Feldspar Gneiss
Amph. Gneiss = Amphibolite Gneiss
Ksp Augen Gneiss = Potassic Feldspar Augen Gneiss
n.r. = no directly observable field relation

Metasedimentary Complex are given in Figure 2.28 and on the geological map in the back pocket (Map 1).

Both the Metasedimentary Complex and Gneiss Complex have undergone polyphase deformation; although the phases within each unit may have resulted from the same deformation "event". For example, the large fold that deforms the Metasedimentary Complex may have formed contemporaneously with the crenulations, minor folds, and mineral lineations. The relation between mineral lineations and crenulations mineral lineations and minor folds and minor folds and crenulations was not determined, and a detailed study of the complex structure within the area is beyond the scope of this study. Within the gneiss three phases of deformation were recorded: 1) an early phase indicated by ptygmatic folding of a granitic vein, wrapped around by the pervasive foliation 2) development of a pervasive foliation 3) folding of the pervasive foliation on different scales including crenulation development. Within the Metasedimentary Complex two phases of deformation were recorded: 1) development of the pervasive foliation 2) folding of the foliation on different scales including the crenulation development and mineral lineation.

The distinctly different foliation orientations between the gneiss complex and metasedimentary complex, strongly indicate that some structural break exists between the two units. From the cross-sections given in Figure 1.28 the key problem in determining the nature of the contact between the two complexes is the lack of outcrop. Many structures or combinations of structures could be imagined to exist

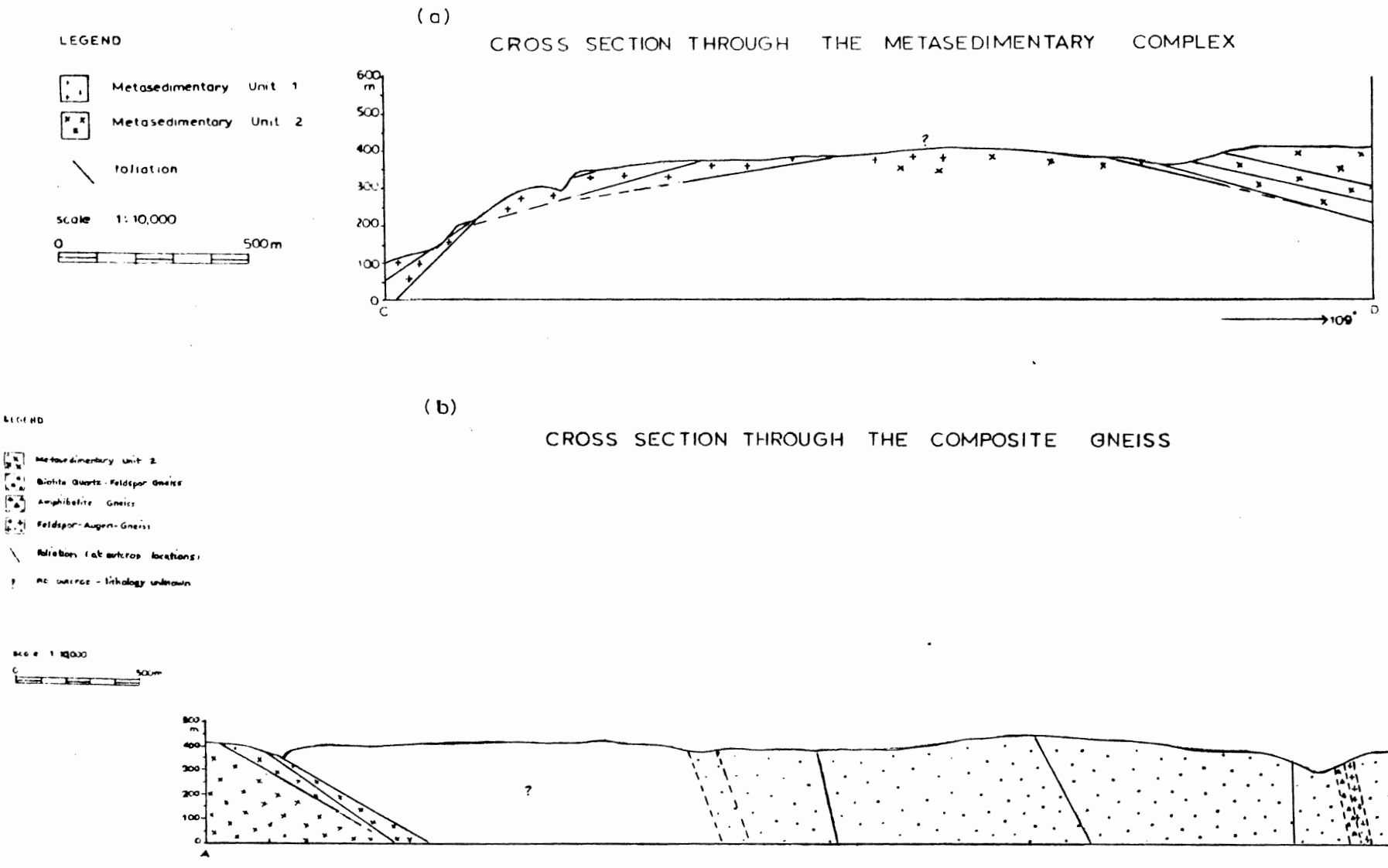

Figure 2.28 Cross-section (a) through the Metasedimentary Complex (b) through the Gneiss Complex. Cross-sections are also given on the Geological Map (Map 1, in the back pocket).

between the two complexes in the area of no outcrop. However if one considers the simplest and most likely possibilities, then there are two likely models. In model 1, it is assumed that the foliation of the Medasedimentary Complex remains constant, across the area of no exposure and is assumed to be the same attitude as that recorded from the last exposure of this complex. In this case the foliation of the Metasedimentary Complex would be truncated by the foliation of the gneiss, and a fault contact would be inferred. In model 2, the assumption is made that the attitude of the foliation within the Metasedimentary Complex changes across the area of no outcrop until it is parallel to that of the Gneiss Complex. In this case, a structurally conformable contact could exist between the two complexes. In either of these two cases, it does not appear likely that the Metasedimentary Complex overlies the Gneiss Complex. These models are purely speculative, but the consistent foliation of the Gneiss Complex being quite different from that found within the Metasedimentary Complex, suggests the existence of some sort of tectonic break between the two complexes.

This study does not support the presence of an unconformity between the two complexes in contrast to the conclusion of Currie (in press) who suggested that the Metasedimentary Complex unconformably overlies the Gneiss Complex and the whole sequence is overturned. This study showed no evidence for a depositional unconformity. The contact between the two complexes was not exposed, facing directions observed in only one location were variable due to local isoclinal folding and no conglomerates, which may represent an erosional boundary, were observed. The coarsest grained metasedimentary rock was located at the top of the

cliff on the north side of the Jumping Brook canyon wall and no gneiss was observed above this outcrop. A complete transect up the north wall just to the west of this outcrop (shown as the top outcrop in the top right of Figure 2.1) showed all of the wall to be the metasedimentary complex in this area.

A structural discontinuity separating the two complexes appears possible. The gneiss could be older as it shows three phases of deformation while the metasedimentary complex shows two and it is of course higher grade. Therefore two interpretations are possible 1) there may have originally been an unconformity separating the Metasedimentary Complex from the Gneiss Complex or 2) the two complexes together may represent different levels of the same sequence. There appears to be no evidence from this study to favor one interpretation over the other.

CHAPTER 3

PETROLOGY

3.1 INTRODUCTION

One hundred and ninety hand samples were collected from within the mapped area during the field mapping. Thin sections from fifty-two selected samples, and seven selected polished thin sections were used in microprobe analysis of the elemental oxides in the major phases. From petrological study of the thin sections, phases were identified, textures and phase relations recorded and relations between textural development and phases considered.

To avoid confusion on lithologic terminology, lithologic terms will be defined for the context in which they are used in this study.

Metasedimentary Unit 1 and 2 consist of interlayered phyllite, psammite and semi-pelite. These lithologies are defined below.

Phyllite:

The phyllite is defined as a medium grained (0.1 mm to 1.0 mm) metamorphosed rock of pelitic origin (Mason, 1978). The composition within the mapped area consists of quartz, feldspar, muscovite, $\pm$ chlorite, biotite, garnet and staurolite.

Psammite:

The psammite is defined as a medium grained (0.1 mm to 1.0 mm) metamorphic rock rich in quartz; a dark grey, metamorphosed sandstone containing quartz and feldspar and a variety of dark rock and mineral fragments (Bates and Jackson, 1980).

Semi-pelite:

The semi-pelite is defined as a quartzose schist (Mason, 1978), a metamorphosed rock intermediate between the phyllite and psammite found within the mapped area, containing at least 25 percent micaceous minerals.

3.2 METASEDIMENTARY COMPLEX

3.2.1 Metasedimentary Unit 1

Unit 1 consists of interlayered phyllite, psammite and semi-pelite. Phyllite is the most common lithology, however semi-pelite and psammite are certainly not uncommon.

Phyllite:

The phyllite of Unit 1 characteristically has layers rich in micaceous minerals alternating with layers rich in quartz and feldspar. These layers are generally 1.5 mm to 4 mm thick. Mineralogically the phyllite consists of quartz; feldspar which is generally rather non-descript and is often difficult to distinguish from quartz without checking the optic sign; muscovite, $\pm$ biotite, $\pm$ chlorite, $\pm$ garnet $\pm$ minor tourmaline, minor opaques and very minor apatite. Phase percentages are given in Table 3.1 however the use of visual Percentage Estimation Charts (after Terry and Chilinger, 1955) as well as the point counting results are used in discussions within the text.

Table 3.1. Phase Percentages Using the Point Counting Method.

Sample	24	16c	31	37.5	81	121	78c	57a	57b	96	160	157
feldspar + quartz	47.7	80.6	52.9	77.3	57.1	78.5	31.3	49.0	57.9	57.9	50.7	59.9
muscovite	25.8	6.2	31.3	0	23.6	0.7	0	24.4	22.8	0	0	0
biotite	19.4	12.8	10.5	9.6	10.7	12.2	0	24.1	13.2	0	6.7	4.5
chlorite	2.3	0.1	1.1	0.3	0.2	1.9	0	0.2	0.6	0	0.2	2.1
garnet	3.6	0.1	3.2	4.7	7.5	0	0	0.1	2.7	0	0.1	4.5
staurolite	0	0	0	0	0.2	0	0	0	0.1	0	0	0
kyanite	0	0	0	0	0	0	0	0	1.4	0	0	0
amphibole	0	0	0	6.9	0	0	64.5	0	0	41.9	25.6	26.9
epidote	0	0.1	0	0	0	6.3	0.3	0.1	0.1	0	9.7	0
sphene	0	0	0	0	0	0	3.9	0.2	0.6	0.2	0	0
rutile	0	0	0	0	0	0	0	0	0	0	0	0
tourmaline	0.2	0	0.2	0	0	0	0	0	0.7	0	0	0
calcite	0	0	0	0	0	0	0	0	0	0	0	0.4
apatite	0.2	0	0	0	0	0	0	0	0	0	0	0
opaques	0.8	0	0.8	1.2	0.5	0.4	0	1.9	0	0	6.9	1.7
unknowns	0	0	0	0	0.2	0	0	0	0	0	0.1	0

*Because of the non-descript nature of the feldspar in many samples distinction between quartz and feldspar is very difficult without checking optical signs. Therefore to avoid gross errors in obtaining percentages for these minerals, the two were combined in the point counting method.

LEGEND

24 - phyllite, Unit 1
16c - psammite, Unit 1
81 - phyllite, Unit 2
37.5 - psammite, Unit 2
31 - phyllite, Unit 2
121 - Jumping Brook Granitoid
78c - Amphibolite Gneiss
57a - Biotite-Quartz-
57b Feldspar Gneiss
96 - Diorite
160 - Diorite
157 - Amphibolite

- sampling target in all cases equals 1000 points per slide

- all values given in volume percent

- point counting was done using a "swift" automatic point counter

Quartz and feldspar together account for approximately 50 percent of the phyllite however this value is quite variable depending on whether the section was taken from an area rich in micaceous minerals or an area rich in quartz and feldspar. Quartz is slightly more abundant than feldspar and quartz and feldspar together make up the matrix of the rock occurring as grains ranging in size from 0.08 mm to 0.3 mm and forming well developed granoblastic polygonal grain boundaries. Twinning is rarely observed in the feldspar but microprobe analysis indicate that much of the feldspar is plagioclase.

Of the micaceous minerals, muscovite is the most abundant and best defines the pervasive schistosity of the rock, by the parallel alignment of its fine sheaths which are approximately 0.02 mm wide. It is the abundance of the muscovite that gives the phyllite its silver grey sheen, and generally the tiny sheaths occur tightly packed together, forming the micaceous horizons. Biotite generally occurs throughout these horizons occurring as small sheaths; slightly larger in size than the muscovite or as porphyroblasts. (The term porphyroblast, in this study, refers to metamorphic minerals that have grain size diameters five to ten times larger than the diameters of matrix minerals). The biotite generally occurs with its long axis aligned parallel to that of the muscovite, however some porphyroblasts with grain widths approximately 0.5 mm, cross-cut the foliation and are interpreted to be post-tectonic to the pervasive schistosity. Chlorite, although not generally abundant, occurs in a similar fashion to the

biotite, occurring as fine sheaths with the long axis parallel to the fabric of the rock or as twinned porphyroblasts cross-cutting the foliation of the rock (Figure 3.1). Porphyroblastic chlorite occurs in samples 12 and 24. Locally biotite is replacing chlorite.

Almandine garnet generally occurs as poikiloblastic porphyroblasts showing preferential growth in the micaceous horizons of the phyllite. Criteria used to determine the relationship between porphyroblasts and fabric defined as schistosity is given in Table 3.2 and discussed in section 3.7.

Within the phyllite, there appear to be two modes of almandine garnets, both porphyroblastic and poikiloblastic. Garnets from sample 12 clearly show matrix material being swung into the garnet to become inclusions. Garnets in this case are clearly syn-tectonic to the development of the schistosity (Figure 3.2). Sample 138b appears to contain two types of garnets - one pre-tectonic and one syn-tectonic to the schistosity. This may be interpreted as two separate generations of garnet growth. The pre-tectonic garnets appear highly broken up and show retrogression to chlorite along fractures and grain boundaries. The syn-tectonic garnets are identified by their inclusion trail pattern. Figure 3.3 shows garnets containing the snowball inclusion trail pattern which is generally indicative of a syn-tectonic relationship to the pervasive schistosity. Sample 24 also shows garnets that are interpreted to be pre- and syn-tectonic with respect to the pervasive schistosity. The syn-tectonic grains are indicated by the matrix

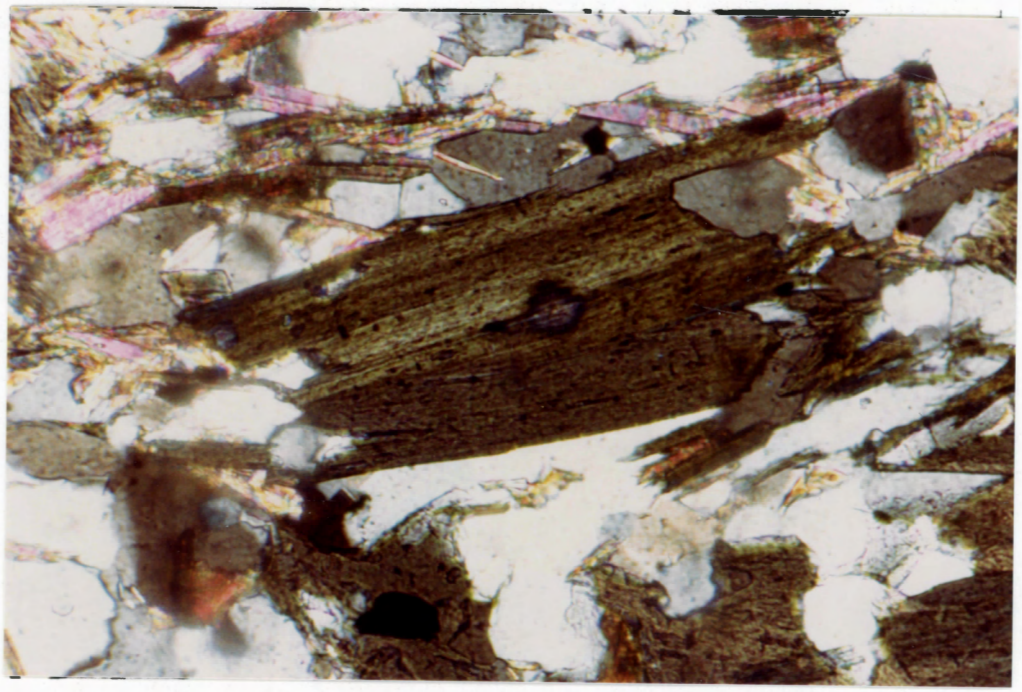

Figure 3.1. Twinned porphyroblastic chlorite cross-cutting the schistosity of the phyllite in Unit 1 of the Metasedimentary Complex. (crossed polars at 125 x).
These are interpreted to be post-tectonic to the pervasive schistosity.

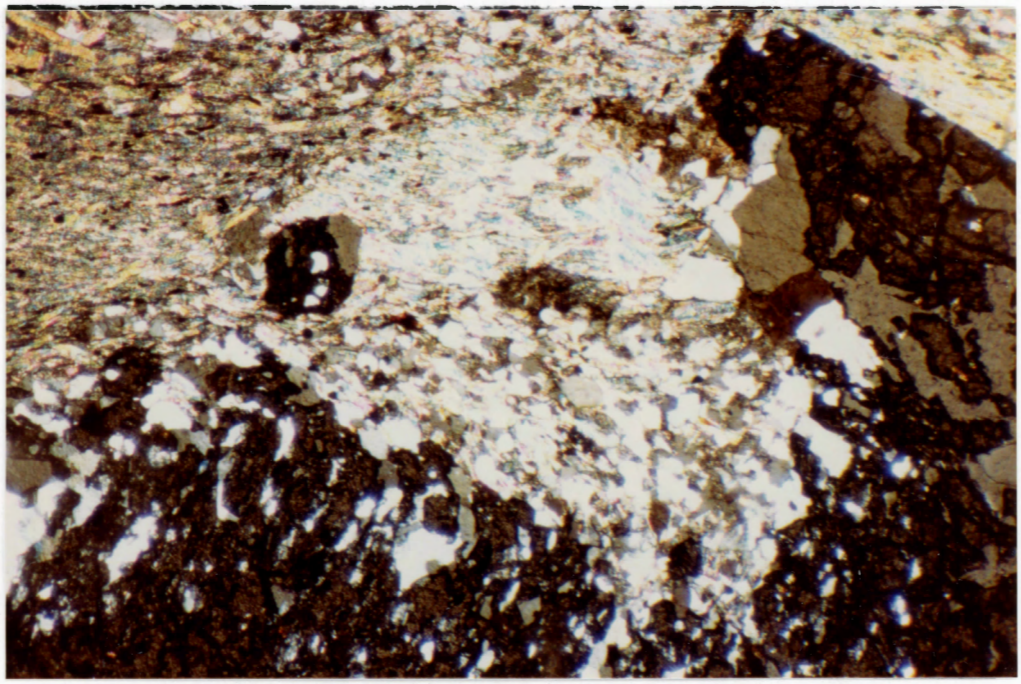

Figure 3.2. Matrix material swinging into garnet porphyroblast. As the porphyroblast grows it is rotated due to the stress that developed the schistosity, and therefore it is syn-tectonic to that schistosity. (crossed polars, x 31.25).

material swinging into the grain, while the pre-tectonic garnets are indicated by their helicitic inclusion trails. These trails are defined by the elongation of the inclusion grains in an orientation that is at an angle to the pervasive schistosity. These garnets tend to be wrapped around by the foliation. In general the garnets tend to be approximately 1.3 mm to 2.1 mm in diameter. Inclusions within the garnets are usually about the same size as the matrix material and have low energy shapes.

Accessory minerals within the phyllite include small grains of tourmaline, 0.04 mm in size, which may be zoned with brown centers and olive rims or olive centers and brown rims. These rounded to idioblastic grains occur scattered throughout the rock or in specific horizons with both the micas and the quartz and feldspar. Opaque minerals (mainly ilmenite) occur as grains approximately 0.5 mm in size and irregular to round in shape. Apatite occurs in very tiny amounts within the matrix and can often be recognized by its grain shape.

It should be noted that the lowest metamorphic grade phyllite contained no biotite but did contain garnets with rotated inclusion trails and showed signs of retrogression to chlorite. The lack of biotite may be a reflection of the bulk composition of the rock or it may be below the biotite isograd for a given event later than that which produced the garnet.

Psammite:

The psammite of unit 1 contains a higher total percentage of quartz and feldspar, and lower percentage of micaceous minerals compared to the phyllite. The micaceous minerals, which include muscovite, chlorite, and biotite in order of abundance, account for only 8 to 18 percent of the total rock. The psammite characteristically contains porphyroclasts of quartz and feldspar that are enclosed by the schistosity. These grains are ellipsoidal in shape with the long axis parallel to the schistosity. The porphyroclast generally consists of one large central grain with irregularly shaped subgrains along the sides and in its "shadows", Figure 3.4.

Biotite within the psammite, as in the phyllite, is brown in color and contains zircons. Biotite sheaths are generally about 0.03 mm wide and may show retrograde alteration to chlorite along grain boundaries. Other samples show chlorite prograding to biotite, but generally the two phases appear to be quite stable in each others presence. Fine needles of muscovite occur with the biotite and chlorite, aiding in defining the weak foliation.

The garnets of the psammite, which account for less than 1 percent of the total rock are almandine, and are rounded in shape and fractured. Because they are rare in this lithology, relation to the foliation is difficult to determine, however they appear to be pre- or early syntectonic with respect to the pervasive schistosity.

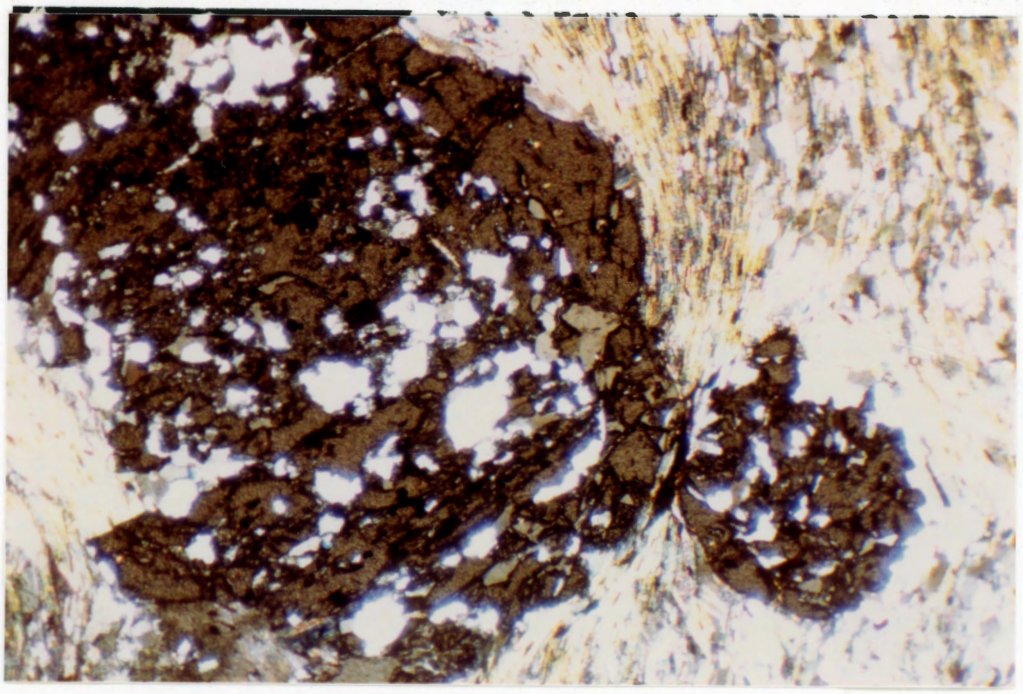

Figure 3.3. Snowball garnets showing the snowball inclusion trails which develop as the garnet rotates, in response to the stress that produced the schistosity (crossed polars, x 31.25).

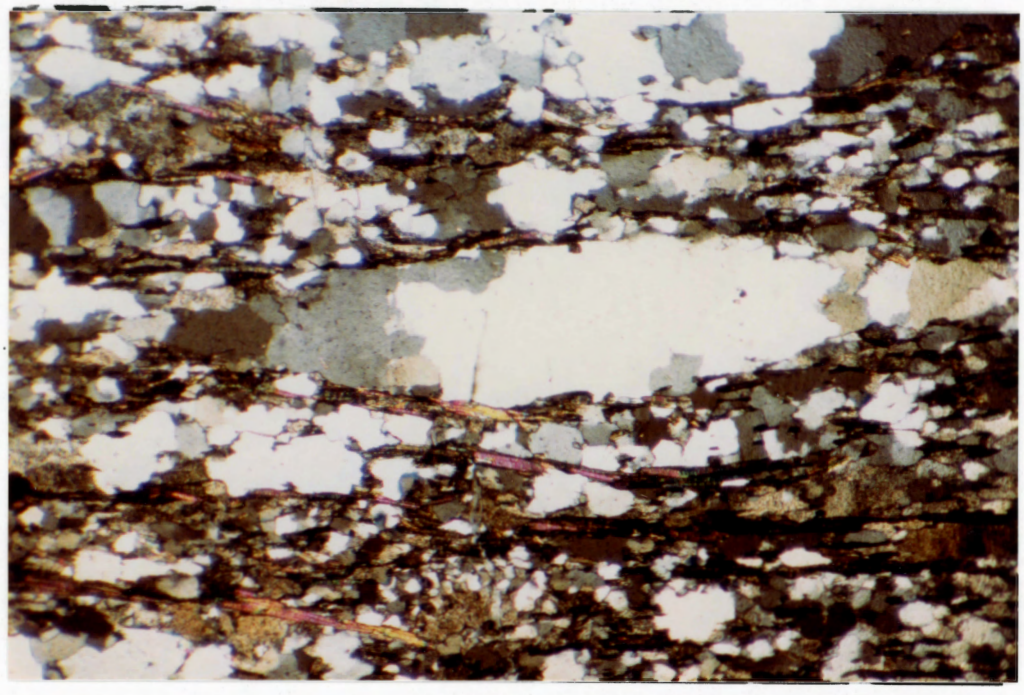

Figure 3.4. Quartz porphyroclast within the psammite of Unit 1. Note the large central grain and subgrain development near the apices of the ellipsoid. The central grain and subgrains are all wrapped around by the pervasive schistosity. The irregular grain boundaries infer textural disequilibrium (crossed polars, x 31.25).

Accessory minerals within the psammite include apatite occurring as small round grains (approximately 0.08 mm in diameter), accounting for much less than 1 percent of the total rock. Opaque minerals account for approximately 2 percent of the rock.

Sericitization of the feldspar is not extensive within the psammite however some grains are preferentially altered while others are fresh. This could be a reflection of the different types of feldspars present.

Semi-Pelite:

The semi-pelite of Unit 1 has a mineralogical composition and texture, intermediate of the mineralogy and texture of the phyllite and psammite, with a higher total percentage of micaceous minerals compared to the phyllite. Grain sizes are similar to those found within the psammite and phyllite and grains show well developed granoblastic polygonal textures.

Almandine garnets from sample 139 are porphyroblastic, poikiloblastic, rounded and are interpreted to be syn-tectonic. Inclusions within the garnet include matrix material (quartz and feldspar) which is approximately the same size as the present matrix grains. Garnets from sample 145 are extremely broken up and stretched parallel to the orientation of the schistosity (Figure 3.5). Many of these garnets are altered to chlorite and a red mineral (possibly hematite). The severely broken nature of the garnets may be due to local shearing within the immediate area from which the sample was taken. This specific sample contains bimodal grain size of the matrix material,

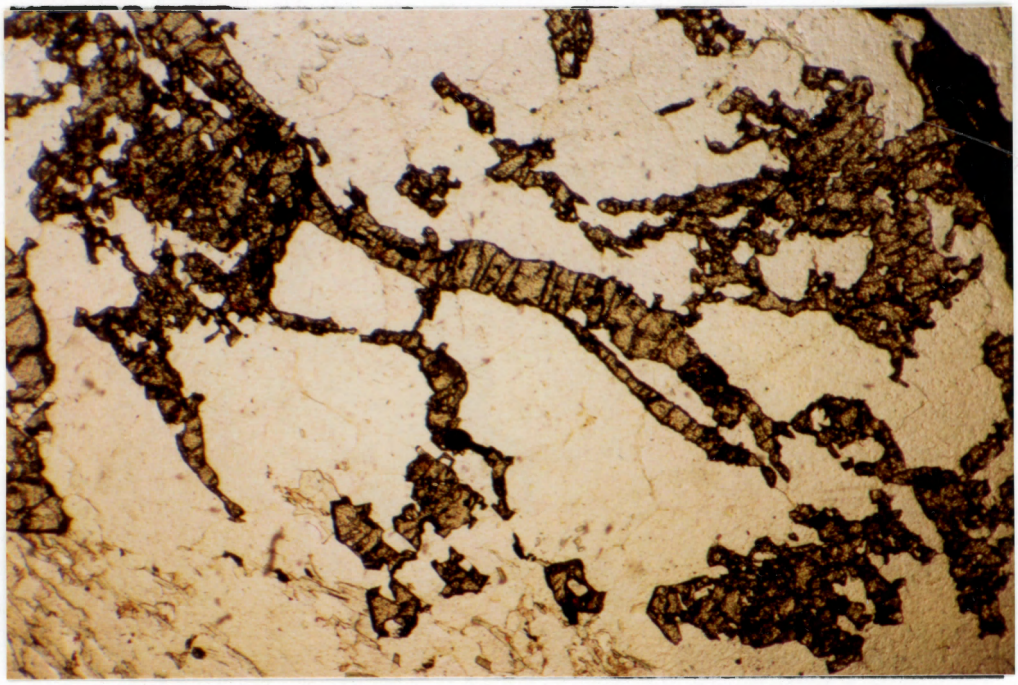

Figure 3.5. Severely broken apart garnet indicating that its growth was pre-tectonic to the pervasive schistosity and that it was broken apart by the stresses that developed the schistosity (plane polarized light, x 31.25).

and this biomodal grain size appears to be typical of samples taken from locations of shearing. The mineral assemblage appears to be in equilibrium.

Accessory minerals within the semi-pelite are the same as those within the psammite and phyllite of Unit 1.

3.2.2 Metasedimentary Unit 2

Phyllite:

Compositional layering, approximately 1.5 centimeters thick, consists of alternating layers of quartz and feldspar with layers of micaceous minerals. All of the phyllitic samples have basically the same mineralogy except for the presence of key metamorphic index minerals. Mineralogically they consist of a matrix of quartz and feldspar, muscovite, biotite, $\pm$ chlorite, garnet, $\pm$ staurolite. Quartz and feldspar account for approximately 50 to 60 percent of the rock, occurring as polygonal grains 0.05 mm to 0.08 mm in size. The pervasive foliation of the rock is a well defined schistosity. In these phyllites, muscovite accounts for approximately 90 percent of the micaceous minerals. The parallel alignment of chlorite and biotite aid in defining the schistosity.

One of the more characteristic features of the phyllite of Unit 2 is the development of porphyroblastic, poikiloblastic biotite flakes. Sample 31 marks the first development of these biotites. These porphyroblasts may be up to 4.5 mm in size, however average sizes are between

0.2 mm to 0.5 mm in diameter. They account for between 8 and 18 percent of the total rock. The percentage of porphyroblasts tends to increase with increasing metamorphic grade. Inclusions include low energy shaped quartz and feldspar, slightly smaller in size than the matrix material. These porphyroblastic biotites are interpreted to be pre- to early syn-tectonic with respect to the pervasive schistosity; as they occur with their long diagonal axis oriented parallel to the schistosity (Figure 3.6 a, b). Their skeletal growth indicates that they had not reached textural equilibrium. Because the grains are not fractured or broken up, it is believed that they grew during the stages of deformation that developed the pervasive schistosity. Some biotites cross-cut the schistosity, and some are randomly oriented kinked grains.

All of the samples studied contained porphyroblastic, poikiloblastic garnet. Garnets from sample 31 contain poikiloblastic cores and non-poikiloblastic rims (Figure 3.7). Grains are generally idioblastic to subidioblastic and contain very tiny inclusions approximately 0.006 mm in size which cannot be optically identified. These inclusions are considerably smaller than the grain size of the present matrix. Many of the inclusions are aligned with their long axes at an angle to the present pervasive schistosity. The alignment of the inclusions in these helicitic grains may be interpreted to represent a relict foliation and the smaller grain size may indicate that the matrix grain size before the formation of the porphyroblast was smaller than the grain size of the matrix after its formation (Spry, 1979), (Figures, 3.7, 3.9). Sample 36a on the other hand, contains porphyroblastic, poikiloblastic garnets, rounded to subidioblastic in shape, that contain inclusions

(a)

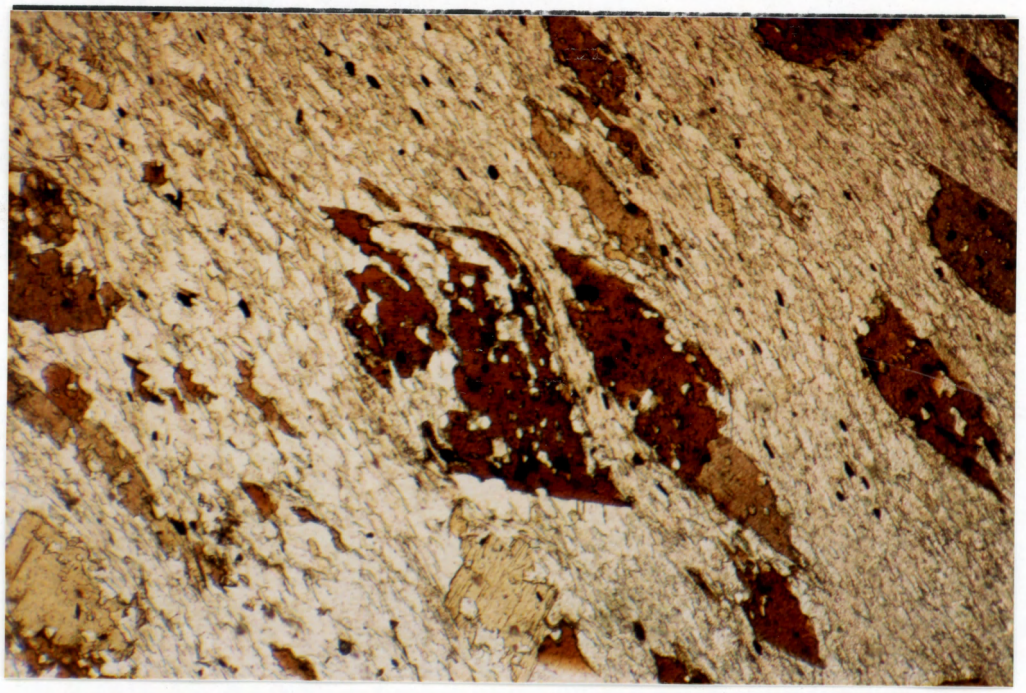

(b)

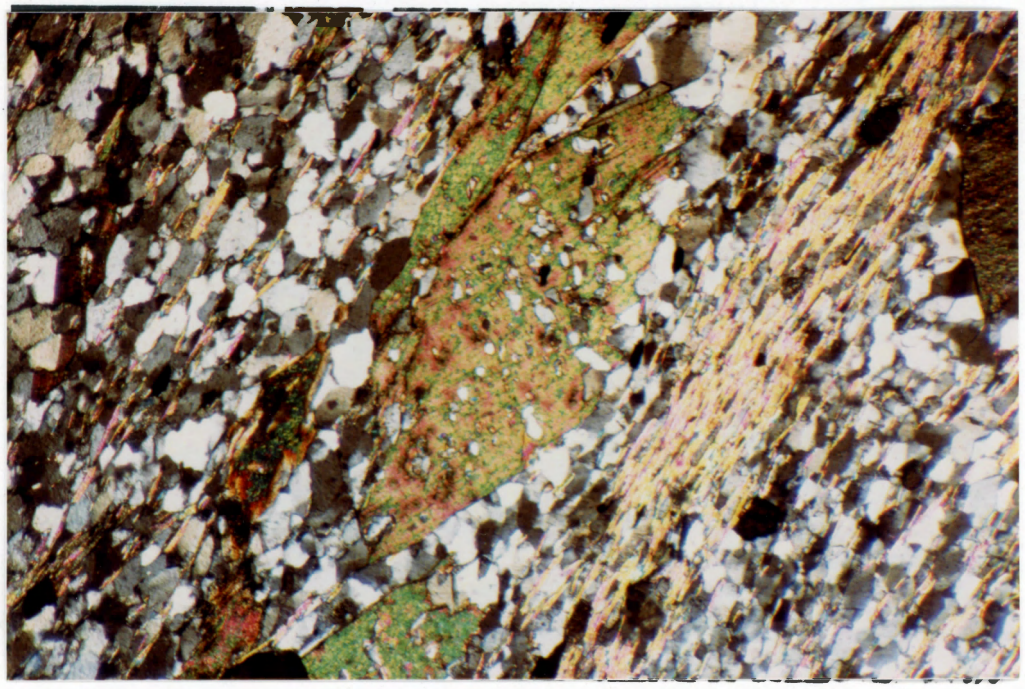

Figure 3.6 a, b. Porphyroblastic and poikiloblastic biotite oriented with the long diagonal axis parallel to the pervasive schistosity, indicating that the grain grew either before the schistosity developed or grew in the early stages of schistosity development and was rotated into its present orientation. (a - taken in plane polarized light; b - taken in crossed polars; x 31.25).

of quartz and feldspar that are elongate parallel to the present pervasive foliation. These inclusions are approximately the same size as the present matrix material. The highest grade phyllite (Sample 81) contains rounded, porphyroblastic, poikiloblastic garnets with inclusions of quartz, feldspar, minor micas and opaques, which are slightly smaller in size than the present matrix material (Figure 3.8). The difference in the size and the orientation of the inclusions within sample 31 compared to samples 36a and 81 suggest that there may be two generations of garnets; one containing a relict foliation and one which grew during the formation of the present foliation.

Porphyroblastic and poikiloblastic staurolite occurs in the highest grade phyllite near the top of French Mountain. The staurolite is up to 1 cm in size and is highly poikiloblastic, engulfing matrix material as it grew. Inclusions within the staurolite include quartz, feldspar, tourmaline, opaques, micas and garnet. The staurolite has been interpreted in this study to be syn- to post-tectonic with respect to the pervasive foliation of the rock. Figure 3.10 shows a slightly rotated staurolite and its highly poikiloblastic nature. The staurolite shows limited alteration to chlorite.

From microprobe analysis much of the feldspar is believed to be plagioclase. Sample 39 contains feldspar that is compositionally zoned.

Accessory minerals within the phyllite include small olive tourmaline grains, approximately 0.04 mm in size which account for less

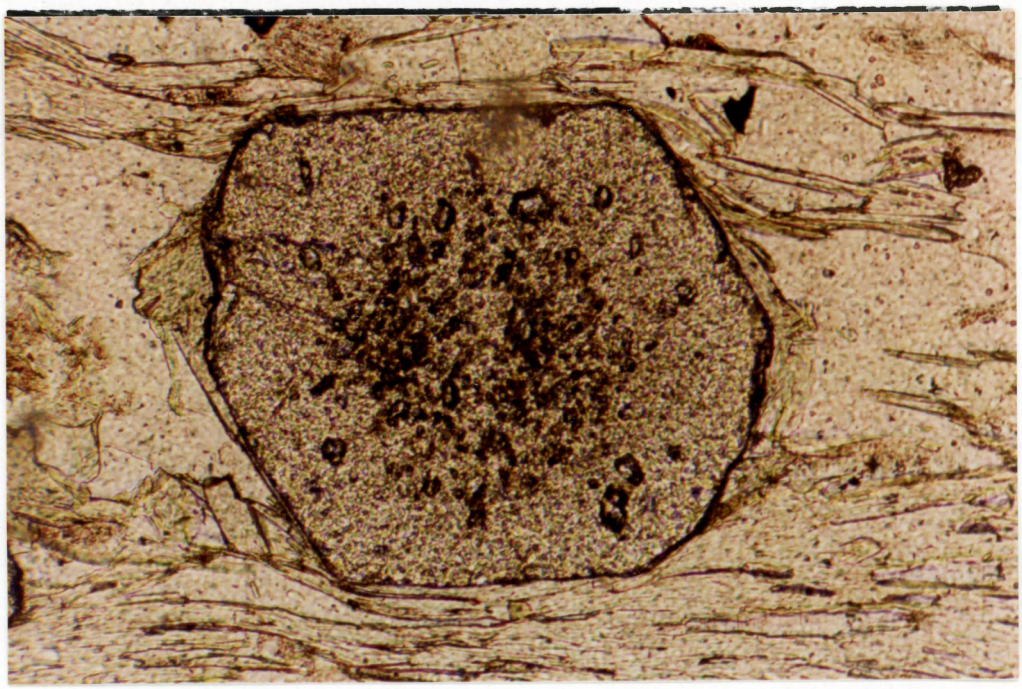

Figure 3.7. Porphyroblastic garnet with poikiloblastic core and non-poikiloblastic rim. Such a texture may indicate two phases of growth or just a "slowing down" of the growth rate of the grain. (plane polarized light, x 125).

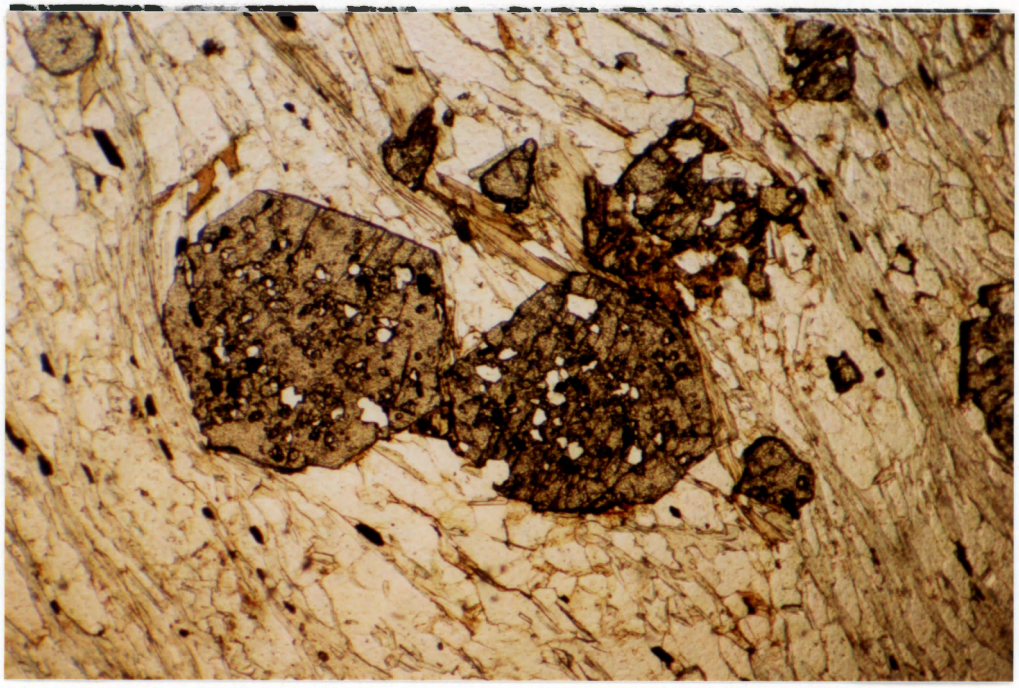

Figure 3.8. Porphyroblastic, poikiloblastic garnet of sample 81. (plane polarized light, x 31.25).

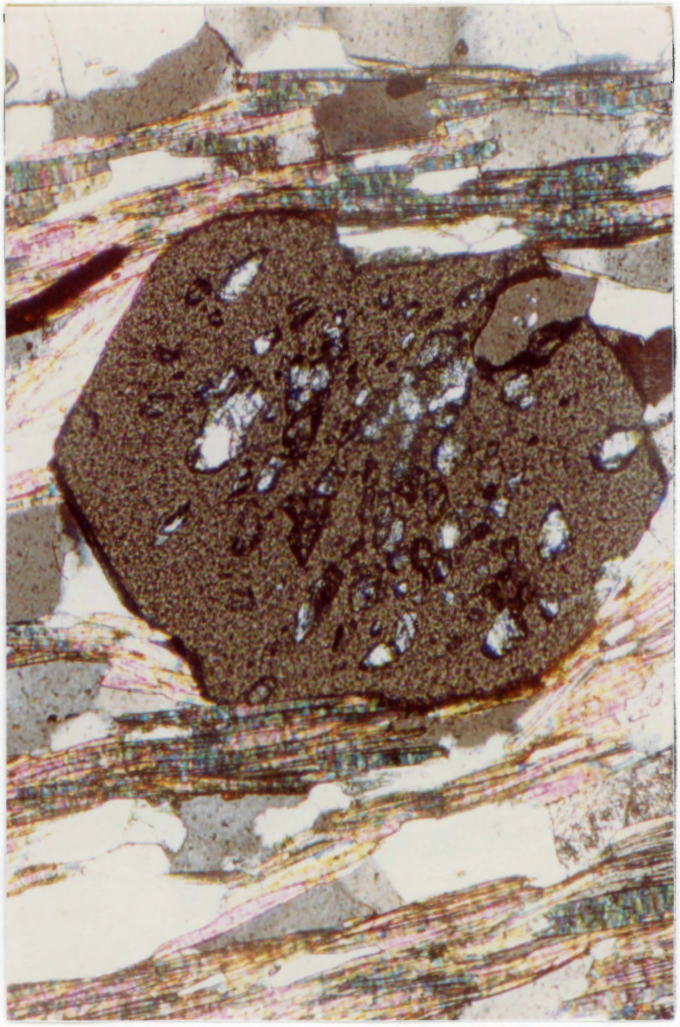

Figure 3.9. Porphyroblastic, poikiloblastic garnet showing the alignment of inclusions at an angle to the main schistosity, indicating that the alignment may be a relict fabric. (crossed polars, x 31.25).

than 1 percent of the rock; opaque minerals, and one tiny grain of fibrolitic sillimanite found in sample 81. This fibrolite was too small to be clearly identified optically and this was the only sample studied that contained any sillimanite.

Psammite:

The psammite of Unit 2 characteristically contains fine idioblastic hornblende. Mineralogically the rock consists of quartz, feldspar, ± hornblende, ± garnet, ± biotite, ± chlorite, ± muscovite. Matrix material accounts for approximately 55 to 75 percent of the rock and consists of granoblastic polygonal quartz and feldspar, approximately 0.04 mm in size. Some of the feldspar grains are zoned and many are believed to be plagioclase because of the presence of albite. twinning.

Typically the psammite lacks a well developed foliation because of the low percentage of micaceous minerals. The psammite consists of horizons rich in micaceous minerals alternating with horizons rich in quartz and feldspar. These horizons are centimeters thick and have sharp boundaries. Sample 37.5 clearly shows these horizons, and shows that biotite is not present in the hornblende-rich horizons and hornblende is not present in the biotite-rich horizons. The schistosity defined by the alignment of micaceous minerals varies in the type of micaceous mineral between samples. Sample 37.5 contains bimodal matrix grain sizes in the hornblende horizon with grains approximately 0.03 mm and 0.08 mm in size. Some samples (example 41) contain porphyroclasts of quartz and feldspar, 0.5 mm in size and similar to the porphyroclasts

of Unit 1. Within the mica-rich horizons garnets from 0.16 mm to 1.1 mm in size may occur.

The hornblende of the psammite occurs as idioblastic, moderately poikiloblastic (containing matrix material) grains in random orientations (Figure 3.11). The hornblende is always concentrated around the outer edges of veins containing feldspar, epidote and zoisite. Mineralogically these veins contain approximately 55 percent feldspar, 30 percent quartz, 25 percent epidote and zoisite, 10 percent hornblende and 1 percent opaque minerals. The feldspar is mainly plagioclase with minor amounts of microcline and grain size is generally 0.45 mm to 1.1 mm in diameter. The epidote and zoisite occur as small round grains generally growing perpendicular to the inner side of the vein wall. The hornblende which is concentrated near to the outer vein wall is generally euhedral/idioblastic. Within the vein, hornblende, epidote and zoisite tend to grow preferentially where the feldspar is most heavily sericitized, and because of the high degree of alteration in these areas of the vein, it is difficult to determine whether the hornblende, epidote and zoisite are replacing the feldspar or vice versa. From this study it appears that these veins represent solutions that moved through the rock and reacted with minerals usually found within minor phyllitic horizons within the psammite, to produce the hornblende. One possible reaction is given below:

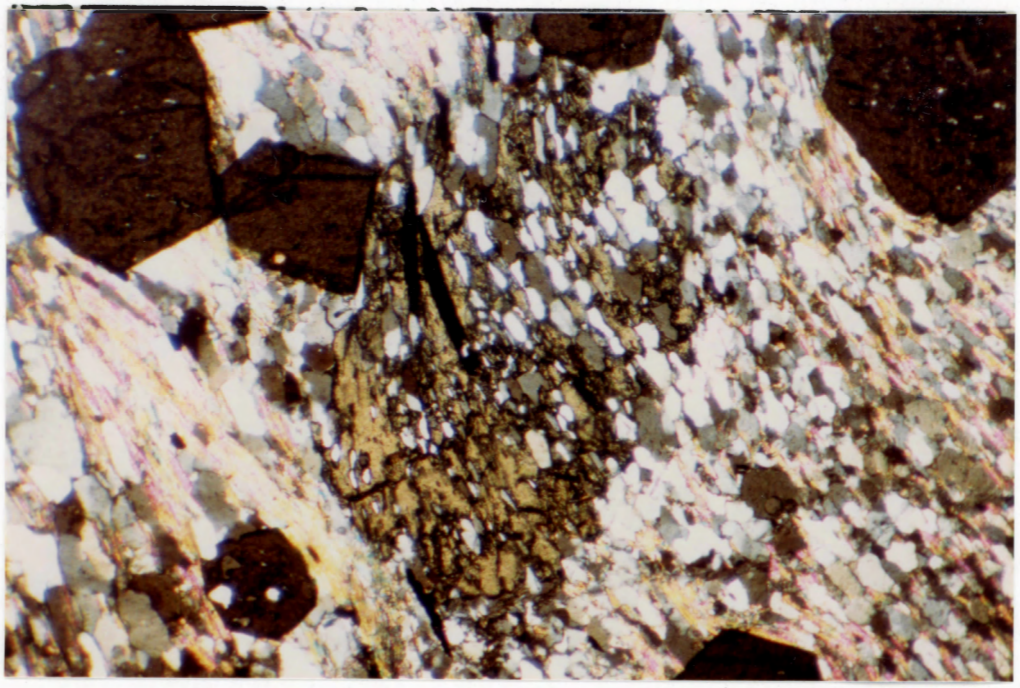

Figure 3.10. Highly poikiloblastic staurolite porphyroblast in the phyllite of Unit 2. The continuous trails of matrix material through the grain suggest that the grain was syn- to post-tectonic with respect to the pervasive foliation (crossed polars, x 31.25).

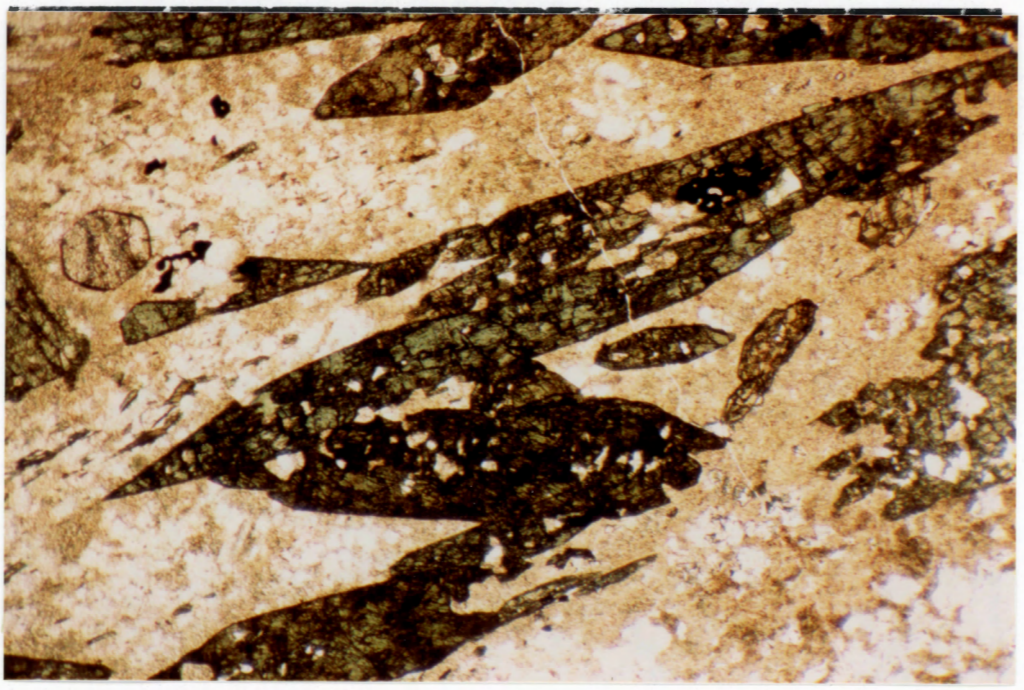

Figure 3.11. Idioblastic, poikiloblastic, hornblende porphyroblasts within the psammite of Unit 2. (crossed polars, x 31.25).

$$3(Mg, Fe)_{10}Al_2Si_6Al_2O_{20}(OH)_{16} + 12Ca_2AlSi_3O_{12}(OH) + SiO_2 =$$

(chlorite) (epidote) (quartz)

$$10Ca_2(Mg, Fe)_3 Al_2(Al_2Si_6)O_{22} (OH)_2 + 4CaAl_2Si_2O_8 + 20H_2O$$

(tschermakitic hornblende) (anorthite)

(Nockolds et al. 1979)

Although this reaction may not be the exact reaction that took place, it does serve to show how perferential growth of the hornblende within the minor phyllitic layers can occur. Because of the general lack of biotite in areas where the hornblende is concentrated, it is more likely that biotite was involved in a similar type of reaction.

Hornblende-rich psammite is distinguished from amphibolite on the basis of the percentage of hornblende in the rock. It has arbitrarily been chosen in this study that a rock with less than 20 percent hornblende is a hornblende-rich psammite.

Locally within the minor phyllitic layers within the psammite porphyroblastic garnet overprints the schistosity, and are interpreted to be post-tectonic to the schistosity.

Accessory minerals of the psammite include apatite and epidote as well as opaque minerals.

Semi-pelite:

The semi-pelite of Unit 2 is intermediate mineralogically between the phyllite and psammite, however this lithology does not contain

hornblende. Some samples contain bimodal grain sizes and a poorly developed schistosity defined by the parallel alignment of tiny biotite and muscovite sheaths. Porphyroblastic and poikiloblastic garnet, 1.1 mm by 0.8 mm in size, have irregular grain boundaries and appear to be quite altered giving them a yellowish brown stain. These garnets may be retrograding to biotite, however this alteration product could not be clearly determined optically.

Accessory minerals are the same as those found within the phyllite and psammite of Unit 2.

3.3 COMPOSITE GNEISS COMPLEX

3.3.1 Biotite-Quartz-Feldspar Gneiss

Mineralogically the gneiss consists of various amounts of biotite, muscovite, quartz, feldspar $\pm$ chlorite $\pm$ garnet $\pm$ kyanite $\pm$ staurolite.

The matrix material consisting of quartz and feldspar, accounts for approximately 50 percent of the rock, however quartz and feldspar may account for as high as 85 percent and as low as 35 percent. Matrix material occurs as irregularly shaped grains about 0.5 mm in size (up to 1.1 mm) with lobate grain boundaries. Feldspar is mainly plagioclase with minor microcline. Myrmekitic texture, although rare is present in a few samples and some grains are chemically zoned. The degree of sericitization of feldspar varies significantly between samples.

Biotite within the gneiss varies from 10 to 35 percent of the total rock. It occurs as "fresh" sheaths 0.5 mm by 0.1 mm to 2.9 mm by 0.2 mm in size defining the schistosity of the rock. The deep red color of many grains reflects the relatively high titanium content (Deer, et al., 1980). Samples 99, 102 and 103 contain green biotite which is a reflection of the +2 oxidation state of the iron within the mineral.

Muscovite occurs as "fresh", well developed sheaths, 0.33 mm by 0.5 mm to 2.3 mm by 0.3 mm in size that often show a pale pink to pale green pleochroism. It accounts for between 1 and 25 percent of the rock and aids in defining the schistosity of the rock.

Chlorite is rare in the gneiss and was only found in sample 63b where it accounts for less than 1 percent of the rock. In this sample biotite is altering to chlorite.

Garnet occurs as poikiloblastic or non-poikiloblastic porphyroblasts interpreted to be pre- to early syn-tectonic with respect to the schistosity. Sample 57b contains garnets with poikiloblastic cores and non-poikiloblastic rims. From petrological study it appears that the garnets within the gneiss complex became elongated and more deformed toward the north and east. Sample 103 contains garnets that are severely broken up, irregular and elongated parallel to the schistosity. Grain sizes range from 3.8 mm to 0.18 mm in diameter. Sample 93 contains garnets with inclusions elongate at an angle to the present pervasive schistosity, and which may represent an earlier relict fabric (Figure 3.12).

Kyanite was identified in sample 57b occurring as elongate fractured grains parallel to the schistosity of the rock. It is retrograding to muscovite with very minor biotite and appears to be pretectonic because of its highly fractured nature (Figure 3.13). This sample also contained a small amount of staurolite occurring as altered grains 0.2 mm in size. Kyanite is preferentially located within the muscovite-rich horizons of the rock.

Accessory minerals include tourmaline, occuring as idioblastic grains 0.2 mm by 0.5 mm in size, and accounting for up to 3 percent of the rock; apatite and opaque minerals which account for less than 1 percent of the rock.

The mineralogy of the gneiss is basically the same as the metasedimentary complex except for the presence of key metamorphic index minerals such as kyanite. However, the average grain size of the gneiss is typically larger.

3.3.2 Amphibolite Gneiss

The amphibolite gneiss consists of approximately 45 percent hornblende, 50 percent feldspar, and 5 percent sphene. Hornblende occurs as dark green, irregularly shaped grains that are aligned with their long axes parallel, defining a foliation. Hornblende averages 0.5 mm in size but grains up to 3 mm in size may occur. Feldspar generally occurs as non-descript, irregularly shaped grains approximately 0.55 mm in size. Preferential sericitization of feldspar grains indicates

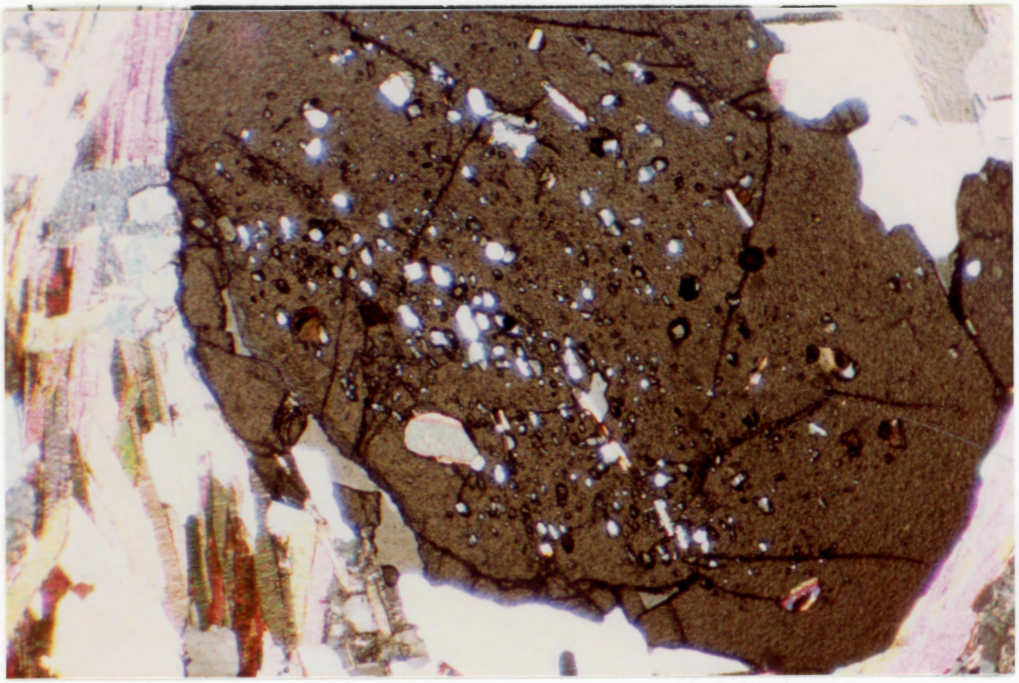

Figure 3.12. Inclusions of quartz, feldspar, and micas elongated at an angle to the pervasive schistosity and which may represent a relict fabric (crossed polars, x 31.25).

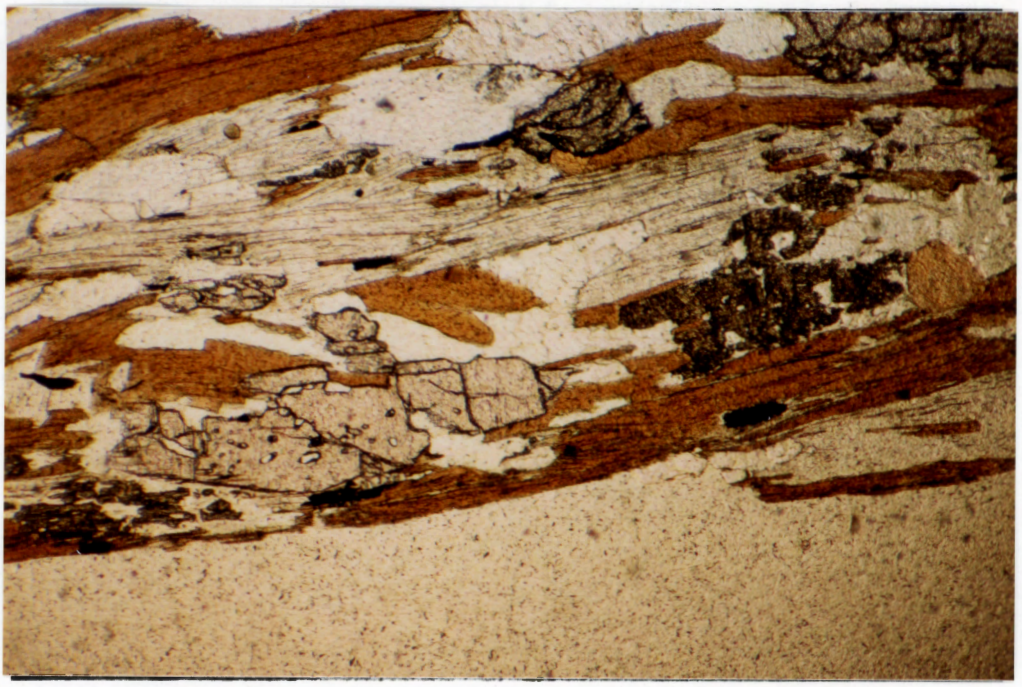

Figure 3.13. Pre-tectonic kyanite in the biotite-quartz-feldspar gneiss, fractured and elongated parallel to the schistosity. (plane polarized light, x 31.25).

different types of feldspars are present. Sphene occurs as ellipsoidal grains approximately 0.16 mm to 0.06 mm in size (Figure 3.14).

Accessory minerals include epidote (pistacite) and pyrite which occurs in cubes approximately 1.5 mm in size. Sample 89 contains epidote rimming small grains that may possibly be apatite although they could not be optically identified. Sample 89 also contains a small amount of highly fractured clinopyroxene along the boundary of the feldspar-rich layers with the hornblende-rich layers. A small amount of biotite was noted in this sample and although garnet was not observed in thin section it was noted in hand sample.

The amphibolite gneiss is distinguished from the amphibolite by its felsic layers approximately 1 centimeter thick which consist of plagioclase, potassic feldspar $\pm$ quartz.

3.3.3 Potassic Feldspar Augen Gneiss

This unit was not studied optically because of its large grain size and time limitations. From hand specimen the augen gneiss consists of large potassic feldspar porphyroclasts up to 1.5 cm by 2.5 cm in size, that characteristically show core and mantle texture. These are wrapped around by a schistosity defined by the alignment of biotite and muscovite. The porphyroclasts are interpreted to be pre-tectonic with respect to the present foliation. Percentages of minerals vary considerably between samples.

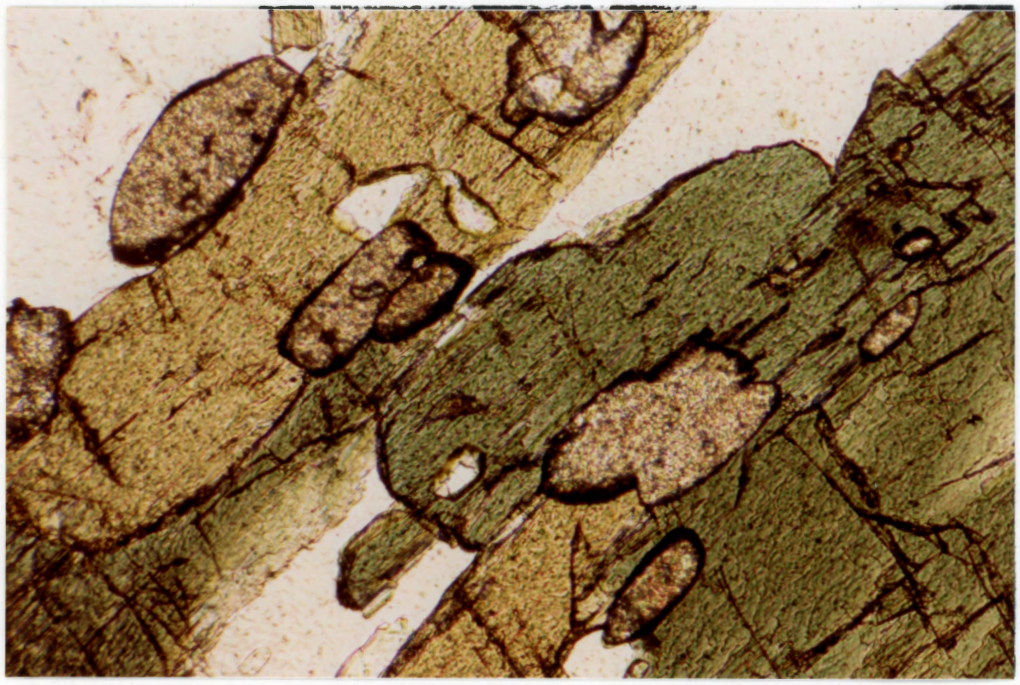

Figure 3.14. Ellipsoidal sphene elongate parallel to the orientation of the hornblende in the amphibolite gneiss (plane polarized light, x 125).

3.4 AMPHIBOLITE

Amphibolite outcrops near the top of French Mountain along the Cabot Trail, near to the intersection with the Fire Tower Road. Hornblende accounts for approximately 40 to 50 percent of the rock and occurs as green porphyroblastic, poikiloblastic grains with irregular to serrated edges, approximately 3.2 mm by 6.5 mm in size.

Feldspar accounting for approximately 42 percent of the rock, occurs as highly sericitized grains which are zoned with oligoclase cores and andesine rims (refer to probe analysis). Grains are approximately 0.1 mm in size and some grains are almost completely obliterated by sericite.

Biotite occurs as altered non-poikiloblastic, patchy, flakes, 0.4 mm by 0.5 mm in size, that occur near to the hornblende. Fine biotite sheaths define a very weak foliation and account for approximately 8 percent of the rock.

Sphene occurs in aggregates surrounding the irregularly shaped rutile which occurs as grains 0.02 mm in size. It appears that the sphene is an alteration product of the rutile.

A small amount of calcite occurring as irregularly shaped grains, 0.32 mm in size was observed in sample 153. This accounts for less than 1 percent of the rock and was found in only one area of the thin section.

Proportions of minerals change significantly between samples and

sample 148d contains as much as 15 percent epidote occuring as aggregates approximately 0.3 mm in size. Opaques form large euhedral to hexagonal grains that are most likely pyrite. It is unclear whether this amphibolite is an ortho- or para-amphibolite.

3.5 DIORITE

Diorite outcrops in two localities 1) on top of French Mountain near French Lake and 2) along the most western extent of the Skyline Trail.

Sample 96 from location (1) consists of 45 percent hornblende, 55 percent plagioclase feldspar and 1 percent sphene. Sample 97 consists of 30 percent hornblende, 14 percent biotite and 55 percent plagioclase feldspar with minor quartz, epidote and chlorite. The hornblende of this diorite occurs as irregularly shaped, sometimes poikiloblastic grains 1.0 to 1.5 mm in size. Sphene occurs as an alteration product of rutile which occurs as small irregular grains. Feldspar is almost all plagioclase occurring as highly sericitized grains approximately 1.0 mm to 0.32 mm in size. Biotite occurs as non-poikiloblastic grains 0.38 mm by 1.3 mm in size, showing limited alteration to chlorite. Accessory minerals include epidote and clinozoicite. A pale purple mineral was observed in hand specimen and believed to be fluorite however no fluorite or other anomalous mineral was found in the thin section.

Samples taken from location(2) contain xenoliths of a hornblende-rich rock finer grained than the diorite. The xenoliths are centimeters in

diameter and contain approximately 40 percent hornblende, 10 percent biotite, 47 percent feldspar and 3 percent epidote. The hornblende occurs as irregular grains averaging 0.32 mm in size or occurs as aggregates about 1.5 mm in size. Biotite occurs as brown flaky grains approximately 0.32 mm in size and the feldspar occurs as irregular grains, 0.33 mm in size. There is no preferred orientation or foliation evident within the xenolith.

The host diorite contains approximately 30 percent irregularly shaped hornblende, 1.0 mm in size and somewhat altered. The alteration product could not be optically identified. Biotite accounts for approximately 5 percent of the rock occurring as broken flakes approximately 0.1 mm in size. It characteristically occurs in "clumps" with the hornblende. Epidote occurs as small rounded to euhedral grains accounting for approximately 4 percent of the rock. Much of the epidote is believed to be clinozoicite. Plagioclase occurs as irregular to euhedral grains with preferential sericitization in the cores of the grains indicating a chemical zoning of the grains. Rutile occurs as small irregular patches, approximately 0.3 mm in size, altering to sphene.

36 JUMPING BROOK GRANITOID

The Jumping Brook Granitoid exposed along the northern wall of the Jumping Brook Canyon is undeformed at the top but becomes progressively foliated, crenulated and sheared toward the base. Mineralogically the Granitoid consists of 30 percent quartz, 50 percent feldspar, 8 percent

biotite, 3 percent chlorite and 9 percent epidote.

Green biotite occurs as randomly oriented broken flakes 0.3 mm by 0.5 mm in size, showing limited alteration to chlorite. Feldspar consists mainly of plagioclase, however microcline was observed, and quartz occurs as irregular grains with the feldspar. Epidote (pistacite), 0.32 mm by 0.13 mm in size tends to occur in the more sericitized parts of the rock forming aggregates or long linear trails, that account for approximately 8 percent of the rock (Figure 3.15).

Traversing down the cliff, the chlorite content increases as the biotite alters to chlorite and the grain size becomes bimodal part-way down the cliff to unimodal near the base. This unimodal grain size is smaller than the grain size found at the top or partway down the cliff. Aggregates of unaltered feldspar become elongated and aggregates of epidote form linear trails. A fabric defined by the alignment of biotite, chlorite, and trails of epidote is crenulated and folded toward the lower eastern part of the exposure (Figure 3.16).

Minor minerals within the Granitoid include small grains of tourmaline and apatite.

3.7 DEFORMATION AND METAMORPHISM RELATIONSHIPS

The relationship between deformation and metamorphism in the rocks of French Mountain was studied through petrological observation of the relationship between metamorphic index minerals and the fabric of the rock. Porphyroblast-matrix microstructural relationships in deformed

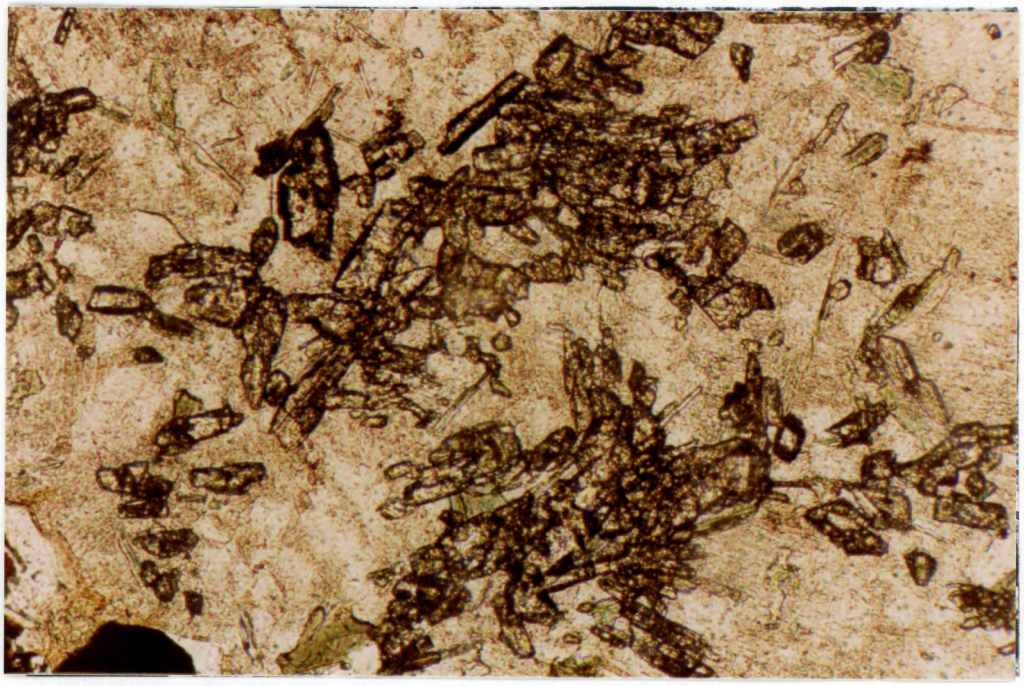

Figure 3.15. Epidote occuring in aggregates within the Jumping Brook Granitoid (plane polarized light, x 125).

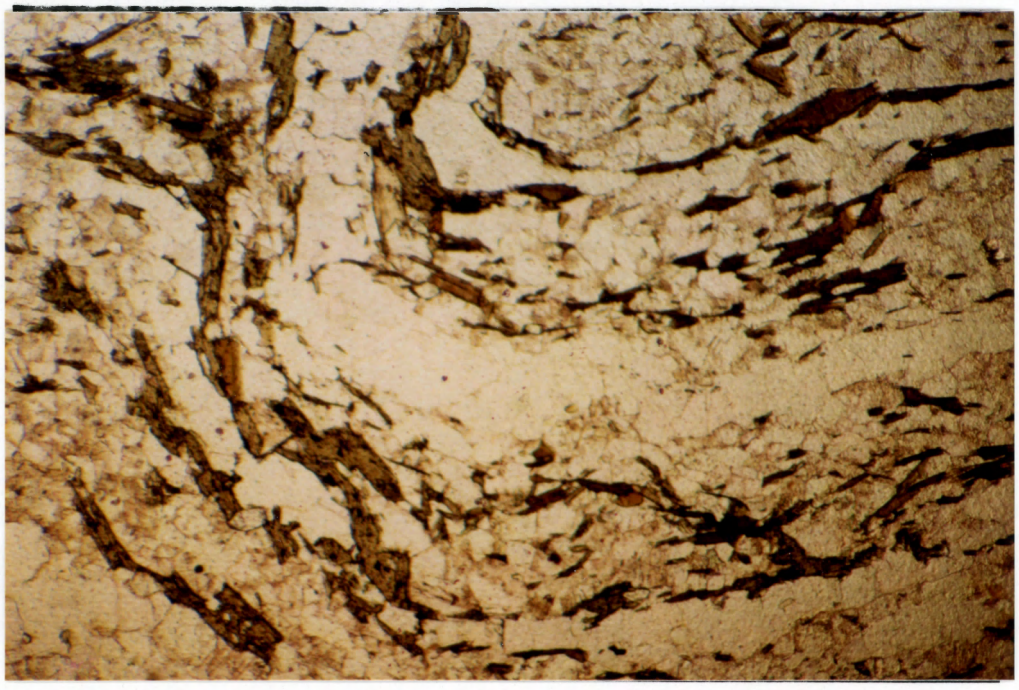

Figure 3.16. Crenulations of the fabric defined by the parallel alignment of biotite, chlorite and epidote in the Jumping Brook Granitoid (plane polarized light, x 31.25).

metamorphic rocks have been used for inferring relative time relationships between metamorphism and deformation, however, according to Vernon (1978) much of the criteria used in determining such relationships is equivocal. Although, often certain porphyroblast-matrix microstructural relations may have more than one interpretation with respect to the relation between metamorphism and deformation, the key metamorphic index minerals and their relation to the fabric of the rock in the French Mountain area were carefully studied and possible interpretations are given.

In order to classify index minerals as pre-, syn- or post-tectonic with respect to the pervasive foliation in the rock the criteria listed in Table 3.2 were used.

Time relationships between growth of the porphyroblast and deformation included the study of relations between margins of the porphyroblast and the pervasive foliation, relations between an internal foliation and the pervasive foliation, and zonation within the porphyroblast.

A summary of the porphyroblast-matrix microstructural relations for the rocks of the French Mountain area, determined in this study, is given in Table 3.3. A broad view of Table 3.3 shows that most of the porphyroblasts are syn-tectonic to their respective pervasive schistosity.

Garnets of samples 138 and 145 are severely broken apart and show alteration to chlorite (Figure 3.5). Although the garnets may be interpreted as being pre-tectonic to (Sem) it is more likely that these rocks were affected by the shear zone that runs diagonally down the north

*Pre-tectonic	Syn-tectonic	Post-tectonic
grain is severely broken and fractured	grain slightly fractured or not fractured	grain clearly overprints the foliation, and grains defining the foliation abut against grain boundary
grain is clearly wrapped around by foliation	inclusions swing into the rotating grain from the matrix	
inclusions within grain are discordant with pervasive foliation		
	grain elongated in direction of foliation, but not highly fractured	inclusions concordant with the matrix

* all relationships are with respect to the pervasive foliation

Table 3.2. Criteria used to determine the relationship between metamorphic index minerals and the deformation that produced the pervasive foliation.

Table 3.3. Summary of the porphyroblast-matrix relationships within the Metasedimentary Complex and Gneiss Complex and the criteria used in making the interpretation.

Sem = pervasive schistosity within the Metasedimentary Complex
Sim = internal and possible relict fabric in minerals within the Metasedimentary Complex
Seg = pervasive schistosity within the Gneiss Complex
Sig = internal and possible relict fabric in minerals within the Gneiss Complex

Table 3.3

Sample	138	145	139	12	24	31
porphyroblast	garnet	garnet	garnet	garnet	garnet	garnet (polyphase growth)
relation of grain to pervasive foliation of rock (Se)	pre-tectonic	pre-tectonic	syn-tectonic	syn-tectonic	syn-tectonic	cores: possibly pre-tectonic
criteria used	grains severely broken up and elongate in shape // to (Sem) grains are wrapped by (Sem)	grains severely broken up and elongate in shape // to (Sem)	matrix material swinging into rotated grains	matrix material swinging into rotated grains	matrix material swinging into rotated grains	cores are poikiloblastic containing inclusions with elongate shapes defining a (Sim) ≠ (Sem) inclusions are smaller in size than present matrix material
porphyroblast	garnet			chlorite	chlorite	
relation of grain to (Se)	pre-early syn-tectonic			post-tectonic	post or late syn-tectonic	rims: syn to post-tectonic
criteria used	grains fractured but show rotation during growth "snowball texture"			grains overgrow the (Sem)	grains overgrow the (Sem) (Sem) abuts the grain boundaries	(Sem) appears to slightly abut the grain boundaries to gently wrap around the grain
porphyroblast						biotite
relation of grain to Se						syn-tectonic
criteria used						grains are generally rotated slightly so that their long diagonal axis is // to (Sem)
Reactions noted in thin section	garnet → chlorite biotite → chlorite	some: garnet → chlorite biotite → chlorite	some: biotite → chlorite	some: biotite → chlorite		

Table 3.3 (continued)

Sample	36a	38	39	143.5	142
porphyroblast	garnet	garnet	garnet	garnet (polyphase growth)	garnet
relation of grain to pervasive foliation of rock (Se)	syn-tectonic	pre- to syn-tectonic	?	cores: possibly pre-tectonic cores are poikiloblastic with inclusions elongate in shape. (Sim) ≠ (Sem) inclusions are ~ 30 times smaller than matrix grains	? poor development of Se does not enable determination of relation between (Se) and grain boundary
criteria used	(Sem) appears to be slightly abut to grain boundaries to gently wrapping around the grain	(Sem) is abutting to gently wrapping around the grains; grains are euhedral, with inclusions much smaller in size than matrix material	because of small percentage of micas, (Sem) is poorly developed and relation between (Se) and grain boundary could not be determined	rims: probably syn-tectonic with (Sem) grains are idioblastic with (Sem) slightly abutting to gently wrapping the grain	
porphyroblast	biotite	hornblende	biotite	garnet	
relation of grain to (Se)	syn-tectonic	post or late syn-tectonic	?	syn-tectonic	
criteria used	(Sem) slightly abut to gently wrapping around the grain	random orientation in a weakly developed (Sem). exact relation between (Se) and grain boundary could not be determined	because of poor development of (Sem) the relation of (Sem) to grain boundary could not be determined	grains are poikiloblastic with inclusions only 5 times smaller than matrix material and no (Sim) development	
porphyroblast			garnets (polyphase growth)	staurolite	
relation of grain to (Se)			cores: inclusions are random and only slightly smaller than matrix material	early syn-tectonic	
criteria used			rims: syn-tectonic non-poikiloblastic (Sem) is slightly abut to gently wrapping around grain	skeletal growth idioblastic grains which are slightly rotated with (Sem)	
Reactions noted in thin section	some ; biotite → chlorite				garnet → biotite biotite → chlorite

Table 3.3 (continued)

Sample	41	81	157	57b	93
porphyroblast	garnet	garnet	garnet	garnet	garnet (polyphase growth)
relation of grain to pervasive foliation of rock (Se)	syn to post tectonic	early syn-tectonic	? possibly pre	late syn or post-tectonic	cores: possibly pre-tectonic poikliobblastic cores with inclusions elongate in shape both (Sig) = (Seg) and (Sig) ≠ (Seg) inclusions generally much smaller than matrix material rims: pre to early syn-tectonic rims are poikiloblastic and (Seg) wraps around grains
criteria used	poikiloblastic grains contain inclusions that are the same size as matrix material and are concordant with (Sem) (Sim) = (Sem)	(Sem) slightly abut to gently wrapping around the grain, grains are idioblastic and poikiloblastic inclusions grain size is equal to grain size of matrix material. Some grains non poikiloblastic and idioblastic	because of poor development of (Sem), relation between (Sem) and grain boundary could not be determined. The grains are quite broken up	grains are rounded and cracked and (Seg) is abut the grain boundary	
porphyroblast	biotite	biotite		kyanite	
relation of grain to (Se)	syn-tectonic	syn to post-tectonic		pre-tectonic (?)	
criteria used	grains are slightly rotated so that the diagonal axis of the grain is parallel to (Sem)	grains are generally elongate in shape // to (Sem) however some over (Sem)		generally grains are severely fractured	
porphyroblast		staurolite		staurolite	
relation of grain to (Se)		last syn to post-tectonic		?	
criteria used		poikiloblastic grains have (Sem) abut the sides of grain however (Sem) can possibly be traced through grain		only one grain found in thin section. grains fairly broken up and altered	
Reactions noted in thin section		staurolite → chlorite	garnet → chlorite biotite → chlorite	kyanite → muscovite + minor biotite staurolite → chlorite	

side of the Jumping Brook Canyon. The snowball texture of some of these garnets (Figure 3.3) show that at least some were syn-tectonic to the pervasive schistosity. Whether or not the severely broken garnets are different from these and can be considered to be pre-tectonic to (Sem) is inconclusive from the petrological study. The garnets of samples 139, 12 and 24 are syn-tectonic to (Sem) as the matrix is observed to swing into the rotating grain (Figure 3.2).

The chlorite of sample 12 and 24 is believed to be post-tectonic to (Sem) as (Sem) was not deflected around the grain but impinges on its boundary. This criteria is disputed by those who believe that the porphyroblast is capable of deflecting (Sem) as it grows and those who believe the (Sem) can be truncated by demonstrable pre-(Sem) porphyroblasts or because of heterogeneous strain both impingement and deflection may occur within the same thin section (Vernon, 1978). Because chlorite is a phyllosilicate one would expect it to be aligned with (Sem) if it were pre- or syn-tectonic with respect to (Sem). Chlorite is not a highly resistent mineral to stress and one would not expect to see clear truncation of the (Sem) along its boundaries if it were pre-tectonic and so in this study it has been interpreted to post-tectonic.

Polyphase growth of the garnets within samples 31, 143.5 and 93 are characterized by poikiloblastic cores and non-poikiloblastic rims. The inclusions in all cases are smaller than the present size of the matrix material. Spry (1979) suggests that the smaller grain size may indicate that the grain size of the matrix was smaller during the growth

of that part of the crystal than after the formation of the rest of the porphyroblast. He does note however that isolated single-crystal inclusions smaller than the matrix material may simply be due to differential dissolution of the inclusions. The smaller inclusions are however, generally interpreted to imply that a coarsening of the matrix took place by the growth of matrix minerals continuing after the porphyroblast incorporated its inclusions (Vernon, 1978). Schoneveld (1977) proposes that inclusions within rotated garnets may be due to the incorporation of grains from the 'pressure shadows' and therefore may have no relation to the size of the surrounding matrix. The inclusions within the samples are elongated in one direction. This (Si) may represent a relict foliation in the rock (Spry, 1969). In this case the growth of the porphyroblast is so gradual that inclusions are incorporated without displacement (Sturt and Harris, 1961). Vernon (1978) has proposed that the inclusions may have changed their shape after incorporation, to minimize interfacial free energy; or that the alignment of the inclusions may be related to the crystal structure of the host. Because of the high symmetry of garnet one would not expect this to occur. Vernon (1978) describes how the orientation of the section taken can control the shapes of the inclusions as seen in two dimensions, if the inclusions are not spheroidal. Whether or not the alignment of inclusions represents a relict foliation remains unresolved from the petrological study.

Zonal variation of the inclusions in the porphyroblastic garnet has been used to interpret tectonic history (Vernon, 1978). Rast

(1958, p. 423) refers to a garnet with an inner zone containing inclusions which he infers to be syn-tectonic and an outer zone free of inclusions which he interprets to be post-tectonic to(Se), although it could equally be due to syn-tectonic growth of the garnet porphyroblast. Because(Se) in the rocks of French Mountain is slightly abutt to gently deflected around the outer non-poikiloblastic rim, the rim is believed to be syn to early post-tectonic with respect to the development of (Se).

Biotite within the Metasedimentary Complex is interpreted in this study to be early syn-tectonic with (Sem) as it is usually oriented with its diagonal axis parallel to (Sem) and it is not broken or fractured. Staurolite within samples 143.5 and 81 is considered to be late syn-tectonic or post-tectonic to (Sem) because it overgrows the schistosity and matrix grains can be traced through its grain.

The kyanite of sample 57b is interpreted to be pre-tectonic with respect to (Seg), because of its highly fractured nature (Figure 3.13). Minor amounts of highly altered staurolite in this sample were poikiloblastic, but relations to(Seg) could not be determined (Figure 3.17).

Although many minerals show evidence for limited retrograde alteration along grain boundaries and fractures, only kyanite clearly shows almost complete grain replacement by a lower grade mineral-muscovite. This could imply that retrogressive metamorphism was most intense in the gneisses or that the kyanite is pre-tectonic to (Seg) whereas most of

the index minerals within the Metasedimentary Complex are early syn- to post-tectonic to (Sem). It is not known if Seg = Sem and therefore interpretation of whether kyanite fits into the progressive sequence, or is pre-tectonic and should not be considered with the other index minerals, is inconclusive. This is an important question in determining the metamorphic history between the gneiss and metasedimentary complex. Unfortunately, little can be deduced from one section containing a few grains of kyanite.

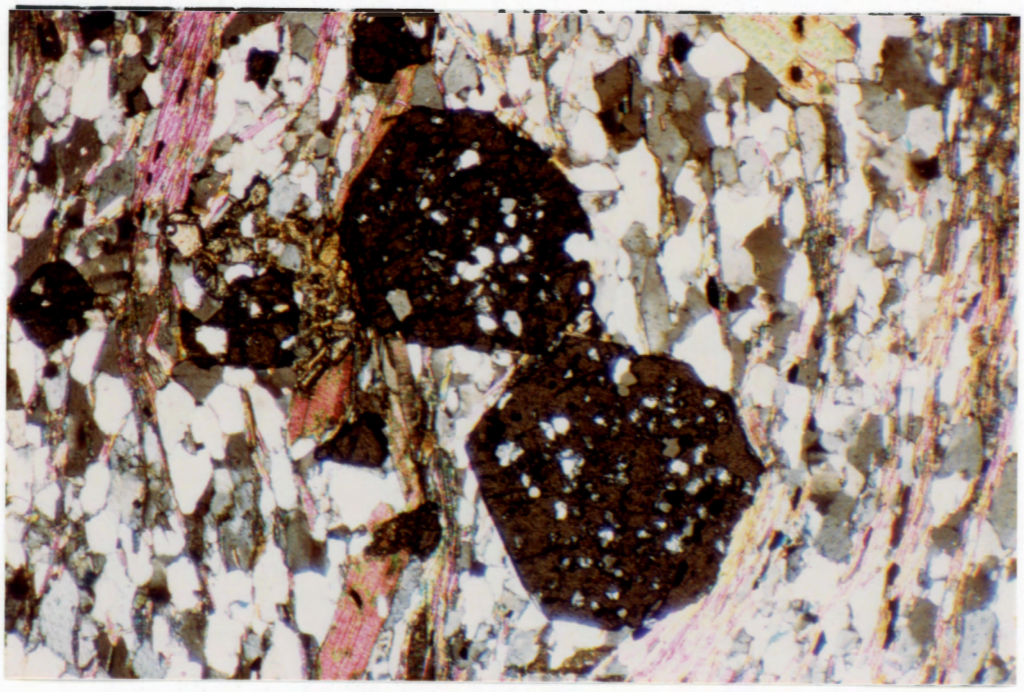

Figure 3.17. Highly altered poikiloblastic staurolite to the left of the upper garnet within the Gneiss. Relations between this grain and the pervasive schistosity are difficult to determine (crossed polars, x 31.25).

CHAPTER 4

MINERAL CHEMISTRY

4.1 INTRODUCTION

Microprobe analysis was carried out on the major phases of seven selected samples, which are described in Table 4.1. Approximately three grains of each major phase for each sample were analysed and analyses are listed according to mineral type, for easier comparison, in Table 4.2, found at the end of this section. The results of the analyses will be discussed briefly below.

4.2 FELDSPAR ANALYSES

Results from the analyses, show that most of the feldspar within both the Metasedimentary and Composite Gneiss Complex is plagioclase showing a general increase in the anorthite content, with increasing metamorphic grade. The anorthite content is quite variable, and with such a small data base, conclusions can only be tentative. A summary of the feldspar analyses is given in Table 4.3. Analyses of the feldspar within the amphibolite suggests that crystal growth occurred simultaneously with an increase in metamorphism. The cores of grains within sample 43a are oligoclase with an anorthite content between 22 and 27 percent. The rims of these grains are andesine with an anorthite content between 37 and 41 percent. The "higher-temperature" plagioclase rimming the "lower-temperature" plagioclase indicates that rim growth took place under conditions of higher temperature than that of the core. The calcium-rich plagioclase most likely developed as a result of the loss of sodium from the oligoclase to the hornblende, and

TABLE 4.1. Description of Samples Used in Microprobe Analysis

Sample Number	Lithology
24	Phyllite of Unit 1 Metasedimentary Complex
31	Poikiloblastic Biotite-Bearing Phyllite of Unit 2 Metasedimentary Complex
37.5	Hornblende-Bearing Psammite of Unit 2 Metasedimentary Complex
38	Epidote-Feldspar Vein-Bearing Psammite of Unit 2 Metasedimentary Complex
81	Staurolite-Bearing Phyllite of Unit 2 Metasedimentary Complex
43a	Amphibolite
57b	Kyanite-Bearing Biotite-Quartz-Feldspar Gneiss of Composite Gneiss Complex

the breakdown of epidote, sphene and chlorite. "The production of more anorthite-rich plagioclase with hornblende may involve such reactions as:

$$3(Mg,Fe)_{10}Al_2Si_6Al_2O_{20}(OH)_{16} + 12Ca_2Al_3Si_3O_{12}(OH) + 14\ SiO_2 =$$

(chlorite) (epidote) (quartz)

$$10Ca_2(Mg,Fe)_3Al_2(Al_2Si_6)O_{22}(OH)_2 + 4CaAl_2Si_2O_8 + 20\ H_2O$$

tschermakitic hornblende (ss) (anorthite)

(Nockolds, et al., 1979)

"The development of oligoclase at about the same grade at which almandine garnet appears is accompanied by a decrease in the amount of epidote, sphene and chlorite. Concurrently, hornblende deepens in color as it gains sodium at the expense of the albite content of plagioclase and titanium from sphene. The characteristic amphibolite facies assemblage is hornblende-andesine ..." (Nockolds et al. 1979). With increasing temperature conditions, one would expect to find plagioclase with high anorthite contents. The gneiss does not seem to follow this trend as it has an anorthite content lower than all of the metasedimentary samples analysed except for sample 24. This may be a reflection of the retrogressive metamorphism that cause the kyanite to alter to muscovite (refer to values given in Table 4.3).

4.3 GARNET ANALYSES

Garnet analyses for the selected samples are given in Table 4.2. Cores and rims of the grains were analysed and the results show calcium and manganese-rich cores and iron and magnesium-rich rims. This trend has been documented as "normal" outward compositional zoning (Hollister,

Table 4.3. Summary of Feldspar Analyses

Lithology	Phyllite	Phyllite	Psammite	Psammite	Phyllite	Amphibolite	Gneiss
Sample Number	24	31	37.5	38	81	43c	57b
# of grains of that plagioclase type	3	1	4	7	1	3	4
Plagioclase Name	oligoclase	andesine	andesine	oligoclase	andesine	oligoclase cores	oligoclase
				core:			core
Anorthite Content in percent	An_{12-19}	An_{33}	$*An_{?-49}$	An_{22-28}	An_{32}	An_{23-29}	An_{18-20}
		2	1	rim:		3	rim:
Plagioclase Name		oligoclase	oligoclase	An_{27-29}		andesine rims	An_{19}
Anorthite Content		An_{29}	$*An_{?}$	1		An_{38-42}	
				albite			
				$An_{0.17}$			
Number of grains analysed per sample	3	3	5	8	1	6	4

increasing metamorphic grade →

*computer program did not calculate all analyses for An percentage

1966). Two models have been proposed to explain variations in the composition of garnet, considering element partitioning between the matrix and the developing garnets. Hollister (1966) and Atherton (1968) propose the variation in MnO in zoned garnets may be explained via a complete fractionation model, where upon initial growth of the garnet, MnO is removed from the matrix and concentrated in the core of the garnet and subsequent growth of the garnet is poor in manganese because the grain is growing in a manganese-poor environment. The decrease in manganese is accompanied by an increase in iron and magnesium to maintain the atomic balance in the garnet.

An alternative model is proposed by Miyashiro and Shido (1973). In this model, garnets are proposed to crystallize in complete equilibrium with the associated matrix minerals. The gradual breakdown of chlorite and biotite is proposed to produce the garnet during increasing progressive metamorphism, gradually increasing the amount of garnet without the addition of manganese to the system. This breakdown of biotite to form the garnet results in a progressive decrease in manganese and an increase in the magnesium content of the garnet.

Changes in the composition of garnet have been linked to the grade of progressive regional metamorphism. A progressive decrease in the MnO content with increasing grade has been documented by Miyashiro (1953). A CaO + MnO decrease and FeO + MgO increase in garnets with progressive regional metamorphism has been documented by Sturt (1962), Atherton (1965) and Cooper (1972).

The garnets analysed in this study have been plotted on a CaO + MnO versus FeO + MgO diagram (Figure 4.1). The data used in constructing this graph are listed in Table 4.4. Figure 4.1 shows the trend of decreasing CaO + MnO content and increasing FeO + MgO content with increasing metamorphic grade. It also shows the trend of manganese-rich cores and magnesium-rich rims.

Figure 4.2 is another display of the composition of the garnets in the rocks of the French Mountain area. The same trend of magnesium and iron-rich rims and calcium and manganese-rich cores is reflected in the triangular plot with the garnet "end-members" at the apices. The lowest grade sample (sample 24) appears to be anomalous in the second trend as it has a rather high iron content compared to the other samples.

4.4 BIOTITE ANALYSES

Analyses of biotite are listed in Table 4.2 at the end of this section. From the results of the analyses there appears to be slight chemical trends with increasing metamorphic grade. There is a slight increase in the magnesium content with increasing metamorphic grade as observed from sample 24 to 81, however the trend does not continue into the gneiss as sample 57b has a smaller magnesium content than sample 81, 37.5 and 31. A second trend, showing a decrease in the iron content with increasing metamorphic grade was observed through samples 24 to 81, again excluding sample 57b which has a higher iron content than sample 81 and 37.5. A plot of the biotite on a triangular diagram with the biotite "end-members" at the apcies is given in Figure 4.3. Variation in the chemical composition of biotite with different grades

Table 4.4. Data Obtained From the Analyses of Garnet Used in the Construction of Figure 4.1

Sample #	Analysis #	core/ rim	Weight percent (MnO + CaO)	Weight percent (FeO + MgO)
24	1	c	4.27	37.11
	2	r	2.32	38.81
	3	c	7.80	31.48
	4	r	2.25	38.98
	5	c	7.50	33.72
	6	r	2.48	38.63
31	1	c	18.69	22.39
	2	r	7.76	32.86
	3	c	8.61	32.17
	4	r	4.60	35.68
	5	c	14.49	26.02
	6	r	7.39	33.47
37.5	1	c	11.45	29.54
	2	r	7.71	32.81
	3	c	12.50	28.35
	4	r	7.49	33.38
	5	c	11.53	29.69
	6	r	5.27	35.76
	7	c	8.55	32.54
	8	r	5.99	35.32
38	1	c	12.80	27.86
	2	r	7.66	32.71
	3	c	12.73	27.97
	4	r	7.41	33.21
	5	c	11.62	29.44
	6	r	7.71	32.80
81	1	c	5.86	34.91
	2	r	4.58	36.32
	3	c	6.28	34.54
	4	r	4.67	36.00
	5	c	7.84	33.27
	6	r	4.14	37.07
57b	1	c	3.74	37.00
	2	r	1.68	37.94
	3	c	2.72	37.49
	4	r	2.80	37.84
	5	c	2.62	37.60

Figure 4.1. Plot of weight percent (FeO + MgO) against (CaO + MnO) for the garnets in the Metasedimentary and Gneiss Complex of the French Mountain area (after Sturt, 1962). The plots show the documented trends of calcium and manganese-rich cores and iron and magnesium-rich rims, and the general progressive increase in iron and magnesium content and decrease in calcium and manganese with increasing metamorphic grade.

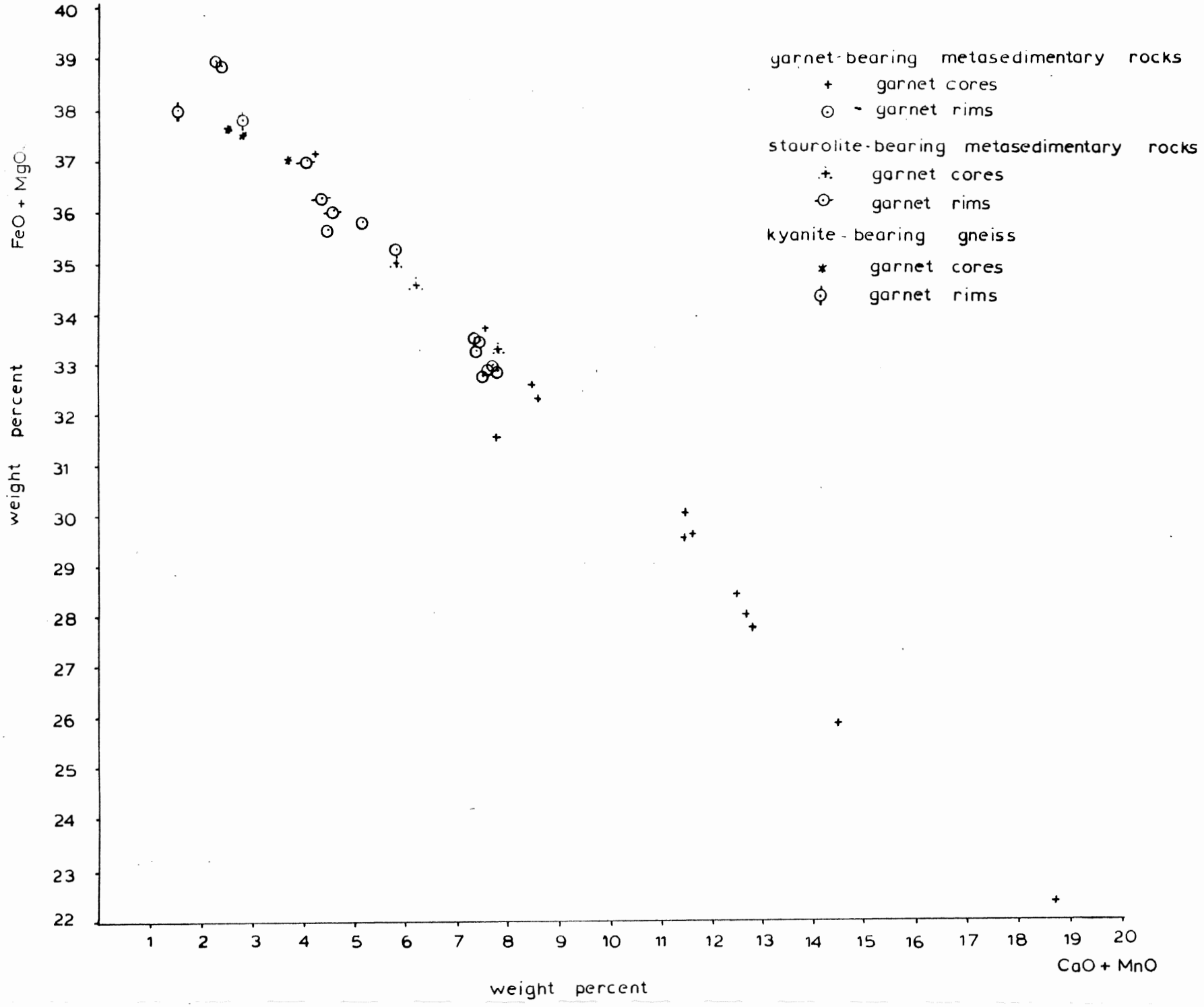
garnet-bearing metasedimentary rocks
garnet cores
garnet rims
staurolite-bearing metasedimentary rocks
garnet cores
garnet rims
kyanite-bearing gneiss
garnet cores
garnet rims
FeO + MgO
weight percent
CaO + MnO
weight percent
40
39
38
37
36
35
34
33
32
31
30
29
28
27
26
25
24
23
22
1
2
3
4
5
6
7
8
9
10
11
12
13
14
15
16
17
18
19
20

Figure 4.2. Garnets from the French Mountain area, plotted on a triangular diagram with "end-member" compositions of the isomorphous series at the apices.

LEGEND: Py - Pyrope, Alm = Almandine, Spess = Spessartine, Gross = Grossular, And = Andradite.

Sample 24 - phyllite of Unit 1 in the Metasedimentary Complex
- ⊙ core of grain
- ⊙ rim of grain

Sample 31 - phyllite of Unit 2 in the Metasedimentary Complex
- △ core of grain
- ⊡ rim of grain

Sample 37.5- psammite of Unit 2 in the Metasedimentary Complex
- + core of grain
- ϕ rim of grain

Sample 38 - psammite of Unit 2 in the Metasedimentary Complex
- × core of grain
- ✳ rim of grain

Sample 81 - staurolite-bearing phyllite of Unit 2 in the Metasedimentary Complex
- • core of grain
- ⊙ rim of grain

Sample 57b - Kyanite-bearing Biotite-Quartz-Feldspar Gneiss
- ◠ core of grain
- ‹·› rim of grain

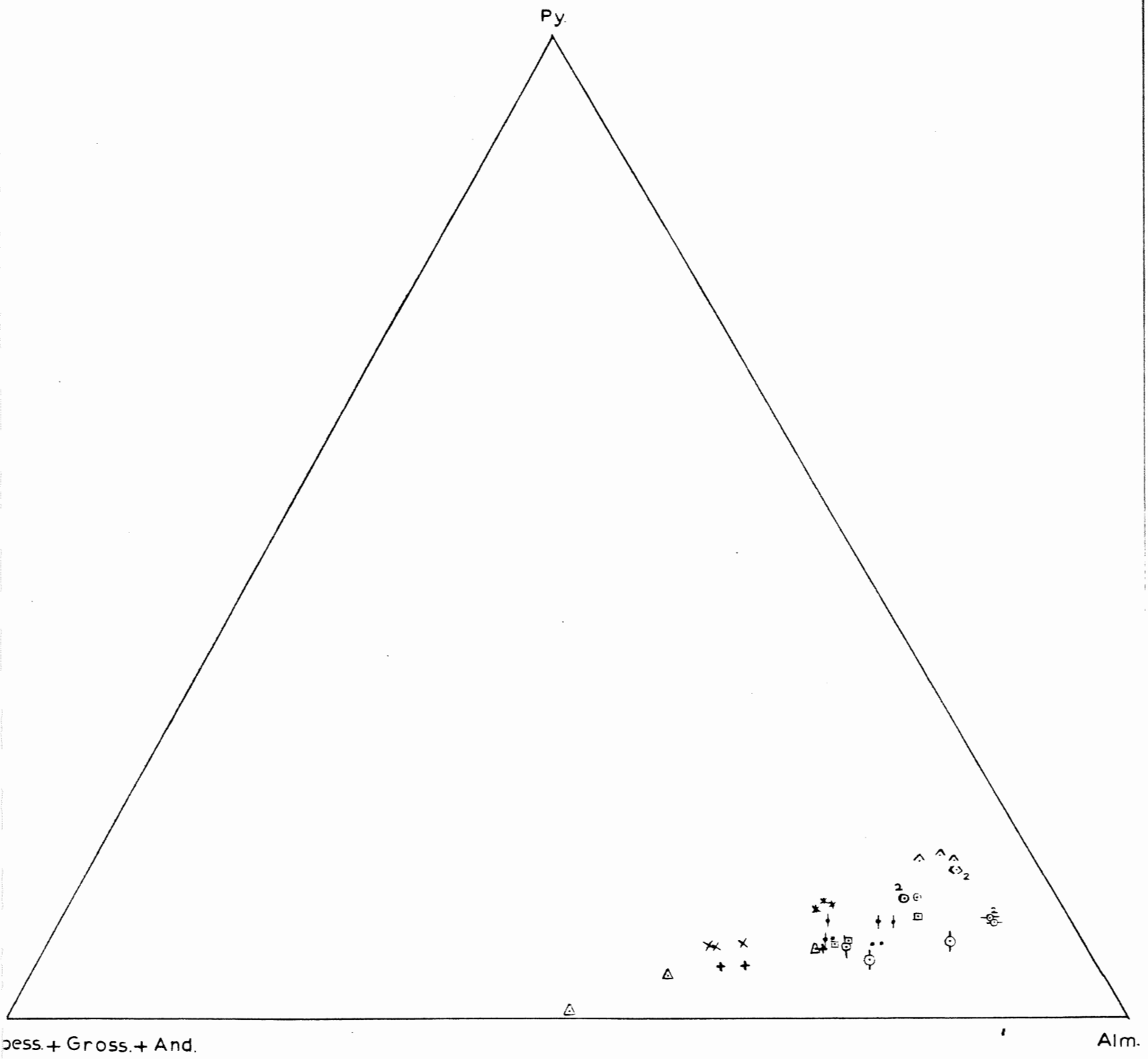
Py.
pess.+ Gross.+ And.
Alm.

Table 4.5. Data Obtained From the Analyses of Biotite Used in the Construction of Figure 4.3.

*

Sample #	24	24	31	31	31	81	81	81	37.5	37.5	37.5	57b	57b	57b	43a	43a
Analysis #	12	13	14	15	21	22	23	27	30	31	32	36	37	40	41	42
Percent Phlogopite	42.63	40.58	49.83	50.86	50.97	54.20	54.58	52.49	50.42	52.62	50.89	48.60	48.78	49.04	65.19	64.67
Percent Annite	57.37	59.42	50.17	49.14	49.03	45.80	54.42	47.51	49.58	47.38	48.25	51.40	51.22	50.74	34.81	35.20
Percent Mn Replacement	0.00	0.00	0.00	0.00	0.00	0.00	0.00	0.00	0.00	0.00	0.86	0.00	0.00	0.00	0.00	0.13

* Analyses obtained from microprobe analysis program

Figure 4.3. Biotite from the French Mountain area plotted on a triangular diagram with the Fe, Mg and Mn end-members plotted at the apices. The plots show a general increase in Mg content with increasing metamorphic grade (excluding sample 57b).

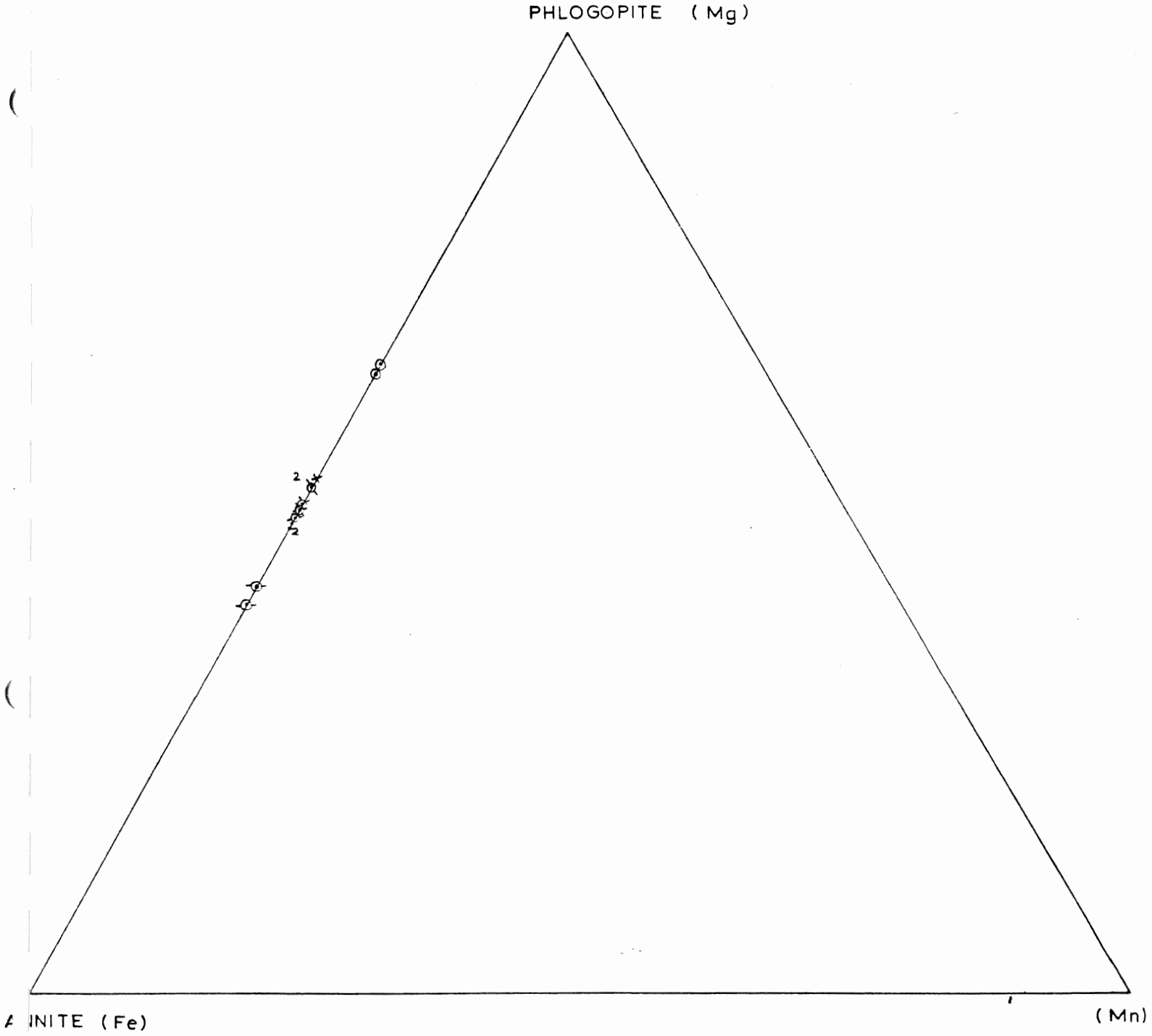

LEGEND :

⊙	sample	24
⊘	sample	31
⊙	sample	37.5
X	sample	81
•	sample	57 b
⊙	sample	43a

of metamorphism has been documented and shows a decrease in Fe^{+2}, Mn and Fe^{+3} and an increase in Ti and Mg with increasing metamorphism (Deer et al., 1980). This trend probably reflects the growth and breakdown of other minerals in the system. For example the growth of staurolite may deplete the system of some of its iron, as there is usually only limited substitution of Mg^{+2} for Fe^{+2} in staurolite, causing the Mg^{+2} to become more readily available for incorporation into the biotite. There does not appear to be any variation trend in the titanium content between samples 24 and 81 however sample 57b has a higher titanium content.

4.5 MUSCOVITE ANALYSES

Analyses given in Table 4.2 show that the muscovite within the rocks of the French Mountain area contain high sodium and aluminium contents and slightly low potassium content when compared to analyses of typical muscovite (Deer et al., 1980). Analyses show an increase in the titanium content with increasing metamorphic grade from sample 31 to 57.

4.6 STAUROLITE, KYANITE AND CHLORITE ANALYSES

Analyses of staurolite, kyanite and chlorite in the rocks of the French Mountain area correspond to typical analyses documented in Deer et al. (1980). The chlorite in sample 24 however has a slightly high iron content.

4.7 HORNBLENDE ANALYSES

Analyses of the hornblende within the amphibolite correspond to typical analyses documented in Deer et al. (1980), however they contain slightly high sodium and aluminum contents. Hornblende within the hornblende-rich psammite has high very high aluminium contents, high iron, slightly high sodium and low magnesium contents when compared to typical analyses given in Deer et al. (1980).

4.8 GEOTHERMOMETRY

The mineral assemblages of the lithologies in the French Mountain area reflect, in a broad sense, conditions of pressure and temperature. To more precisely define the temperature conditions of metamorphism, analyses of selected samples were applied to the garnet-biotite geothermometers of Ferry and Spear (1978) and Thompson (1976).

The calibration of element partitioning between mineral phases is a particularly useful method for estimating the temperature at which minerals within the rock crystallize. The usefulness of this method is a reflection of the fact that the partitioning of elements between mineral phases is a temperature dependent phenomenon, and is independent of the activity of volatile components in the geological environment. Studies have shown that the partitioning of iron and magnesium between coexisting garnet and biotite in an equilibrium assemblage can be used to determine the temperature at which they were last at equilibrium (Thompson, 1976; Goldman and Albee, 1977; and Ferry and Spear, 1978).

Table 4.6. Microprobe Analyses Data Used in Geothermometry Calculations

Sample #	24		31		81	
Mineral	*garnet	**biotite	garnet	biotite	garnet	biotite
SiO_2	36.49	35.36	36.17	36.34	37.03	36.41
TiO_2	0.00	1.65	0.00	1.51	0.00	1.52
Al_2O_3	20.55	19.70	20.47	19.89	20.83	19.77
Cr_2O_3	0.00	0.00	0.00	0.06	0.00	0.00
Fe_2O_3	0.79	0.00	0.82	0.00	0.53	0.00
FeO	36.67	21.46	33.05	18.79	32.91	18.02
MnO	0.52	0.00	1.31	0.00	0.34	0.00
MgO	2.54	8.58	2.63	10.47	3.09	11.17
CaO	1.83	0.00	3.29	0.00	4.33	0.00
Na_2O	0.00	0.00	0.00	0.00	0.00	0.00
K_2O	0.00	8.26	0.00	8.76	0.00	8.19
H_2O	-	3.92	-	4.01	-	4.00
Sum	98.91	98.92	97.66	99.83	99.01	99.08
Si	5.981	5.399	5.972	5.435	5.991	5.449
Al^{iv}	0.019	2.601	0.028	2.565	0.009	2.551
Al^{vi}	3.950	0.945	3.955	0.940	3.962	0.935
Ti	0.000	0.190	0.000	0.170	0.000	0.171
Cr	0.000	0.000	0.000	0.007	0.000	0.000
Fe^{+3}	0.098	0.000	0.102	0.000	0.065	0.000
Fe^{+2}	4.971	2.742	4.564	2.350	4.453	2.255
Mn	0.072	0.000	0.183	0.000	0.047	0.000
Mg	0.621	1.953	0.647	2.334	0.745	2.492
Ca	0.321	0.000	0.582	0.000	0.751	0.000
Na	0.000	0.000	0.000	0.000	0.000	0.000
K	0.000	1.607	0.000	1.671	0.000	1.563
H	-	4.000	-	4.000	-	4.000
O	24.000	24.000	24.000	24.000	24.000	24.000

* averaged from 3 analyses

Table 4.6 (continued). Microprobe Analysis Data Used in Geothermometry Calculations .

Sample #	57b	
Mineral	garnet	biotite
SiO_2	36.89	37.17
TiO_2	0.00	0.19
Al_2O_3	20.90	19.64
Cr_2O_3	0.00	0.00
Fe_2O_3	0.00	0.00
FeO	34.07	18.81
MnO	1.44	0.00
MgO	3.87	10.05
CaO	1.24	0.00
Na_2O	0.00	0.00
K_2O	0.00	8.57
H_2O	-	4.04
Sum	98.41	100.27
Si	6.001	5.516
Al^{iv}	0.000	2.484
Al^{vi}	4.006	0.951
Ti	0.000	0.222
Cr	0.000	0.000
Fe^{+3}	0.000	0.000
Fe^{+2}	4.635	2.335
Mn	0.198	0.000
Mg	0.938	2.223
Ca	0.216	0.000
Na	0.000	0.000
K	0.000	1.622
H	-	4.000
O	24.000	24.000

Table 4.7. Temperatures Obtained According to the Ferry and Spear (1978) Geothermometer

Sample Number	ln K*	Temperature (°C)	$\frac{Ca+Mn}{Ca+Mn+Mg+Fe}$	$\frac{Al^{vi}+Ti}{Al^{vi}+Ti+Fe+Mg}$
24	-1.7405417	563	0.07	0.19
31	-1.9467767	500	0.13	0.19
81	-1.887885	517	0.13	0.19
57b	-1.5484875	632	0.07	0.20

*where $\ln K = \frac{-2109}{T°K} + 0.782$

temperatures obtained are accurate to $\pm$ 25°C

Table 4.8. Temperatures Obtained According to Thompson's (1976) Geothermometer

Sample	* ln K	Temperature (°C)
21	1.7407243	564
31	1.9467766	513
81	1.8798633	531
57b	1.5929293	597

* where $\ln K_D = \ln \frac{Fe^{gnt} \cdot Mg^{bt}}{Mg^{gnt} \cdot Fe^{bt}}$ (after Doucet, 1983)

temperatures obtained are accurate to $\pm$ 25°C

Figure 4.4. Temperatures obtained for the rocks of the French Mountain area using the geothermometer of Ferry and Spear (1978), plotted on a graph of ln k verses 10000/T°K where ln k = (Mg/Fe)gnt/(Mg/Fe)bt. Temperatures are accurate to ± 25°C.

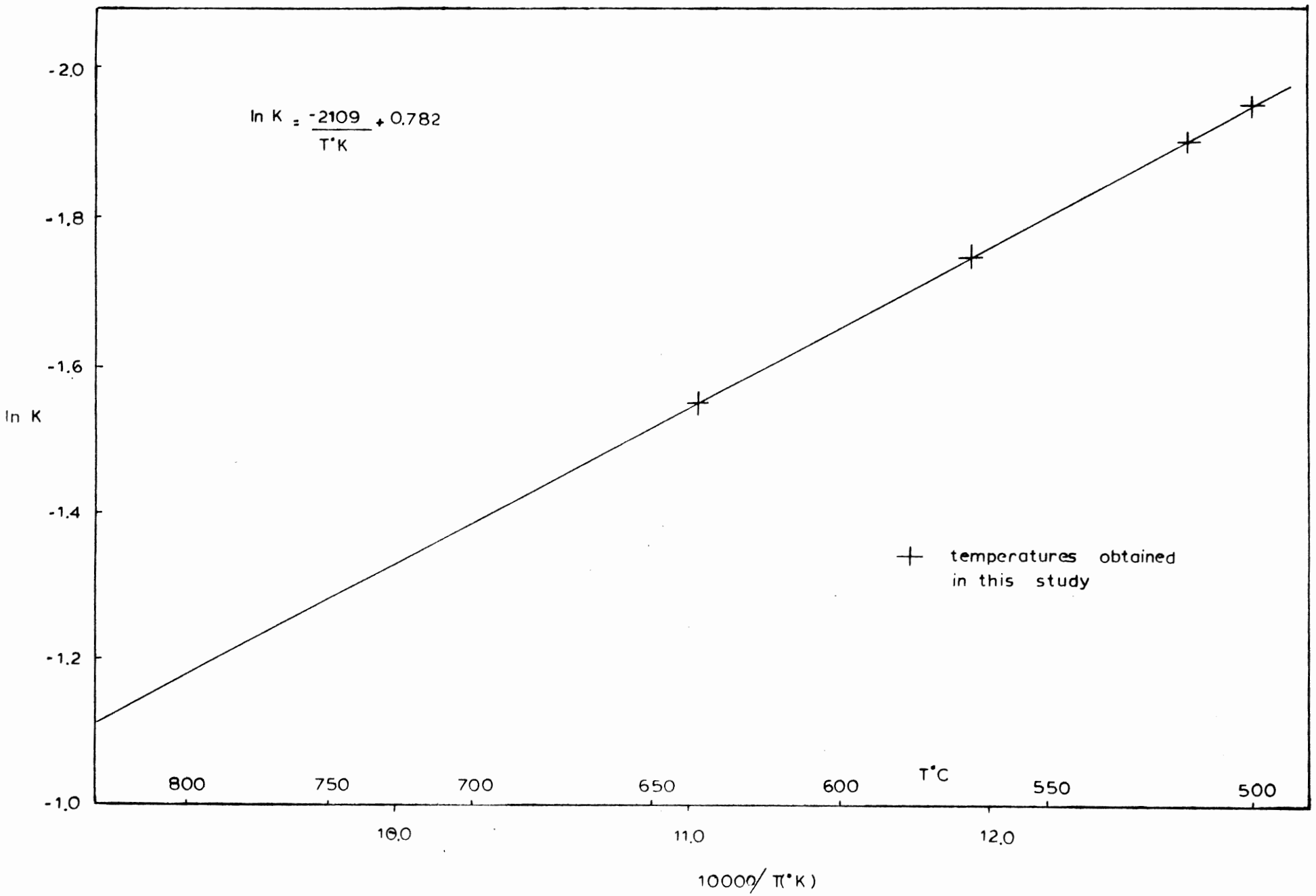
$\ln K = \frac{-2109}{T°K} + 0.782$
-2.0
-1.8
-1.6
-1.4
-1.2
-1.0
ln K
800
750
700
650
600
550
500
T°C
10.0
11.0
12.0
10000/ T(°K)
temperatures obtained
in this study

Figure 4.5. Temperatures obtained for the rocks of the French Mountain area using the geothermometer of Thompson (1976), plotted on a graph of ln K_D against $10^4/T°K$ where

$$\ln K_D = \frac{Fe^{gnt} \cdot Mg^{bt}}{Mg^{gnt} \cdot Fe^{bt}}$$

Temperatures are accurate to $\pm$ 25°C.

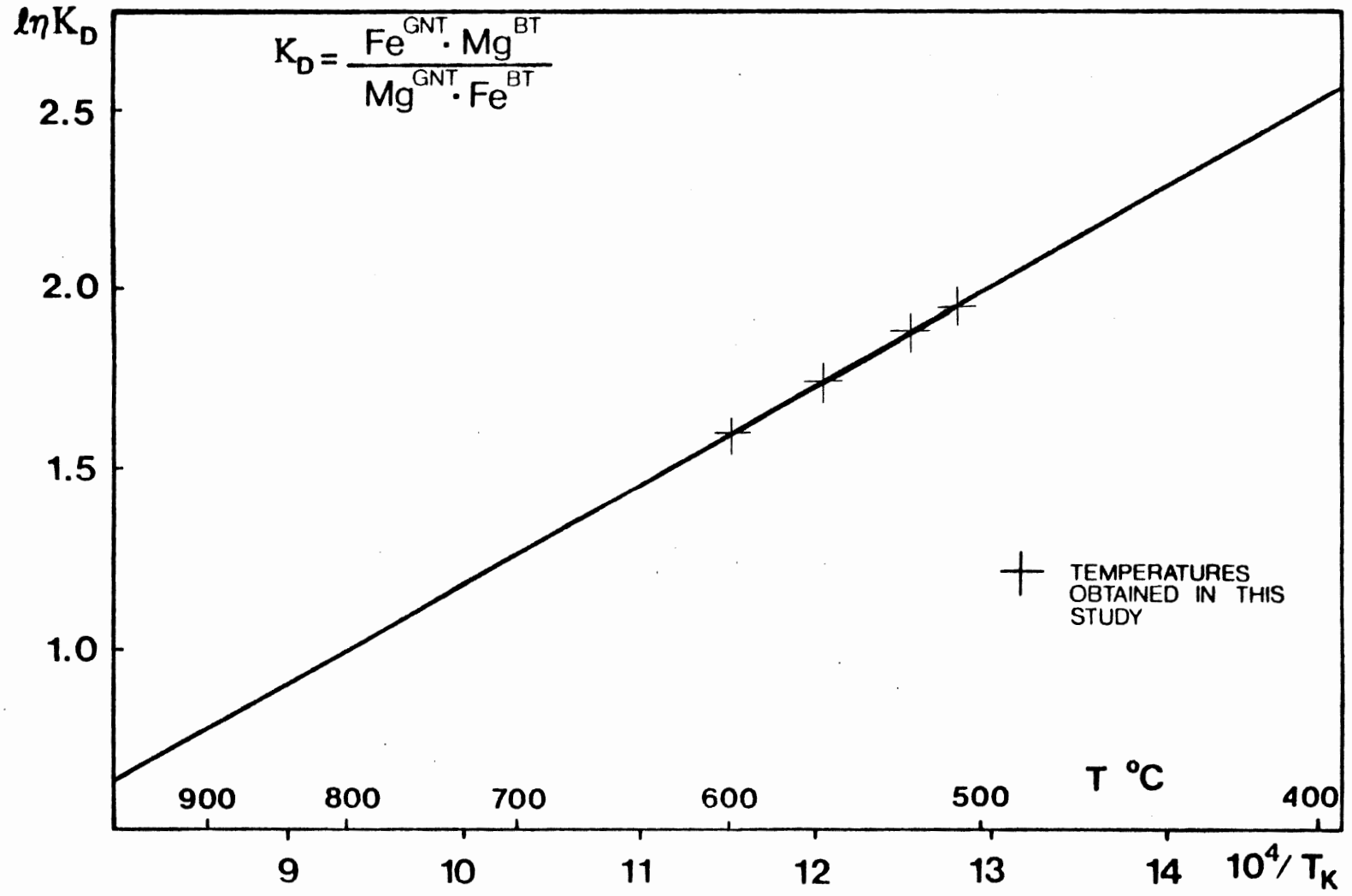
ln K_D
K_D = Fe^GNT · Mg^BT / Mg^GNT · Fe^BT
2.5
2.0
1.5
1.0
TEMPERATURES OBTAINED IN THIS STUDY
T °C
900
800
700
600
500
400
9
10
11
12
13
14
10^4/ T_K

Four samples were used in determining more precise conditions of temperature: one lower grade metasedimentary sample (sample 24), one medium grade metasedimentary sample (sample 31), one high grade metasedimentary sample (sample 81) and one gneiss sample (sample 57b). Data used in calculating these geothermometers are given in Table 4.6. The temperatures obtained according to the geothermometer of Ferry and Spear (1978) and Thompson (1976) are given in Tables 4.7 and 4.8 respectively. Ferry and Spear's (1978) calibration was determined using synthetically produced garnets and biotites. They propose that their calibration could be applied without correction, for systems in which $(Al^{vi} + Ti)/(Al^{vi} + Ti + Fe + Mg) \sim 0.15$ in biotite and $(Ca + Mn)/(Ca + Mn + Fe + Mg) \sim 0.2$ in garnet. From Table 4.7 the biotite exceeds this limit and the results according to this method may be invalid. In both geothermometer calculations the Fe^{+2} of garnet was used in determining K_D. The resulting temperatures from these calculations are plotted in Figures 4.4 and 4.5.

From the geothermometers, temperatures range from 500°C to 632°C. These temperatures are consistent with temperatures indicated by the presence of staurolite in the highest grade metasedimentary rocks but not the kyanite in the gneiss. The metamorphic index mineral kyanite suggests peak temperatures between 650 and 700°C, depending on what reactions took place. This discrepancy between temperatures calculated using the garnet-biotite geothermometers and those indicated by the metamorphic assemblage may be resolved if the garnets and biotites re-equilibrated during a

retrograde metamorphic event. The petrologic study revealed that only a limited amount of retrograde metamorphism had taken place as was indicated by the presence of retrograde chlorite along the grain boundaries and grain fractures in the garnet and staurolite in the Metasedimentary Complex; however extensive retrograde metamorphism was observed in the gneiss complex where muscovite is almost completely replacing kyanite.

Table 4.2. Microprobe Analayses of the Major Phases Within the Metasedimentary and Gneiss Complexes of the French Mountain Area.

Microprobe Analyses of Feldspar

Sample #	81	57b	57b	57b	57b	31
Analysis #	5	6	7	8	9*	10
SiO_2	59.29	63.69	63.79	63.67	63.58	60.87
TiO_2	.06	0.00	.08	0.00	0.00	0.00
Al_2O_3	24.93	22.63	23.52	22.94	23.16	24.69
Cr_2O_3	0.00	0.00	.07	.05	0.00	0.00
Fe_2O_3	0.00	0.00	0.00	0.00	0.00	0.00
FeO	.19	0.00	0.00	0.00	.06	0.00
MnO	0.00	0.00	.18	0.00	0.00	0.00
MgO	0.00	0.00	0.00	0.00	0.00	0.00
CaO	6.39	3.78	4.37	3.77	3.96	6.02
Na_2O	7.38	9.43	9.30	9.23	9.04	8.00
K_2O	0.00	.10	.22	.07	0.00	.04
Sum	98.24	99.63	101.46	99.68	99.80	99.62
Si	10.725	11.282	11.138	11.261	11.230	10.844
Ti	.008	0.000	.011	0.000	0.000	0.000
Al	5.314	4.724	4.839	4.781	4.820	5.183
Fe^{+3}	0.000	0.000	0.000	0.000	0.000	0.000
Fe^{+2}	.029	0.000	0.000	0.000	.009	0.000
Mn	0.000	0.000	.027	0.000	0.000	0.000
Mg	0.000	0.000	0.000	0.000	0.000	0.000
Ca	1.238	.717	.817	.714	.749	1.149
Na	2.588	3.239	3.148	3.165	3.096	2.763
K	0.000	.023	.049	.016	0.000	.009
O	32.000	32.000	32.000	32.000	32.000	32.000
Orthoclase	0.000	.568	1.220	.405	0.000	.232
Albite	67.637	81.401	78.417	81.254	80.511	70.466
Anorthite	32.363	18.301	20.362	18.340	19.489	29.303

* rim of grain

Microprobe Analyses of Feldspar

Sample #	31	31	24	24	24
Analysis #	11	12	13	14	15
SiO_2	60.25	59.71	64.70	65.39	63.91
TiO_2	0.00	0.00	0.00	0.00	0.00
Al_2O_3	25.44	25.81	23.05	22.01	23.18
Cr_2O_3	0.00	0.00	0.00	0.00	0.00
Fe_2O_3	0.00	0.00	0.00	0.00	0.00
FeO	.08	0.00	.08	.04	.17
MnO	0.00	0.00	0.00	0.00	0.00
MgO	0.00	0.00	0.00	0.00	0.00
CaO	6.92	6.53	3.74	2.53	3.89
Na_2O	7.71	7.30	9.46	9.97	9.34
K_2O	0.00	.16	.05	.14	0.00
Sum	100.40	99.51	101.08	100.08	100.49
Si	10.685	10.661	11.287	11.485	11.226
Ti	0.000	0.000	0.000	0.000	0.000
Al	5.316	5.430	4.738	4.555	4.798
Fe^{+3}	0.000	0.000	0.000	0.000	0.000
Fe^{+2}	.012	0.000	.012	.006	.025
Mn	0.000	0.000	0.000	0.000	0.000
Mg	0.000	0.000	0.000	0.000	0.000
Ca	1.315	1.249	.699	.476	.732
Na	2.651	2.527	3.200	3.395	3.181
K	0.000	.036	.011	.031	0.000
O	32.000	32.000	32.000	32.000	32.000
Orthoclase	0.000	.956	.285	.804	0.000
Albite	66.845	66.280	81.836	86.997	81.290
Anorthite	33.155	32.764	17.879	12.200	18.710

Microprobe Analyses of Feldspar

Sample #	38	38	38	38	38	38
Analysis #	1	4	5	6*	7	8*
SiO_2	70.24	62.98	61.13	60.60	62.79	61.24
TiO_2	0.00	0.00	0.00	0.00	0.00	0.00
Al_2O_3	20.65	23.68	24.39	24.53	23.37	24.23
Cr_2O_3	0.00	0.00	0.00	0.00	0.00	0.00
Fe_2O_3	0.00	0.00	0.00	0.00	0.00	0.00
FeO	0.00	.17	.11	.25	.07	0.00
MnO	0.00	0.00	0.00	0.00	.07	0.00
MgO	0.00	0.00	0.00	0.00	0.00	0.00
CaO	.04	4.80	5.85	6.10	4.80	5.73
Na_2O	12.98	9.09	8.43	8.19	9.13	8.39
K_2O	.05	.13	.09	.04	.11	0.00
Sum	103.96	100.85	100.00	99.71	100.34	99.59
Si	11.852	11.073	10.869	10.816	11.096	10.912
Ti	0.000	0.000	0.000	0.000	0.000	0.000
Al	4.106	4.906	5.111	5.159	4.866	5.087
Fe^{+3}	0.000	0.000	0.000	0.000	0.000	0.000
Fe^{+2}	0.000	.025	.016	.037	.010	0.000
Mn	0.000	0.000	0.000	0.000	.010	0.000
Mg	0.000	0.000	0.000	0.000	0.000	0.000
Ca	.007	.904	1.114	1.167	.909	1.094
Na	4.246	3.099	2.906	2.834	3.128	2.898
K	.011	.029	.020	.009	.025	0.000
O	32.00	32.000	32.000	32.000	32.000	32.000
Orthoclase	0.252	0.723	0.505	0.227	0.610	0.000
Albite	99.578	76.851	71.916	70.681	77.015	72.600
Anorthite	0.170	22.426	27.579	29.092	22.375	27.400

* = rim of grain

Microprobe Analyses of Feldspar

Sample #	38	37.5	37.5	37.5	37.5
Analysis #	11	12	13	14	15*
SiO_2	59.23	58.86	60.61	58.00	57.27
TiO_2	0.00	0.00	0.00	0.00	0.00
Al_2O_3	25.64	26.06	24.55	26.30	26.93
Cr_2O_3	0.00	0.00	0.00	0.00	0.00
Fe_2O_3	0.00	0.00	0.00	0.00	0.00
FeO	0.00	0.00	.13	0.00	0.00
MnO	0.00	0.00	0.00	0.00	0.00
MgO	0.00	0.00	0.00	0.00	0.00
CaO	7.40	7.61	6.28	8.27	9.08
Na_2O	7.34	7.57	8.36	6.94	6.61
K_2O	0.00	0.00	.19	0.00	.08
Sum	99.61	100.10	100.12	99.51	99.97
Si	10.598	10.505	10.794	10.422	10.276
Ti	0.000	0.000	0.000	0.000	0.000
Al	5.406	5.481	5.152	5.569	5.694
Fe^{+3}	0.000	0.000	0.000	0.000	0.000
Fe^{+2}	0.000	0.000	.019	0.000	0.000
Mn	0.000	0.000	0.000	0.000	0.000
Mg	0.000	0.000	0.000	0.000	0.000
Ca	1.419	1.455	1.198	1.592	1.746
Na	2.546	2.620	2.886	2.418	2.299
K	0.000	0.000	.043	0.000	.018
O	32.000	32.000	32.000	32.000	32.000
Orthoclase	0.000	0.000	.043	0.000	.018
Albite	2.546	2.620	2.886	2.418	2.298
Anorthite	1.419	1.455	1.198	1.592	1.746

* = rim of grain

□ = grains within epidote-feldspar veins

Microprobe Analyses of Feldspar

Sample #	37.5	37.5	43a	43a	43a
Analysis #	16	17*	18	19	20
SiO_2	64.81	55.45	60.92	58.10	60.17
TiO_2	0.00	0.00	0.00	0.00	0.00
Al_2O_3	21.71	27.68	23.99	26.28	24.06
Cr_2O_3	0.00	0.00	0.00	0.00	0.00
Fe_2O_3	0.00	0.00	0.00	0.00	0.00
FeO	0.00	0.00	0.00	.10	0.00
MnO	0.00	0.00	0.00	0.00	0.00
MgO	0.00	0.00	0.00	0.00	0.00
CaO	5.44	10.22	5.77	8.06	5.95
Na_2O	7.51	5.85	8.28	7.15	8.14
K_2O	0.00	0.00	0.00	.23	.12
Sum	99.47	99.20	98.96	99.92	98.44
Si	11.451	10.055	10.923	10.418	10.864
Ti	0.000	0.000	0.000	0.000	0.000
Al	4.520	5.915	5.069	5.553	5.119
Fe^{+3}	0.000	0.000	0.000	0.000	0.000
Fe^{+2}	0.000	0.000	0.000	.015	0.000
Mn	0.000	0.000	0.000	0.000	0.000
Mg	0.000	0.000	0.000	0.000	0.000
Ca	1.030	1.986	1.108	1.548	1.151
Na	2.573	2.057	2.878	2.486	2.850
K	0.000	0.000	0.000	.053	.028
O	32.000	32.000	32.000	32.000	32.000
Orthoclase	0.000	0.000	0.000	1.287	.686
Albite	2.573	50.880	72.197	60.823	70.740
Anorthite	1.030	49.120	27.803	37.890	28.574

* = rim of grain

Microprobe Analyses of Feldspar

Sample #	43a	43a	43a
Analysis #	21	23	24
SiO_2	57.79	62.31	57.28
TiO_2	0.00	0.00	0.00
Al_2O_3	25.88	23.53	25.56
Cr_2O_3	0.00	0.00	0.00
Fe_2O_3	0.00	0.00	0.00
FeO	0.00	0.00	0.61
MnO	0.00	0.00	0.00
MgO	0.00	0.00	0.40
CaO	7.90	4.82	8.68
Na_2O	7.03	9.08	6.69
K_2O	0.00	0.06	0.08
Sum	98.60	99.80	99.30
Si	10.470	11.063	10.373
Ti	0.000	0.000	0.000
Al	5.525	4.923	5.455
Fe^{+3}	0.000	0.000	0.000
Fe^{+2}	0.000	0.000	.092
Mn	0.000	0.000	0.000
Mg	0.000	0.000	.108
Ca	1.534	.917	1.684
Na	2.469	3.126	2.349
K	0.000	.014	.018
O	32.000	32.000	32.000
Orthoclase	0.000	.335	.456
Albite	61.690	77.060	57.976
Anorthite	38.310	22.605	41.568

Microprobe Analyses of Garnet

Sample #	24					
Analysis #	1	1	2	2	3	3
Core or Rim	core	rim	core	rim	core	rim
SiO_2	36.50	36.49	34.91	36.55	36.09	36.43
TiO_2	0.00	0.00	0.00	0.00	0.00	0.00
Al_2O_3	20.73	20.58	19.59	20.64	20.38	20.42
Fe_2O_3	1.12	0.69	2.52	1.09	1.35	0.60
FeO	35.07	36.22	29.67	36.42	32.22	36.16
MnO	1.87	0.54	5.24	0.46	4.90	0.56
MgO	2.04	2.59	1.81	2.56	1.50	2.47
CaO	2.40	1.78	2,56	1.79	2.60	1.92
Na_2O	0.00	0.00	0.00	0.00	0.00	0.00
K_2O	0.00	0.00	0.00	0.00	0.00	0.00
Total	99.62	98.82	96.15	99.44	98.91	98.50
Si	5.958	5.982	5.937	5.968	5.959	5.994
Al^{iv}	0.042	0.018	0.063	0.032	0.041	0.006
Al^{vi}	3.946	3.957	3.863	3.939	3.924	3.953
Ti	0.000	0.000	0.000	0.000	0.000	0.000
Fe^{+3}	0.137	0.085	0.323	0.134	0.168	0.074
Fe^{+2}	4.788	4.966	4.220	4.972	4.449	4.976
Mn	0.259	0.075	0.755	0.064	0.685	0.078
Mg	0.496	0.633	0.459	0.623	0.369	0.606
Ca	0.420	0.313	0.466	0.313	0.460	0.338
Na	0.000	0.000	0.000	0.000	0.000	0.000
K	0.000	0.000	0.022	0.000	0.000	0.000
O	24.000	24.000	24.000	24.000	24.000	24.000
Fe/Mg	10.444	8.099	11.546	8.299	14.365	8.465
Fe/Fe+Mg	0.913	0.890	0.920	0.892	0.935	0.894
almandine	80.28	82.93	71.70	83.24	74.59	82.95
andradite	3.47	2.18	6.52	3.39	4.15	1.88
grossular	3.58	3.05	1.33	1.85	3.57	3.76
pyrope	8.32	10.58	7.73	10.44	6.19	10.11
spessartine	4.35	1.25	12.72	1.07	11.50	1.30

Microprobe Analyses of Garnet

Sample #	31					
Analysis #	1	1	2	2	3	3
Core or Rim	core	rim	core	rim	core	rim
SiO_2	36.72	36.53	36.69	36.17	36.43	36.80
TiO_2	0.00	0.00	0.00	0.00	0.00	0.00
Al_2O_3	20.48	20.55	20.47	20.47	20.25	20.59
Fe_2O_3	0.94	1.45	0.63	0.82	0.76	0.26
FeO	22.07	30.90	30.31	33.05	24.92	31.47
MnO	9.87	2.29	2.82	1.31	6.90	1.74
MgO	0.32	1.96	1.86	2.63	1.10	2.00
CaO	8.82	5.47	5.79	3.29	7.59	5.65
Na_2O	0.00	0.00	0.00	0.00	0.00	0.00
K_2O	0.00	0.00	0.00	0.00	0.00	0.00
Total	99.13	99.00	98.51	97.66	97.87	98.48
Si	5.991	5.962	6.000	5.972	6.001	6.007
Al^{iv}	0.009	0.038	0.000	0.028	0.000	0.000
Al^{vi}	3.928	3.915	3.944	3.955	3.931	3.961
Ti	0.000	0.000	0.000	0.000	0.000	0.000
Fe^{+3}	0.115	0.178	0.077	0.102	0.094	0.031
Fe^{+2}	3.012	4.217	4.146	4.564	3.433	4.296
Mn	1.364	0.317	0.391	0.183	0.963	0.241
Mg	0.078	0.477	0.453	0.647	0.270	0.487
Ca	1.542	0.957	1.014	0.582	1.340	0.988
Na	0.000	0.000	0.000	0.000	0.000	0.000
K	0.000	0.000	0.000	0.000	0.000	0.000
O	24.000	24.000	24.000	24.000	24.000	24.000
Fe/Mg	57.714(?)	9.882	10.177	7.492	16.622	9.387
Fe/Fe+Mg	0.983	0.908	0.911	0.882	0.943	0.904
almandine	50.19	70.63	69.03	76.36	57.12	71.36
andradite	2.93	4.60	1.87	2.49	2.40	0.83
grossular	22.81	11.45	15.03	7.26	19.93	15.67
pyrope	1.30	8.00	7.55	10.83	4.50	8.13
spessartine	22.77	5.32	6.52	3.06	16.05	4.02

Microprobe Analyses of Garnet

Sample #	38					
Analysis #	1	1	2	2	3	3
Core or Rim	core	rim	core	rim	core	rim
SiO_2	36.63	36.78	36.61	36.98	36.89	36.88
TiO_2	0.00	0.00	0.00	0.00	0.00	0.00
Al_2O_3	20.70	20.86	20.65	21.00	20.65	21.10
Fe_2O_3	1.67	1.46	1.75	1.21	0.69	0.89
FeO	25.94	29.71	26.07	30.19	27.47	29.89
MnO	7.18	3.18	7.26	3.02	6.42	3.05
MgO	1.92	3.00	1.90	3.02	1.97	2.91
CaO	5.62	4.48	5.47	4.39	5.20	4.66
Na_2O	0.00	0.00	0.00	0.00	0.00	0.00
K_2O	0.00	0.00	0.00	0.00	0.00	0.00
Total	99.50	99.32	99.53	99.69	99.22	99.29
Si	5.949	5.950	5.949	5.956	5.993	5.954
Al^{iv}	0.051	0.050	0.051	0.044	0.007	0.046
Al^{vi}	3.910	3.927	3.903	3.941	3.946	3.969
Ti	0.000	0.000	0.000	0.000	0.000	0.000
Fe^{+3}	0.205	0.177	0.214	0.147	0.084	0.108
Fe^{+2}	3.524	4.019	3.543	4.066	3.732	4.035
Mn	0.988	0.436	0.999	0.412	0.883	0.417
Mg	0.465	0.723	0.460	0.725	0.477	0.700
Ca	0.978	0.777	0.952	0.758	0.905	0.806
Na	0.000	0.000	0.000	0.000	0.000	0.000
K	0.000	0.000	0.000	0.000	0.000	0.000
O	24,000	24.000	24.000	24.000	24.000	24.000
Fe/Mg	10.147	6.404	10.334	6.380	9.852	6.513
Fe/Fe+Mg	0.910	0.865	0.912	0.864	0.908	0.867
almandine	59.14	67.46	59.47	68.18	62.21	67.70
andradite	5.30	4.46	5.37	3.70	2.03	2.65
grossular	11.14	8.60	10.63	9.02	13.07	10.89
pyrope	7.82	12.15	7.73	12.17	7.96	11.76
spessartine	16.61	7.33	16.79	6.92	14.73	7.00

Microprobe Analyses of Garnet

Sample #	37.5					
Analysis #	1	1	2	2	3	3
Core or Rim	core	rim	core	rim	core	rim
SiO_2	36.90	36.83	36.66	37.31	36.99	37.17
TiO_2	0.06	0.00	0.00	0.00	0.00	0.00
Al_2O_3	20.67	20.80	20.84	21.06	20.66	20.98
Fe_2O_3	0.84	0.30	0.86	0.42	0.21	0.00
FeO	28.08	30.72	27.03	30.76	28.31	33.23
MnO	4.24	0.93	5.70	1.42	4.78	0.43
MgO	1.46	2.09	1.32	2.62	1.38	2.53
CaO	7.21	6.78	6.80	6.07	6.75	4.84
Na_2O	0.00	0.00	0.00	0.00	0.00	0.00
K_2O	0.00	0.00	0.00	0.00	0.00	0.00
Total	99.37	98.42	99.13	99.62	99.06	99.18
Si	5.982	5.992	5.965	5.989	6.011	6.005
Al^{iv}	0.018	0.008	0.035	0.011	0.000	0.000
Al^{vi}	3.931	3.979	3.960	3.973	3.956	3.994
Ti	0.007	0.000	0.000	0.000	0.000	0.000
Fe^{+3}	0.102	0.037	0.106	0.051	0.025	0.000
Fe^{+2}	3.807	4.179	3.678	4.130	3.848	4.490
Mn	0.582	0.128	0.786	0.193	0.658	0.059
Mg	0.353	0.507	0.320	0.627	0.334	0.609
Ca	1.252	1.182	1.185	1.044	1.175	0.838
Na	0.000	0.000	0.000	0.000	0.000	0.000
K	0.000	0.000	0.000	0.000	0.000	0.000
O	24.000	24.000	24.000	24.000	24.000	24.000
Fe/Mg	12.739	8.572	14.275	6.977	13.556	7.466
Fe/Fe+Mg	0.927	0.896	0.935	0.875	0.931	0.882
almandine	63.48	69.68	61.59	68.88	63.67	74.86
andradite	2.55	0.90	2.64	1.35	0.53	0.00
grossular	18.17	18.83	17.23	16.08	19.17	13.99
pyrope	5.89	8.46	5.36	10.47	5.60	10.17
spessartine	9.72	2.14	13.18	3.22	11.03	0.98

Microprobe Analyses of Garnet

Sample #	81					
Analysis #	1	1	2	2	3	3
Core or Rim	core	rim	core	rim	core	rim
SiO_2	36.72	37.21	36.76	37.03	37.08	37.29
TiO_2	0.00	0.00	0.00	0.00	0.00	0.00
Al_2O_3	20.89	21.15	20.76	20.83	20.97	21.22
Fe_2O_3	0.08	0.39	0.50	0.53	0.59	0.53
FeO	32.86	33.15	32.55	32.91	31.24	33.87
MnO	0.30	0.52	0.59	0.34	1.99	0.95
MgO	2.05	3.17	1.99	3.09	2.03	3.20
CaO	5.56	4.06	5.69	4.33	5.85	3.19
Na_2O	0.00	0.00	0.00	0.00	0.00	0.00
K_2O	0.00	0.00	0.00	0.00	0.00	0.00
Total	98.45	99.61	98.79	99.01	99.69	100.20
Si	5.988	5.980	5.986	5.991	5.981	5.974
Al^{iv}	0.012	0.020	0.014	0.009	0.019	0.026
Al^{vi}	4.002	3.985	3.969	3.962	3.967	3.979
Ti	0.000	0.000	0.000	0.000	0.000	0.000
Fe^{+3}	0.010	0.047	0.061	0.065	0.071	0.064
Fe^{+2}	4.481	4.455	4.433	4.453	4.215	4.537
Mn	0.041	0.071	0.081	0.047	0.272	0.129
Mg	0.498	0.759	0.483	0.745	0.488	0.764
Ca	0.971	0.699	0.993	0.751	1.011	0.548
Na	0.000	0.000	0.000	0.000	0.000	0.000
K	0.000	0.000	0.000	0.000	0.000	0.000
O	24.000	24.000	24.000	24.000	24.000	24.000
Fe/Mg	9.096	6.023	9.473	6.125	9.338	6.191
Fe/Fe+Mg	0.901	0.858	0.905	0.860	0.903	0.861
almandine	74.78	74.43	73.99	74.24	70.39	75.88
andradite	0.23	1.20	1.50	1.73	1.81	1.58
grossular	15.99	10.48	15.09	10.81	15.10	7.59
pyrope	8.32	12.69	8.07	12.44	8.16	12.79
spessartine	0.68	1.19	1.35	0.78	4.55	2.16

Microprobe Analyses of Garnet

Sample #	37.5	
Analysis #	4	4
Core or Rim	core	rim
SiO_2	36.98	37.48
TiO_2	0.00	0.00
Al_2O_3	20.85	21.09
Fe_2O_3	0.38	0.00
FeO	30.69	32.79
MnO	2.59	0.73
MgO	1.85	2.53
CaO	5.96	5.26
Na_2O	0.00	0.00
K_2O	0.00	0.00
Total	99.27	99.88
Si	5.992	6.009
Al^{iv}	0.008	0.000
Al^{vi}	3.973	3.984
Ti	0.000	0.000
Fe^{+3}	0.047	0.000
Fe^{+2}	4.159	4.396
Mn	0.355	0.099
Mg	0.447	0.605
Ca	1.035	0.904
Na	0.000	0.000
K	0.000	0.000
O	24.000	24.000
Fe/Mg	10.210	7.436
Fe/Fe+Mg	0.911	0.881
almandine	69.34	73.09
andradite	1.20	0.00
grossular	16.07	15.13
pyrope	7.46	10.12
spessartine	5.92	1.66

Microprobe Analyses of Garnet

Sample #	57b				
Analysis #	1	1	2	2	3
Core of Rim	core	rim	core	rim	core
SiO_2	36.98	36.89	36.77	36.73	36.75
TiO_2	0.00	0.00	0.00	0.00	0.00
Al_2O_3	21.26	20.90	21.00	21.04	21.09
Fe_2O_3	1.08	0.00	1.30	0.89	1.86
FeO	32.91	34.07	33.30	34.09	33.19
MnO	2.73	1.44	1.18	1.53	1.57
MgO	4.09	3.87	4.19	3.75	4.41
CaO	1.01	1.24	1.59	1.27	1.05
Na_2O	0.00	0.00	0.00	0.00	0.00
K_2O	0.00	0.00	0.00	0.00	0.00
Total	99.95	98.41	99.20	99.21	99.73
Si	5.942	6.001	5.945	5.953	5.921
Al^{iv}	0.058	0.000	0.055	0.047	0.079
Al^{vi}	3.967	4.006	3.945	3.971	3.924
Ti	0.000	0.000	0.000	0.000	0.000
Fe^{+3}	0.131	0.000	0.158	0.108	0.225
Fe^{+2}	4.421	4.635	4.503	4.621	4.471
Mn	0.372	0.198	0.162	0.210	0.214
Mg	0.979	0.938	1.010	0.906	1.059
Ca	0.174	0.216	0.275	0.221	0.181
Na	0.000	0.000	0.000	0.000	0.000
K	0.000	0.000	0.000	0.000	0.000
O	24.000	24.000	24.000	24.000	24.000
Fe/Mg	5.027	5.151	4.776	5.452	4.637
Fe/Fe+Mg	0.834	0.837	0.827	0.845	0.823
almandine	73.93	77.42	75.66	77.54	76.83
andradite	2.93	0.00	4.01	2.80	3.10
grossular	0.00	3.61	0.61	0.92	1.15
pyrope	16.48	15.67	16.99	15.22	16.10
spessartine	6.26	3.31	2.72	3.53	2.82

Microprobe Analyses of Biotite

Sample #	24	24	31	31	31	31	31
Analysis #	12	13	14	15	21	22	23
SiO_2	36.08	34.63	36.34	35.03	36.59	37.11	36.84
TiO_2	1.46	1.84	1.51	1.23	1.61	1.42	1.57
Al_2O_3	20.13	19.27	19.89	19.21	19.92	20.05	20.26
Cr_2O_3	0.00	0.00	.06	0.00	0.00	0.00	0.00
Fe_2O_3	0.00	0.00	0.00	0.00	0.00	0.00	0.00
FeO	21.08	21.84	18.79	19.01	18.02	16.70	16.76
MnO	0.00	0.00	0.00	0.00	0.00	0.00	0.00
MgO	8.79	8.37	10.47	11.04	10.51	11.09	11.30
CaO	0.00	0.00	0.00	0.00	0.00	0.00	0.00
Na_2O	0.00	0.00	0.00	0.00	0.00	0.00	0.00
K_2O	8.60	7.91	8.76	7.87	8.82	8.76	8.45
H_2O	3.98	3.86	4.01	3.90	4.01	4.03	4.03
Sum	100.12	97.72	99.83	97.29	99.48	99.16	99.21
Si	5.430	5.369	5.435	5.380	5.469	5.520	5.472
Al	2.570	2.631	2.565	2.620	2.531	2.480	2.528
Al	1.001	.890	.940	.856	.978	1.035	1.018
Ti	.165	.215	.170	.142	.181	.159	.175
Cr	0.000	0.000	.007	0.000	0.000	0.000	0.000
Fe^{+3}	0.000	0.000	0.000	0.000	0.000	0.000	0.000
Fe^{+2}	2.653	2.832	2.350	2.442	2.252	2.078	2.082
Mn	0.000	0.000	0.000	0.000	0.000	0.000	0.000
Mg	1.972	1.934	2.334	2.527	2.341	2.459	2.502
Ca	0.000	0.000	0.000	0.000	0.000	0.000	0.000
Na	0.000	0.000	0.000	0.000	0.000	0.000	0.000
K	1.651	1.564	1.671	1.542	1.681	1.662	1.601
H	4.000	4.000	4.000	4.000	4.000	4.000	4.000
O	24.000	24.000	24.000	24.000	24.000	24.000	24.000

Microprobe Analyses of Biotite

Sample #	81	37.5	37.5	37.5	57b	57b
Analysis #	27	30	31	32	36	37
SiO_2	36.41	36.21	36.99	33.32	36.99	37.17
TiO_2	1.52	1.75	1.78	6.54	2.03	1.99
Al_2O_3	19.77	18.34	19.04	18.05	19.89	19.64
Cr_2O_3	0.00	0.00	0.00	0.00	0.00	0.00
Fe_2O_3	0.00	0.00	0.00	0.00	0.00	0.00
FeO	18.02	18.68	17.94	16.59	18.74	18.81
MnO	0.00	0.00	0.00	.29	0.00	0.00
MgO	11.17	10.66	11.18	9.76	9.94	10.05
CaO	0.00	0.00	0.00	2.49	0.00	0.00
Na_2O	0.00	0.00	0.00	0.00	0.00	0.00
K_2O	8.19	8.99	9.09	7.40	8.53	8.57
H_2O	4.00	3.94	4.02	3.93	4.03	4.04
Sum	99.08	98.57	100.04	98.27	100.15	100.27
Si	5.449	5.504	5.506	5.078	5.494	5.516
Al	2.551	2.496	2.494	2.922	2.506	2.484
Al	.935	.789	.846	.319	.974	.951
Ti	.171	.200	.199	.749	.227	.222
Cr	0.000	0.000	0.000	0.000	0.000	0.000
Fe^{+3}	0.000	0.000	0.000	0.000	0.000	0.000
Fe^{+2}	2.255	2.375	2.233	2.102	2.328	2.335
Mn	0.000	0.000	0.000	.037	0.000	0.000
Mg	2.492	2.415	2.481	2.217	2.200	2.223
Ca	0.000	0.000	0.000	.407	0.000	0.000
Na	0.000	0.000	0.000	0.000	0.000	0.000
K	1.563	1.743	1.726	1.438	1.616	1.622
H	4.000	4.000	4.000	4.000	4.000	4.000
O	24.000	24.000	24.000	24.000	24.000	24.000

Microprobe Analysis of Biotite

Sample #	57b	43a	43a
Analysis #	40	41	42
SiO_2	37.85	37.93	38.62
TiO_2	1.98	1.69	1.64
Al_2O_3	20.16	17.62	18.16
Cr_2O_3	.08	0.00	0.00
Fe_2O_3	0.00	0.00	0.00
FeO	18.81	13.80	14.04
MnO	.08	0.00	.05
MgO	10.20	14.50	14.47
CaO	0.00	0.00	0.00
Na_2O	.11	0.00	0.00
K_2O	8.67	9.89	9.11
H_2O	4.10	4.06	4.11
Sum	101.77	99.49	100.20
Si	5.493	5.600	5.627
Al	2.507	2.400	2.373
Al	.965	.665	.746
Ti	.218	.188	.180
Cr	.009	0.000	0.000
Fe^{+3}	0.000	0.000	0.000
Fe^{+2}	2.299	1.704	1.711
Mn	.010	0.000	.006
Mg	2.222	3.191	3.143
Ca	0.000	0.000	0.000
Na	.031	0.000	0.000
K	1.616	1.862	1.693
H	4.000	4.000	4.000
O	24.000	24.000	24.000

Microprobe Analyses of Chlorite

Sample #	38	38	38	24	24	24
Analysis #	5	6	7	8	9	10
SiO_2	25.44	25.31	24.92	24.31	24.00	24.07
TiO_2	0.00	0.00	06	.09	0.00	0.00
Al_2O_3	22.01	22.31	22.63	23.68	23.86	23.86
Fe_2O_3	0.00	0.00	0.00	0.00	0.00	0.00
FeO	23.76	21.93	21.81	26.97	27.25	27.36
MnO	0.00	0.00	0.00	0.00	0.00	0.00
MgO	16.33	17.69	17.04	13.43	13.30	13.31
CaO	0.00	0.00	0.00	0.00	0.00	0.00
Na_2O	0.00	0.00	0.00	0.00	0.00	0.00
K_2O	0.00	0.00	0.00	0.00	0.00	0.00
H_2O	11.47	11.54	11.43	11.40	11.37	11.39
Sum	99.01	98.78	97.89	99.99	99.78	99.99
Si	5.316	5.258	5.223	5.110	5.060	5.066
Al^{iv}	2.684	2.742	2.777	2.890	2.940	2.934
Al^{vi}	2.735	2.720	2.813	2.976	2.988	2.983
Ti	0.000	0.000	.009	.014	0.000	0.000
Fe^{+3}	0.000	0.000	0.000	0.000	0.000	0.000
Fe	4.152	3.810	3.823	4.741	4.805	4.815
Mn	0.000	0.000	0.000	0.000	0.000	0.000
Mg	5.068	5.478	5.324	4.208	4.180	4.175
Ca	0.000	0.000	0.000	0.000	0.000	0.000
Na	0.000	0.000	0.000	0.000	0.000	0.000
K	0.000	0.000	0.000	0.000	0.000	0.000
H	16.000	16.000	16.000	16.000	16.000	16.000
O	36.000	36.000	36.000	36.000	36.000	36.000

Microprobe Analyses of Chlorite

Sample #	24	31	31	81	31
Analysis #	11	16	17	24*	25*
SiO_2	24.15	24.67	24.45	24.59	23.89
TiO_2	0.00	.05	0.00	0.00	.08
Al_2O_3	23.89	23.77	23.98	23.92	23.98
Fe_2O_3	0.00	0.00	0.00	0.00	0.00
FeO	27.04	23.83	24.39	23.62	26.15
MnO	0.00	0.00	0.00	0.00	0.00
MgO	13.08	14.93	15.11	13.93	13.06
CaO	0.00	0.00	0.00	0.00	0.00
Na_2O	0.00	0.00	0.00	0.00	0.00
K_2O	0.00	0.00	0.00	.17	.05
H_2O	11.35	11.44	11.49	11.31	11.27
Sum	99.51	98.69	99.42	97.54	98.48
Si	5.098	5.169	5.101	5.212	5.080
Al^{iv}	2.902	2.831	2.899	2.788	2.920
Al^{vi}	3.040	3.038	2.995	3.187	3.089
Ti	0.000	.008	0.000	0.000	.013
Fe^{+3}	0.000	0.000	0.000	0.000	0.000
Fe	4.773	4.176	4.255	4.187	4.651
Mn	0.000	0.000	0.000	0.000	0.000
Mg	4.115	4.663	4.698	4.401	4.140
Ca	0.000	0.000	0.000	0.000	0.000
Na	0.000	0.000	0.000	0.000	0.000
K	0.000	0.000	0.000	.046	.014
H	16.000	16.000	16.000	16.000	16.000
O	36.000	36.000	36.000	36.000	36.000

* retrograde chlorite

Microprobe Analyses of Chlorite

Sample #	81	37.5
Analysis #	26*	33
SiO_2	24.58	24.82
TiO_2	.08	0.00
Al_2O_3	23.64	23.49
Fe_2O_3	0.00	0.00
FeO	22.52	23.16
MnO	0.00	0.00
MgO	15.88	16.01
CaO	0.00	0.00
Na_2O	0.00	0.00
K_2O	0.00	0.00
H_2O	11.43	11.50
Sum	98.13	98.98
Si	5.152	5.171
Al^{iv}	2.848	2.829
Al^{vi}	2.991	2.937
Ti	.013	0.000
Fe^{+3}	0.000	0.000
Fe^{+2}	3.948	4.035
Mn	0.000	0.000
Mg	4.961	4.971
Ca	0.000	0.000
Na	0.000	0.000
K	0.000	0.000
H	16.000	16.000
O	36.000	36.000

* retrograde chlorite

Microprobe Analyses of Muscovite

Sample #	31	31	31	81	81	57b	57b
Analysis #	18	19	20	28	29	38	39
SiO_2	46.43	46.02	4.604	44.79	44.90	47.34	47.18
TiO_2	.15	.29	.25	.37	.33	.97	.87
Al_2O_3	36.84	36.90	35.88	35.50	36.54	36.62	36.60
Cr_2O_3	0.00	.05	0.00	.05	0.00	0.00	0.00
Fe_2O_3	0.00	0.00	0.00	0.00	0.00	0.00	0.00
FeO	.92	.82	.95	.89	1.06	.75	.81
MnO	0.00	.04	0.00	0.00	0.00	0.00	0.00
MgO	.44	.42	.39	.37	.21	.40	.48
CaO	0.00	0.00	0.00	.12	0.00	0.00	0.00
Na_2O	1.29	1.73	1.33	1.40	1.08	1.26	1.29
K_2O	9.36	8.72	8.82	7.62	7.25	9.29	9.32
H_2O	4.54	4.53	4.47	4.37	4.41	4.61	4.60
Sum	99.97	99.52	98.13	95.48	95.78	101.24	101.15
Si	6.121	6.086	6.169	6.135	6.106	6.153	6.143
Al	1.879	1.914	1.831	1.865	1.894	1.847	1.857
Al	3.844	3.835	3.834	3.865	3.961	3.762	3.758
Ti	.015	.029	.025	.038	.034	.095	.085
Cr	0.000	.005	0.000	.005	0.000	0.000	0.000
Fe^{+3}	0.000	0.000	0.000	0.000	0.000	0.000	0.000
Fe^{+2}	.101	.091	.106	.102	.121	.082	.088
Mn	0.000	.004	0.000	0.000	0.000	0.000	0.000
Mg	.086	.083	.078	.076	.043	.077	.093
Ca	0.000	0.000	0.000	.018	0.000	0.000	0.000
Na	.330	.444	.346	.372	.285	.318	.326
K	1.574	1.471	1.507	1.331	1.258	1.540	1.548
H	4.000	4.000	4.000	4.000	4.000	4.000	4.000
O	24.000	24.000	24.000	24.000	24.000	24.000	24.000

Microprobe Analyses of Staurolite

Sample #	81	81	81	81
Analysis #	24	25	26	27
SiO_2	27.55	27.35	27.21	27.56
TiO_2	.61	.44	.47	.44
Al_2O_3	52.67	52.27	53.53	53.01
Cr_2O_3	0.00	0.00	0.00	0.00
Fe_2O_3	0.00	0.00	0.00	0.00
FeO	13.53	13.39	13.16	12.97
MnO	.11	0.00	.06	0.00
MgO	2.04	1.65	1.58	1.55
CaO	0.00	0.00	0.00	0.00
Na_2O	0.00	0.00	0.00	0.00
K_2O	.04	0.00	0.00	0.00
Sum	96.55	95.10	96.01	95.53
Si	4.041	4.066	4.002	4.066
Al	1.959	1.934	1.998	1.934
Al	7.145	7.222	7.279	7.282
Ti	.067	.049	.052	.049
Cr	0.000	0.000	0.000	0.000
Fe^{+3}	0.000	0.000	0.000	0.000
Fe^{+2}	1.660	1.665	1.619	1.600
Mn	.014	0.000	.007	0.000
Mg	.446	.366	.346	.341
Ca	0.000	0.000	0.000	0.000
Na	0.000	0.000	0.000	0.000
K	.007	0.000	0.000	0.000
O	24.000	24.000	24.000	24.000

Microprobe Analyses of Kyanite

Sample #	57b	57b	57b	57b
Analysis #	43	44	45	46
SiO_2	36.44	36.47	36.85	36.00
TiO_2	0.00	0.00	0.00	0.00
Al_2O_3	61.92	61.40	61.89	60.70
Cr_2O_3	.05	0.00	.06	0.00
Fe_2O_3	0.00	0.00	0.00	0.00
FeO	.23	.15	.25	.27
MnO	0.00	0.00	.04	.08
MgO	0.00	0.00	0.00	0.00
CaO	0.00	0.00	.06	.07
Na_2O	0.00	0.00	0.00	0.00
K_2O	.10	.07	.15	.09
Sum	98.74	98.09	99.30	97.21
Si	4.787	4.818	4.817	4.807
Al	1.213	1.183	1.183	1.193
Al	8.373	8.376	8.350	8.357
Ti	0.000	0.000	0.000	0.000
Cr	.005	0.000	.006	0.000
Fe^{+3}	0.000	0.000	0.000	0.000
Fe^{+2}	.025	.017	.027	.030
Mn	0.000	0.000	.004	.009
Mg	0.000	0.000	0.000	0.000
Ca	0.000	0.000	.008	.010
Na	0.000	0.000	0.000	0.000
K	.017	.012	.025	.015
O	24.000	24.000	24.000	24.000

Microprobe Analyses of Hornblende

Sample #	37.5	37.5	37.5	37.5	37.5	37.5	37.5
Analysis #	11	12	13	16	17	18	19
SiO_2	40.63	40.95	41.07	39.99	40.02	40.01	40.52
TiO_2	.30	.31	.26	.25	.36	.23	.24
Al_2O_3	20.30	19.42	20.13	18.96	18.83	19.09	18.91
Cr_2O_3	0.00	0.00	0.00	0.00	0.00	0.00	0.00
Fe_2O_3	0.00	0.00	0.00	0.00	0.00	0.00	0.00
FeO	17.83	17.44	18.32	17.32	16.59	17.83	16.85
MnO	0.00	0.00	0.00	0.00	0.00	0.00	0.00
MgO	6.65	6.45	6.65	6.59	6.79	6.15	6.63
CaO	11.27	11.20	11.25	11.19	11.16	11.18	11.07
Na_2O	1.35	1.20	1.24	.94	1.25	1.00	1.13
K_2O	.47	.29	.42	.34	.42	.29	.36
H_2O	2.03	2.01	2.04	1.97	1.97	1.97	1.98
Sum	100.83	99.27	101.38	97.55	97.39	97.75	97.69

Microprobe Analyses of Hornblende

Sample #	38	38	38	38	38	38
Analysis #	20	21	22	23	24*	25*
SiO_2	41.35	42.45	41.95	42.25	40.06	39.61
TiO_2	.24	.12	.22	.46	.25	.39
Al_2O_3	18.47	18.25	18.17	18.42	18.47	18.45
Cr_2O_3	0.00	0.00	0.00	0.00	0.00	0.00
Fe_2O_3	0.00	0.00	0.00	0.00	0.00	0.00
FeO	18.49	18.79	19.08	18.63	23.72	22.49
MnO	.05	.05	.13	.17	.08	.13
MgO	7.16	7.49	6.96	7.70	3.81	4.62
CaO	10.68	10.72	10.80	10.93	11.22	10.84
Na_2O	1.86	1.85	1.63	1.90	1.27	1.34
K_2O	.28	.22	.20	.30	.28	.29
H_2O	2.02	2.05	2.03	2.07	1.98	1.97
Sum	100.60	101.99	101.17	102.83	101.14	100.13

* grain from within epidote-feldspar veins

Microprobe Analyses of Hornblende

Sample #	38	38	38	38
Analysis #	27	28	29*	30*
SiO_2	40.65	41.13	39.97	39.50
TiO_2	.19	.24	.13	.26
Al_2O_3	18.10	18.85	18.87	18.38
Cr_2O_3	0.00	0.00	0.00	0.00
Fe_2O_3	0.00	0.00	0.00	0.00
FeO	19.33	18.93	23.06	22.20
MnO	.18	.13	.06	0.00
MgO	7.63	6.87	3.92	4.69
CaO	9.78	10.77	11.28	10.85
Na_2O	1.43	1.67	1.38	1.45
K_2O	.20	.28	.34	.29
H_2O	2.00	2.02	1.98	1.96
Sum	99.49	100.89	100.81	99.58

* grain from within epidote-feldspar vein

Microprobe Analyses of Opaque Minerals

Sample #	38	38	38
Analysis #	2	3	4
SiO_2	11.03	0.00	0.36
TiO_2	44.64	49.69	49.05
Al_2O_3	2.68	0.00	0.00
FeO	27.15	47.26	46.04
MnO	5.83	0.52	0.68
MgO	0.00	0.00	0.00
CaO	7.81	0.11	0.26
Na_2O	0.72	0.00	0.00
K_2O	0.00	0.00	0.00
Total	99.86	97.76	96.58

Microprobe Analayses of Hornblende

Sample #	43a	43a	43a	43a	43a	43a
Analysis #	4	5	6	8	9	10
SiO_2	44.09	44.03	44.19	45.19	43.56	46.28
TiO_2	.25	.60	.44	.55	.44	.32
Al_2O_3	14.56	14.49	14.76	15.32	15.55	11.50
Cr_2O_3	0.00	0.00	.10	.11	.06	0.00
Fe_2O_3	0.00	0.00	0.00	0.00	0.00	0.00
FeO	12.85	13.15	14.56	12.93	13.01	12.15
MnO	.11	.14	.21	.36	.26	.15
MgO	11.10	11.34	10.65	11.64	10.63	12.51
CaO	11.88	12.19	11.50	11.75	11.81	12.09
Na_2O	1.17	1.20	1.62	1.79	1.34	1.00
K_2O	.27	.45	.26	.26	.28	.35
H_2O	2.03	2.05	2.05	2.10	2.04	2.04
Sum	98.31	99.64	100.34	102.00	98.98	98.39

Microprobe Analyses of Opaque Minerals

Sample #	31	31	31	31	24	24
Analysis #	1	2	3	4	1	2
SiO_2	0.12	0.11	0.00	0.00	0.00	0.00
TiO_2	52.58	52.98	51.97	52.81	52.94	52.18
Al_2O_3	0.00	0.00	0.00	0.00	0.00	0.00
FeO	45.24	45.08	45.74	46.03	46.05	45.43
MnO	0.74	0.73	0.67	.55	0.11	0.14
MgO	0.00	0.00	0.00	0.00	0.00	0.00
CaO	0.00	0.00	0.07	0.07	0.00	0.00
Na_2O	0.00	0.00	0.04	0.09	0.00	0.05
K_2O	0.00	0.00	0.00	0.00	0.05	0.00
Total	98.67	98.89	98.49	99.56	99.15	97.79

Microprobe Analyses of Opaque Minerals

Sample #	24	24	81	81	81	57b
Analysis #	3	4	1	2	4	1(r)
SiO_2	0.00	0.00	0.00	0.00	0.37	0.00
TiO_2	50.62	51.03	51.65	52.92	53.71	97.53
Al_2O_3	0.00	0.00	0.00	0.00	0.00	0.00
FeO	46.31	45.88	44.85	44.61	43.70	0.00
MnO	0.07	0.11	0.67	1.05	0.31	0.00
MgO	0.29	0.00	0.13	0.14	0.32	0.00
CaO	0.00	0.00	0.07	0.00	0.00	0.00
Na_2O	0.16	0.00	0.05	0.10	.09	0.00
K_2O	0.00	0.07	0.00	0.00	.07	0.00
Total	97.46	97.08	97.41	98.82	98.58	97.53

Note: r = rim of grain

c = core of grain

Microprobe Analyses of Opaque Minerals

Sample #	57b	37.5	37.5	37.5	38
Analysis #	1(c)	1	2	3	1
SiO_2	0.00	0.00	0.00	0.00	0.00
TiO_2	99.28	52.20	51.98	52.88	49.83
Al_2O_3	0.00	0.00	0.00	0.00	0.00
FeO	0.00	46.23	46.59	46.00	44.86
MnO	0.12	0.34	0.64	0.41	3.29
MgO	0.07	0.00	0.00	0.00	0.00
CaO	0.00	0.00	0.08	0.08	0.10
Na_2O	0.11	0.08	0.14	0.00	0.00
K_2O	0.07	0.00	0.00	0.00	0.00
Total	99.70	98.84	99.43	99.38	98.07

CHAPTER 5

METAMORPHISM

5.1 INTRODUCTION

The metasedimentary rocks exposed along the southwestern slopes of French Mountain and the gneissic rocks on the top of French Mountain show a progressive metamorphic sequence with metamorphic index minerals including chlorite, biotite, garnet, staurolite and kyanite. The Metasedimentary Complex shows mainly progressive metamorphism features with minor retrograde metamorphism along some metamorphic grain boundaries and fractures which may be observed in the garnet and staurolite. The Gneiss Complex shows extensive retrograde metamorphism with kyanite altering extensively to muscovite.

5.2 METAMORPHIC MINERAL ASSEMBLAGES

5.2.1 Metasedimentary Mineral Assemblage

The lowest grade rocks within the mapped area fall into the almandine zone near the boundary between the greenschist and epidote-amphibolite facies. The mineral assemblage of these rocks consist of quartz, plagioclase, muscovite, biotite, chlorite, garnet $\pm$ tourmaline, + ilmenite + minor apatite. Only two samples of this grade did not contain biotite. This lack of biotite is believed to be a reflection of the bulk composition of the rock because of its field relation to samples that do contain biotite. Rocks outside of the mapped area, south of Corney Brook along the coast and approximately three kilometers up the Cheticamp River have been correlated with the Metasedimentary Complex as part of

the "Jumping Brook Complex" (Currie, in press). These rocks outside of the mapped area, yet correlative with the Metasedimentary Complex, have the lowest grade mineral assemblage consisting of prehnite, epidote, actinolite and quartz for correlative volcanic units; and chlorite, epidote and quartz for correlative metasedimentary units (Currie, in press). This classifies the lowest grade rocks into the chlorite zone between the prehnite-pumpellyite and greenschist facies. South of the Cheticamp River, rocks correlative with the Jumping Brook Complex contain mineral assemblages of biotite, muscovite, chlorite $\pm$ garnet (Currie, in press), putting these rocks into the biotite zone of the greenschist facies. Within the mapped area the metamorphic grade increases from west to east up to the staurolite zone. The mineral assemblage of these rocks consists of quartz, feldspar, garnet, staurolite, muscovite, biotite and retrograde chlorite.

5.2.2 Amphibolite Assemblage

The mineral assemblage of the Amphibolite located at the top of French Mountain along the Cabot Trail consists of hornblende, biotite, plagioclase with oligoclase cores and andesine rims, epidote, minor sphene and minor opaque minerals. This mineral assemblage classifies the rock into the epidote-amphibolite facies which corresponds to the staurolite zone of the staurolite-bearing phyllites found in the immediate area.

5.2.3 Biotite-Quartz-Feldspar Gneiss Assemblage

The mineral assemblage of the gneiss is very similar to the mineral assemblage of the metasedimentary complex, except for the presence of relict kyanite, retrograde muscovite and a general lack of chlorite. Sample 57b contains relict kyanite, a minor amount of altered staurolite, oligoclase, muscovite, biotite, garnet, ilmenite and minor potassic feldspar. Andalusite and cordierite have been documented to occur at the intersection of the Cabot Trail with the Fishing Cove River (Currie, in press), however this could not be confirmed in this study, as the samples chosen for thin sectioning did not include one from that particular outcrop.

5.2.4 Amphibolite Gneiss Assemblage

The mineral assemblage of the gneiss is similar to that of the amphibolite containing hornblende, sphene, and plagioclase, minor quartz, minor epidote and very minor clinopyroxene.

5.2.5 Summary and Discussion of Assemblages

A summary of the mineral assemblages for the metamorphic rocks of the French Mountain area is given in Figure 5.1. The incoming of key index minerals is strongly dependent on the composition of the rock. The progressive metamorphic sequence is best observed in the phyllitic horizons and their gneissic equivalents, where the key metamorphic index minerals preferentially grow. The psammitic layers tend to be

Figure 5.1. Metamorphic Mineral Assemblages in the Rocks of the French Mountain Area.

Metamorphic Facies	Greenschist		Epidote-Amphibolite		Amphibolite	
Metamorphic Zones	chlorite	biotite	almandine	staurolite	kyanite	sillimanite
Approximate Temperature (°C)	350 - 550		550 - 650		650 - 800	
Metasedimentary* Complex and Quartz-Feldspar-Gneiss**						
*chlorite (prograde)	———	- -				
muscovite (prograde)	———	———	———	———	———	
biotite (prograde)	———	———	———	———	———	
almandine		———	———	———	———	
staurolite				———	- -	
**kyanite					— -	
chlorite (retrograde)	———	———	———	- - -		
**muscovite (retrograde)					— -	
sericite (retrograde)	———	———	———	———	———	
Amphibolite and Amphibolite Gneiss						
biotite				———	———	
hornblende				———	———	
epidote				———	- -	
chlorite (retrograde)					- - -	
sericite (retrograde)				———	———	
plagioclase				———	———	

Note: Because even the lowest grade rocks contained significant amounts of almandine the rocks were classified into the almandine zone of the Greenschist Facies.

devoid of index minerals; although they locally contain garnet. From this study, peak metamorphism in the rocks of French Mountain are indicated by the mineral assemblage: relict kyanite, minor staurolite, quartz, oligoclase, biotite and muscovite. Some of the muscovite is replacing kyanite, however much of the muscovite in the sample occurs away from the pre-tectonic (with respect to the pervasive schistosity) kyanite grains. Minor tourmaline and ilmenite are also present in this sample and are controlled by boron and titanium respectively.

5.2.6 Thompson AFM and ACF Diagrams

The mineral assemblages of the selected samples were plotted on the appropriate AFM or ACF diagrams. These diagrams were constructed using the data obtained from the microprobe analyses. The diagrams are given in Figure 5.2 while the data used in their construction is given in Table 5.1.

5.3 THE ORIGIN OF THE MIGMATITES AND PEGMATITES

Although local veins and pods of quartz and potassic feldspar are present within the Metasedimentary Complex, many of these are believed to be boudinaged veins. True pegmatite begins to outcrop where the first gneiss outcrops along the Fire Tower Road. Much of the pegmatite contains coarse grained potassic feldspar, "books" of biotite and muscovite, quartz and probably plagioclase feldspar. Pegmatite is quite common throughout the Gneiss Complex occurring as veins of various widths that cut across or run parallel to the pervasive

Figure 5.2. Thompson AFM and ACF Diagrams constructed from Microprobe Analyses of the Major Phases for 5 selected samples from the French Mountain Area. The microprobe data used in constructing these diagrams are given in Table 5.1. Analyses are plotted on triangular diagrams where

$A = [Al_2O_3] - 3[K_2O]$,

$F = [FeO] - [TiO_2] - [Fe_2O_3]$

$M = [MgO]$

for the AFM plot, and

$A = [Al_2O_3] - [Na_2O] - [K_2O]$

$C = [CaO] - 10/3[P_2O_5] - [CO_2]$

$F = [MgO] + [FeO] - [TiO_2] - [Fe_2O_3]$

for the ACF plot.

SAMPLE 24
(PHYLLITE OF UNIT 1,
METASEDIMENTARY COMPLEX)

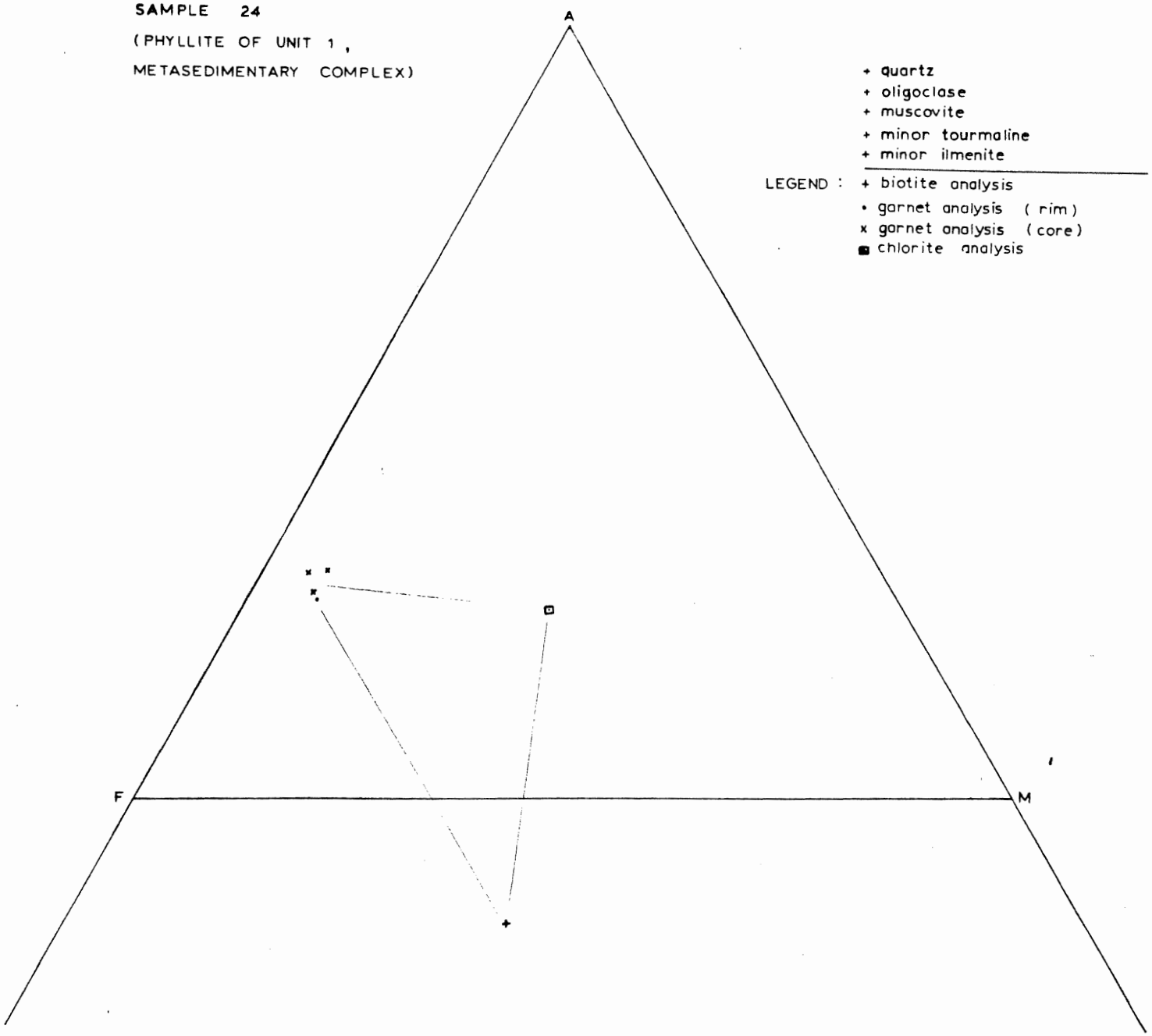

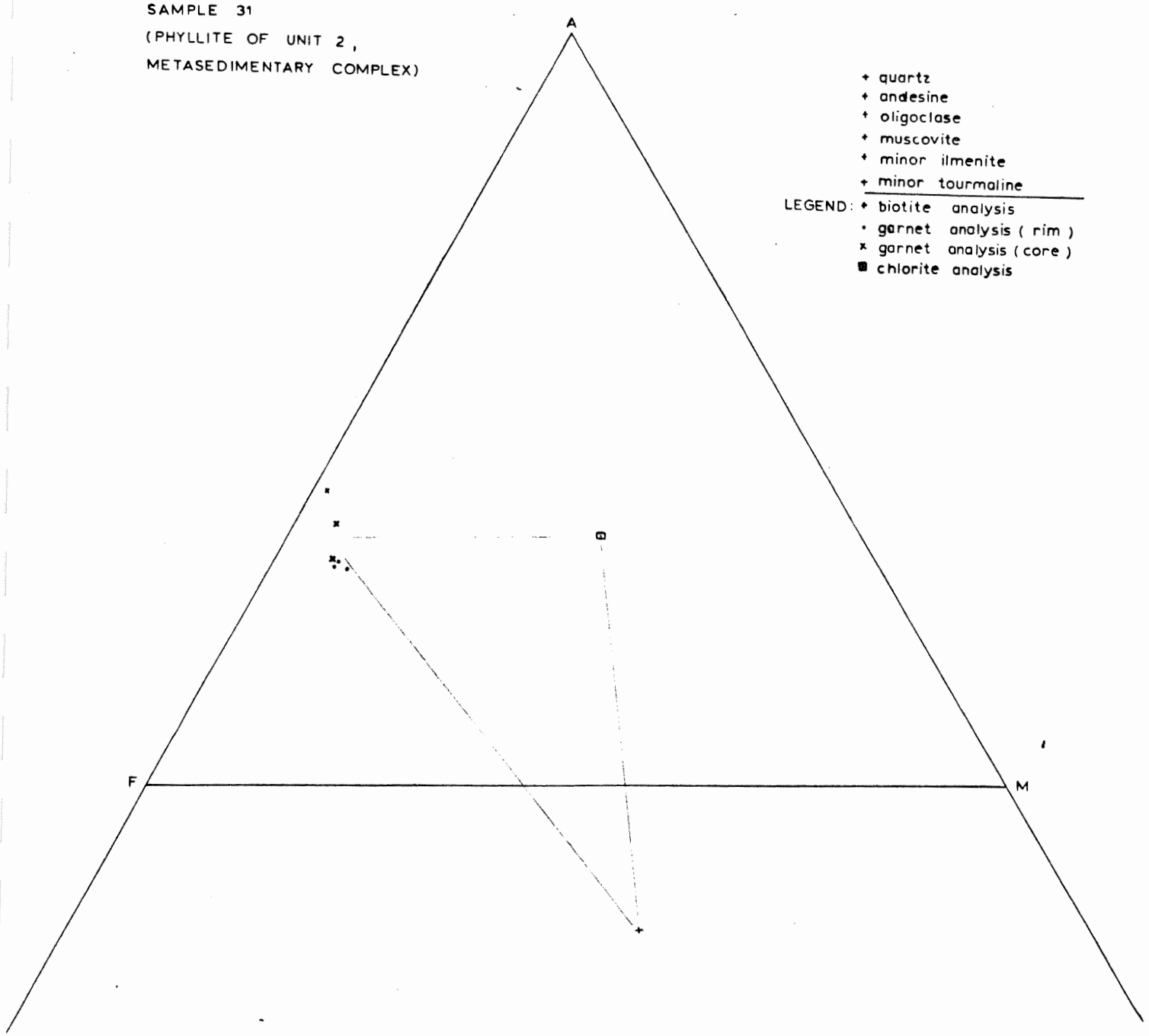
SAMPLE 31
(PHYLLITE OF UNIT 2,
METASEDIMENTARY COMPLEX)
A
F
M
+ quartz
+ andesine
+ oligoclase
+ muscovite
+ minor ilmenite
+ minor tourmaline
LEGEND: + biotite analysis
· garnet analysis (rim)
× garnet analysis (core)
■ chlorite analysis

SAMPLE 81
(STAUROLITE – BEARING PHYLLITE
OF UNIT 2, METASEDIMENTARY COMPLEX)

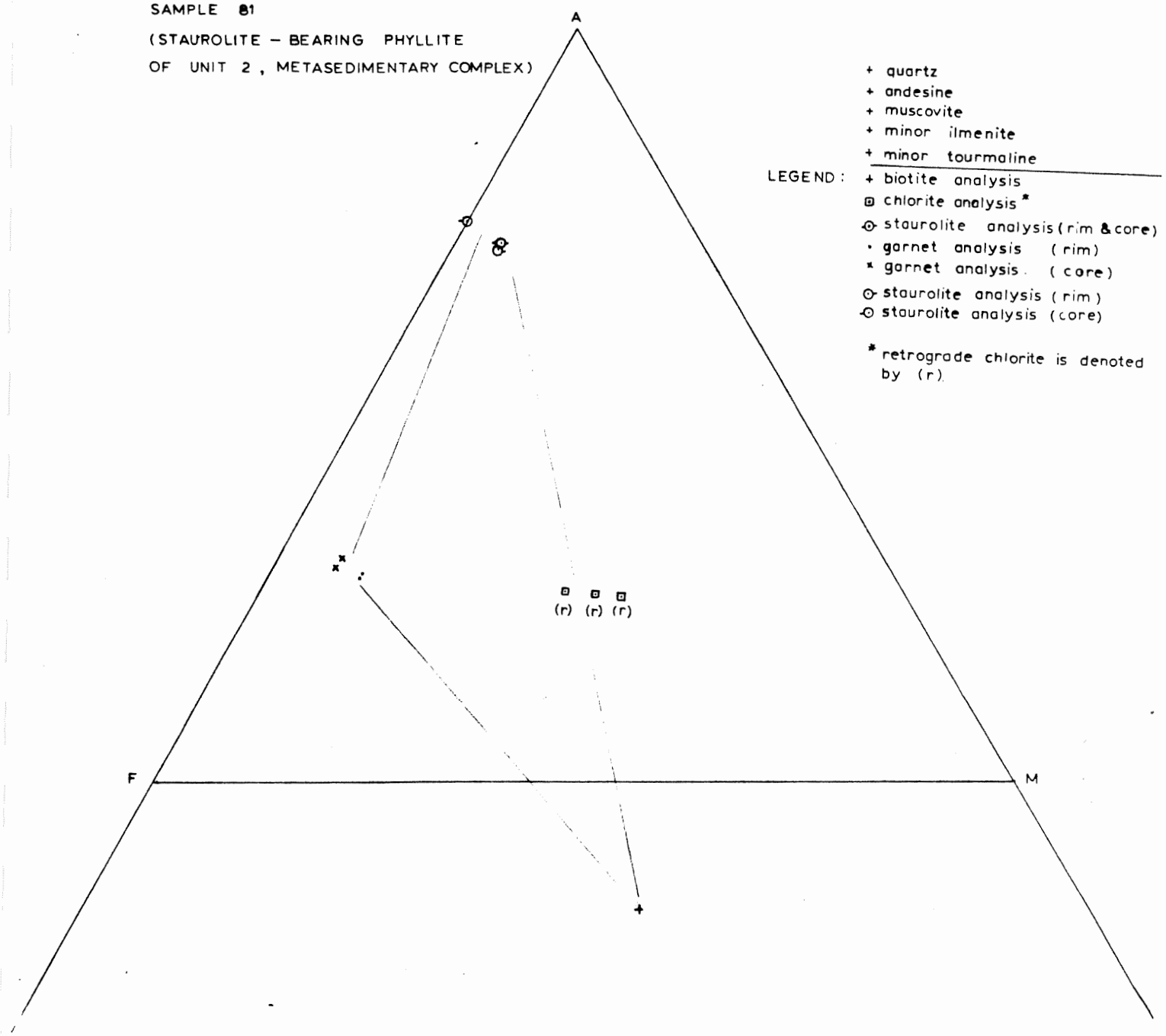

+ quartz
+ andesine
+ muscovite
+ minor ilmenite
+ minor tourmaline

LEGEND:
+ biotite analysis
⊡ chlorite analysis *
⊙ staurolite analysis (rim & core)
· garnet analysis (rim)
× garnet analysis (core)
⊙ staurolite analysis (rim)
⊙ staurolite analysis (core)

* retrograde chlorite is denoted by (r)

SAMPLE 57b
(KYANITE - BEARING QUARTZ-
FELDSPAR GNEISS)

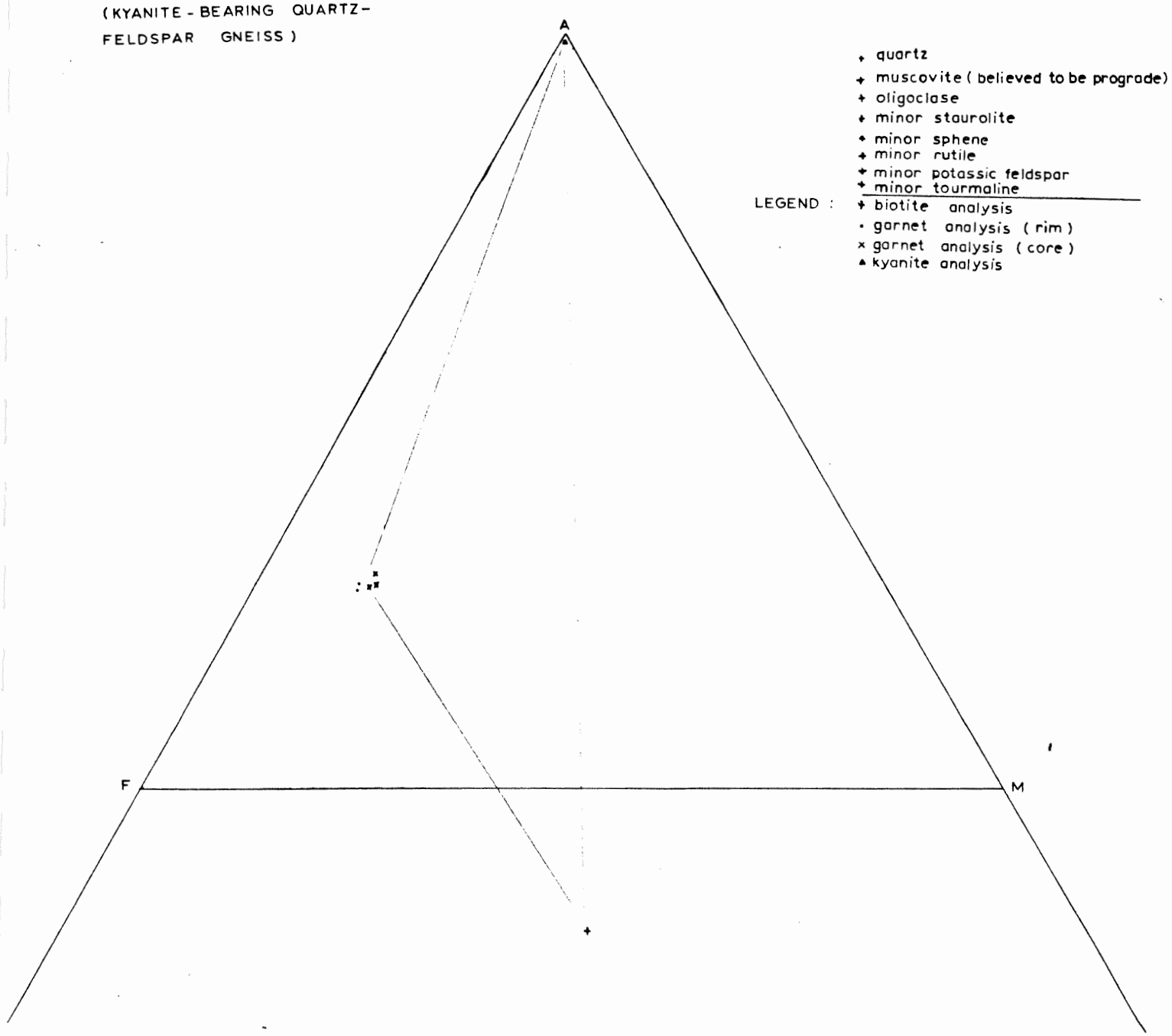

LEGEND :
- quartz
- muscovite (believed to be prograde)
- oligoclase
- minor staurolite
- minor sphene
- minor rutile
- minor potassic feldspar
- minor tourmaline

- biotite analysis
- garnet analysis (rim)
- garnet analysis (core)
- kyanite analysis

SAMPLE 43C

(AMPHIBOLITE)

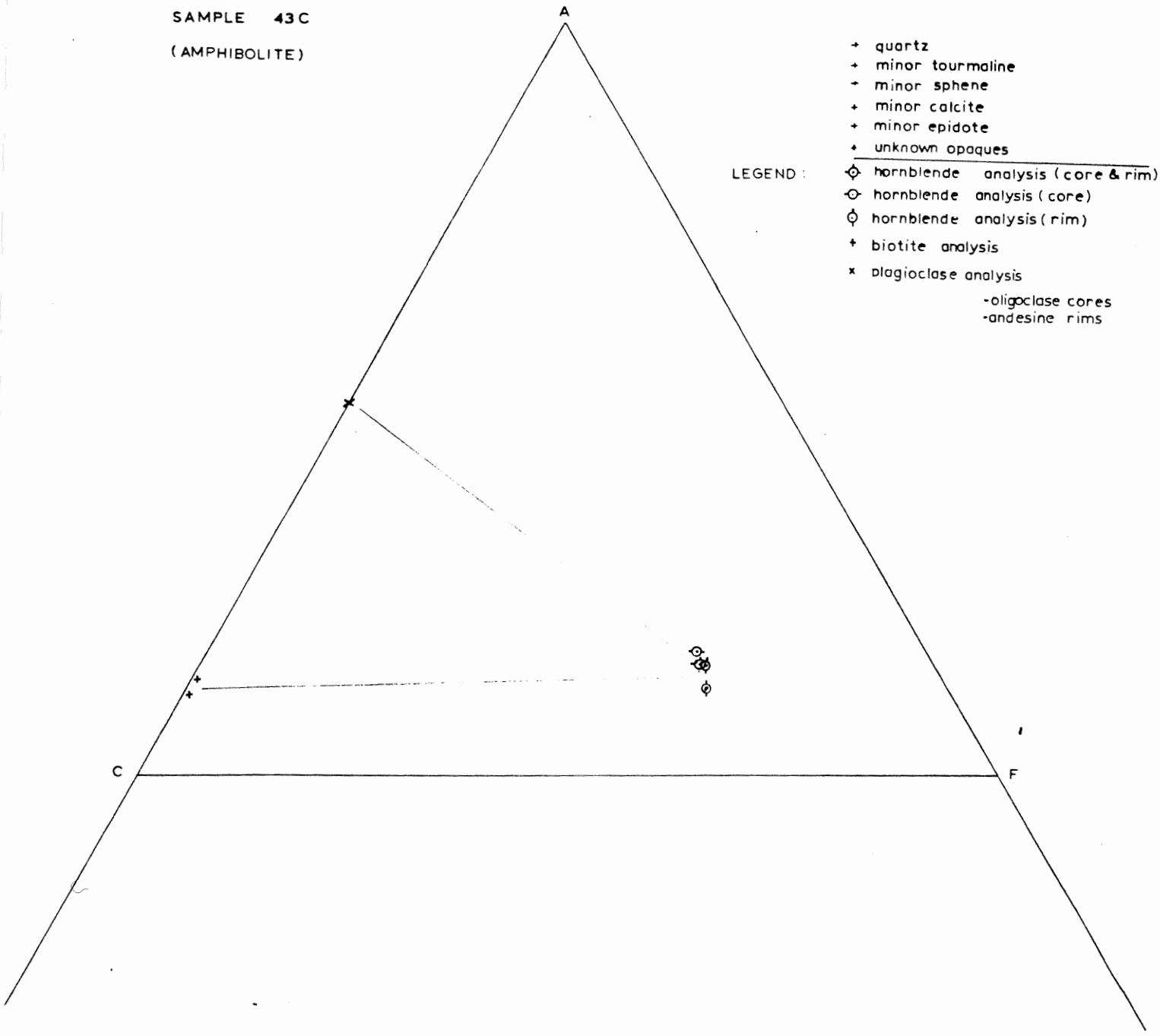

- quartz
- minor tourmaline
- minor sphene
- minor calcite
- minor epidote
- unknown opaques

LEGEND :

- hornblende analysis (core & rim)
- hornblende analysis (core)
- hornblende analysis (rim)
- biotite analysis
- plagioclase analysis
  - oligoclase cores
  - andesine rims

Table 5.1. Microprobe Analyses Data Used in the Construction of Thompson AFM and ACF Diagrams*.

* These tables consist of averages of the microprobe analyses given in Table 4.2

Table 5.1.

Mineral: biotite						
Sample	24*	31**	37.5	81	43a	57b
SiO_2	35.35	35.99	36.60	36.79	38.27	37.25
TiO_2	1.65	4.35	1.76	1.50	1.66	2.00
Al_2O_3	19.70	19.67	18.69	20.03	18.11	19.90
Cr_2O_3	0.00	0.002	0.00	0.00	0.00	0.03
Fe_2O_3	0.00	0.00	0.00	0.00	0.00	0.00
FeO	21.46	18.61	18.31	17.16	13.92	18.79
MnO	0.00	0.00	0.00	0.00	0.02	0.03
MgO	8.58	10.67	10.92	11.19	14.48	10.06
CaO	0.00	0.00	0.00	0.00	0.00	0.00
Na_2O	0.00	0.00	0.00	0.00	0.00	0.04
K_2O	8.25	8.48	9.04	8.47	9.50	8.59
H_2O	3.92	3.97	3.98	4.02	4.08	4.06

* average of 2 analyses

** average of 3 analyses

Table 5.1 (continued)

Mineral: chlorite							
Sample	24***	31*	37.5	38**	81+	81+	81+
SiO_2	24.13	24.56	24.82	25.22	24.59	23.89	24.58
TiO_2	0.02	0.02	0.00	0.02	0.00	0.08	0.08
Al_2O_3	23.82	35.76	23.49	22.32	23.92	23.98	23.64
Fe_2O_3	0.00	0.00	0.00	0.00	0.00	0.00	0.00
FeO	27.15	24.11	23.16	22.50	23.62	26.15	22.52
MnO	0.00	0.00	0.00	0.00	0.00	0.00	0.00
MgO	13.28	15.02	16.01	17.02	13.93	13.06	15.88
CaO	0.00	0.00	0.00	0.00	0.00	0.00	0.00
Na_2O	0.00	0.00	0.00	0.00	0.00	0.00	0.00
K_2O	0.00	0.00	0.00	0.00	0.17	0.05	0.00
H_2O	11.38	11.46	11.50	11.48	11.31	11.27	11.43

* average of 2 analyses

** average of 3 analyses

*** average of 4 analyses

\+ retrograde chlorite

Table 5.1 (continued)

Mineral: staurolite			
Sample	81	81	81
SiO_2	27.55	27.35	27.21
TiO_2	0.61	0.44	0.47
Al_2O_3	52.67	52.27	53.53
Cr_2O_3	0.00	0.00	0.00
Fe_2O_3	0.00	0.00	0.00
FeO	13.53	13.39	13.16
MnO	0.11	0.00	0.06
MgO	2.04	1.65	1.58
CaO	0.00	0.00	0.00
Na_2O	0.00	0.00	0.00
K_2O	0.04	0.00	0.00
Sum	99.55	95.10	96.01

Table 5.1 (continued)

Mineral: kyanite				
Sample	57b	57b	57b	57b
SiO_2	36.44	36.47	36.85	36.00
TiO_2	0.00	0.00	0.00	0.00
Al_2O_3	61.92	61.40	61.89	60.70
Cr_2O_3	0.05	0.00	0.06	0.00
Fe_2O_3	0.00	0.00	0.00	0.00
FeO	0.23	0.15	0.25	0.27
MnO	0.00	0.00	0.04	0.08
MgO	0.00	0.00	0.00	0.00
CaO	0.00	0.00	0.06	0.07
Na_2O	0.00	0.00	0.00	0.00
K_2O	0.10	0.07	0.15	0.09
Sum	98.74	98.09	99.30	97.21

Table 5.1 (continued)

Mineral: feldspar						
Sample	43a	43a	43a	43a	43a	43a
SiO_2	60.92	59.10	60.17	57.79	62.31	57.28
TiO_2	0.00	0.00	0.00	0.00	0.00	0.00
Al_2O_3	23.99	26.28	24.06	25.88	23.53	25.56
Cr_2O_3	0.00	0.00	0.00	0.00	0.00	0.00
Fe_2O_3	0.00	0.00	0.00	0.00	0.00	0.00
FeO	0.00	0.10	0.00	0.00	0.00	0.61
MnO	0.00	0.00	0.00	0.00	0.00	0.00
MgO	0.00	0.00	0.00	0.00	0.00	0.40
CaO	5.77	8.06	5.95	7.90	4.82	8.68
Na_2O	8.28	7.15	8.14	7.03	9.08	6.69
K_2O	0.00	0.23	0.12	0.00	0.06	0.08

Table 5.1 (continued)

Mineral: hornblende				
Sample	43a*	43a	43a	43a
SiO_2	44.10	45.19	43.56	46.28
TiO_2	0.43	0.55	0.44	0.32
Al_2O_3	14.60	15.32	15.55	11.50
Cr_2O_3	0.03	0.11	0.06	0.00
Fe_2O_3	0.00	0.00	0.00	0.00
FeO	13.52	12,93	13.01	12.15
MnO	0.15	0.36	0.26	0.15
MgO	11.03	11.64	10.63	12.51
CaO	11.86	11.75	11.81	12.09
Na_2O	1.33	1.79	1.34	1.00
K_2O	0.33	0.26	0.28	0.35
H_2O	2.04	2.10	2.04	2.04

* average of 3 analyses

foliation of the gneiss. Grain size within the pegmatite varies from being fine grained to very coarse grained with potassic feldspar grains up to 4 centimeters in size. Some pegmatite contains garnet (e.g. sample 45a). Some of the granite dykes throughout the gneiss may actually be fine grained pegmatite and the potassic feldspar augen gneiss may actually be foliated and sheared pegmatite. Large potassic feldspar "eyes" can sometimes be observed within the biotite-quartz-feldspar gneiss (e.g. sample 53). These "eyes" are wrapped around by the pervasive foliation of the gneiss. The question of origin of these pegmatites is thus posed. Is the pegmatite injected into the gneiss as evidenced by those dykes cross-cutting the foliation of the gneiss or are they segregated from the gneiss as leucosomatic material?

Migmatitic textures were observed in the gneiss and are best displayed along the northern part of the Fire Tower Road, where highly contorted leucosomes can be seen. Some of these leucosomes are bounded by biotite-rich melanosomes, which are interpreted to be residual material after anatexis (Mehnert, 1968). The question is also posed whether these migmatites formed via anatexis or via metamorphic segregation.

The leucosomes are mainly white and are most likely composed of plagioclase along with quartz. They may be ptygmatically folded.

Four mechanisms have been proposed for the development of the thin leucosomes and larger pegmatites: 1) metamorphic segregation, 2) in situ partial melting of the parent rock or anatexis, 3) igneous injection

of granitic magma from outside the parent rock and 4) "external metasomatism" which involves the infiltration of a fluid into the rock (Yardley, 1978).

Currie (in press) proposes that many of the granitic "schlieren" within the Jumping Brook Complex and Pleasant Bay Complex may have resulted from anatexis. Currie claims that on the basis of the mineral assemblages, metamorphic conditions may have reached 650°C at 3 to 4 kilobars, which he claims is adequate for partial melting.

Studies done by Craw (in press) in the Cheticamp River area, suggest that the leucosomes did not form via anatexis but owe their origin to hydrothermally-induced metamorphic segregation. Much of this conclusion was based on the lack of potassic feldspar in the leucosomes. Craw (in press) concludes that the high grade pelitic assemblages of the Jumping Brook Complex, exposed along the Cheticamp River, had a maximum metamorphic temperature near to 550°C and a maximum pressure between 4 and 5 kilobars, and claims that such temperatures are too low for anatexis to have occurred.

Although a detailed study of the migmatites is beyond the scope of this study, metamorphic assemblages of the kyanite-bearing gneiss suggest that temperatures were approximately 650°C and the geothermometers indicate temperatures were between 600°C and 630°C, which is sufficiently high for anatexis to have occurred according to "wet" melting of muscovite-bearing pelites (Thompson, 1982). Although potassic feldspar is present in the gneissic rocks it does not appear

to be overly abundant. Temperatures greater than 700°C have been proposed for the experimental melting of biotite-plagioclase (An_{50})-quartz mixtures (Hoschek, 1976). Anatectic reactions invoked by Hoschek (1976) produce significant amounts of potassic feldspar in the leucosome. Melanosomes in the migmatites of French Mountain are rare. Because the leucosomes in the migmatites of French Mountain appear to contain only limited amounts of potassic feldspar it is most likely that they formed as a result of metamorphic segregation or the introduction of a fluid from outside the rock.

The pegmatites that cross-cut the pervasive foliation have most likely been injected into the gneiss as the boundaries between the pegmatite and gneiss are sharp. The origin of the pegmatite that occurs as pods wrapped around by the pervasive foliation or as "veins" running parallel to the foliation of the gneiss remains unresolved.

5.4 CONDITIONS OF METAMORPHISM

A sequence of progressive metamorphism is observed in the metasedimentary rocks of the southwestern slopes of French Mountain. Petrologic study of selected samples indicate that the garnet is syn-tectonic, the biotite early syn-tectonic and the staurolite late syn- to post-tectonic with respect to the pervasive schistosity. Metamorphism is therefore interpreted to begin during the early stages of deformation and continue into the last stages and possibly after deformation ceased if the staurolite is truly post-tectonic to the pervasive schistosity. A summary table of the discussion between the index minerals and

deformational fabrics of Chapter 3 is given in Table 5.2. It is unknown whether the pervasive schistosity of the gneiss was developed by the same event that produced the schistosity of the metasedimentary rocks and so the two have been considered separately. The Metasedimentary Complex shows mainly progressive metamorphism with limited local retrogressive metamorphism. Interpretation of the relationship between the kyanite and the fabric is somewhat difficult because only a few grains were observed. The fact that they are generally highly fractured and show alteration to muscovite leads to their interpretation as being pre-tectonic to the pervasive schistosity and that the Gneiss Complex has undergone extensive retrogression.

There are a number of possible chemical reactions that result in the formation of staurolite and kyanite during progressive metamorphism.

The following reactions have been proposed for the formation of staurolite:

*(1) chlorite + muscovite = staurolite + biotite + quartz + $H_2O_{(v)}$ (Hoschek, 1969)

*(2) chloritoid + aluminum silicate (andalusite, kyanite) = staurolite + quartz + $H_2O_{(v)}$ (Hoschek, 1969)

*(3) chloritoid + quartz = staurolite + garnet + $H_2O_{(v)}$ (Hoschek, 1969)

*(4) chloritoid + chlorite + muscovite = staurolite + biotite + quartz + $H_2O_{(v)}$ (Hoschek, 1969)

(5) chlorite + garnet + muscovite = staurolite + biotite + quartz + $H_2O_{(v)}$ (Albee, 1965; Carmichael, 1969)

* reactions that have been experimentally demonstrated.

Table 5.2. Index Mineral-Fabric Relationships

Metamorphic Mineral	Tectonic relationship to the schistosity in metasedimentary rocks	Tectonic relationship to the schistosity in the gneissic rocks
chlorite (prograde)	syn- (locally post)	absent
biotite	early syn- (locally post)	syn-
muscovite (prograde)	syn-	syn-
garnet	mainly syn- (few pre-)	syn- (locally pre-)
staurolite	late syn- to post-	?
kyanite	absent	pre-

? = difficult to determine relationship because of too few grains

Because the rocks of the Metasedimentary Complex do not contain chloritoid, reactions (1) and (5) are most favored for the formation of the staurolite in the rocks of French Mountain. Reaction (5) requires that the formation of the staurolite occurred at the expense of the garnet. No decrease in the percent of garnet was observed in the staurolite-bearing phyllite. Therefore reaction (1) appears to be the most likely reaction resulting in the formation of the staurolite. This reaction is confirmed by the AFM diagram in Figure 5.3. From Figure 5.3 the tie-line between garnet and chlorite of sample 31 is replaced by the tie-line between biotite and staurolite in sample 81. This is schematically shown in Figure 5.4. Garnet is present in both assemblages and the reaction from the assemblages suggests that the chlorite reacted with muscovite to yield staurolite and biotite. A decrease in muscovite and increase in biotite was noted between samples 31 and 81 which also confirms the likeliness of this reaction over other possible reactions. Although not evident in the point counting tables sample 81 can contain up to 25 percent biotite in specific horizons compared to sample 31 which contains approximately 10 percent biotite.

The formation of kyanite is grouped into two sets of possible reactions, those that involve the breakdown of staurolite and those that do not. The following reactions have been proposed:

(6) staurolite + muscovite + quartz = aluminium silicate + biotite + $H_2O_{(v)}$ (Hoschek, 1969)

Figure 5.3. Plots from Figure 5.2 superimposed on AFM diagram.

MINERAL ASSEMBLAGES OF
SAMPLES 24 , 31 , 81 , and 57b

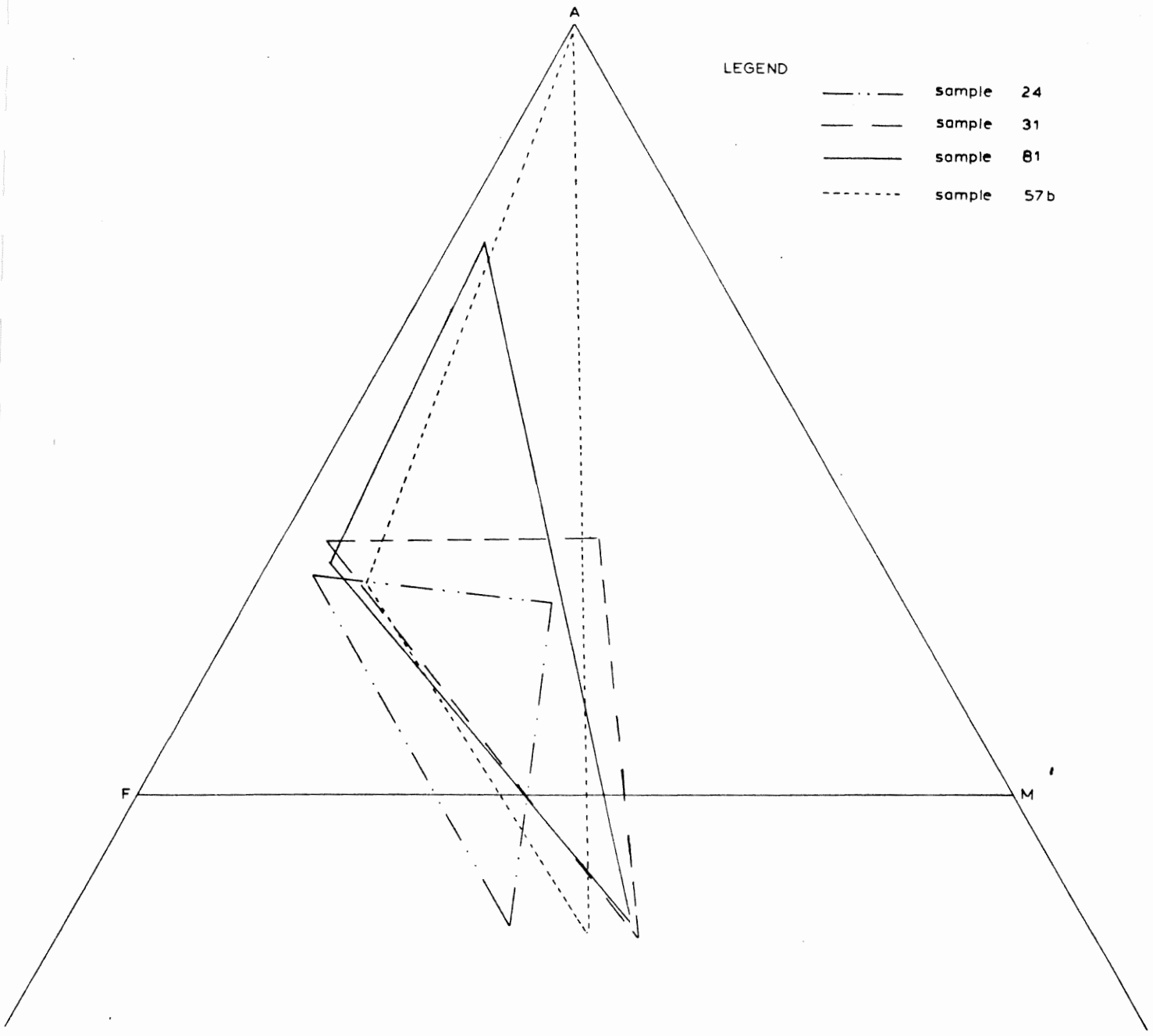

Figure 5.4. The change in the tie-lines between minerals from sample 31 to sample 81 suggest that reaction (1) was the one involved in the formation of the staurolite in Unit 2 of the Metasedimentary Complex.

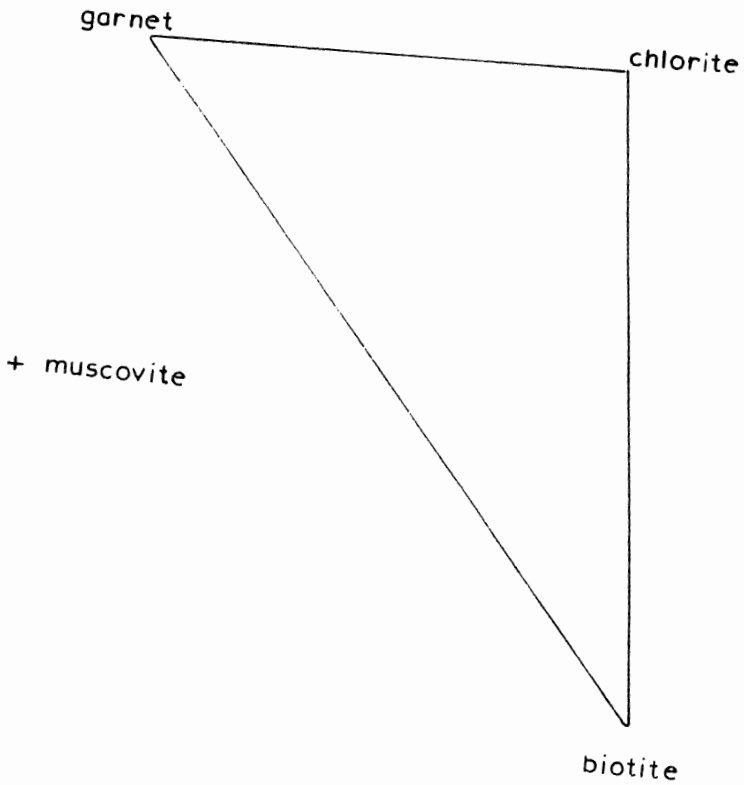

SAMPLE 31

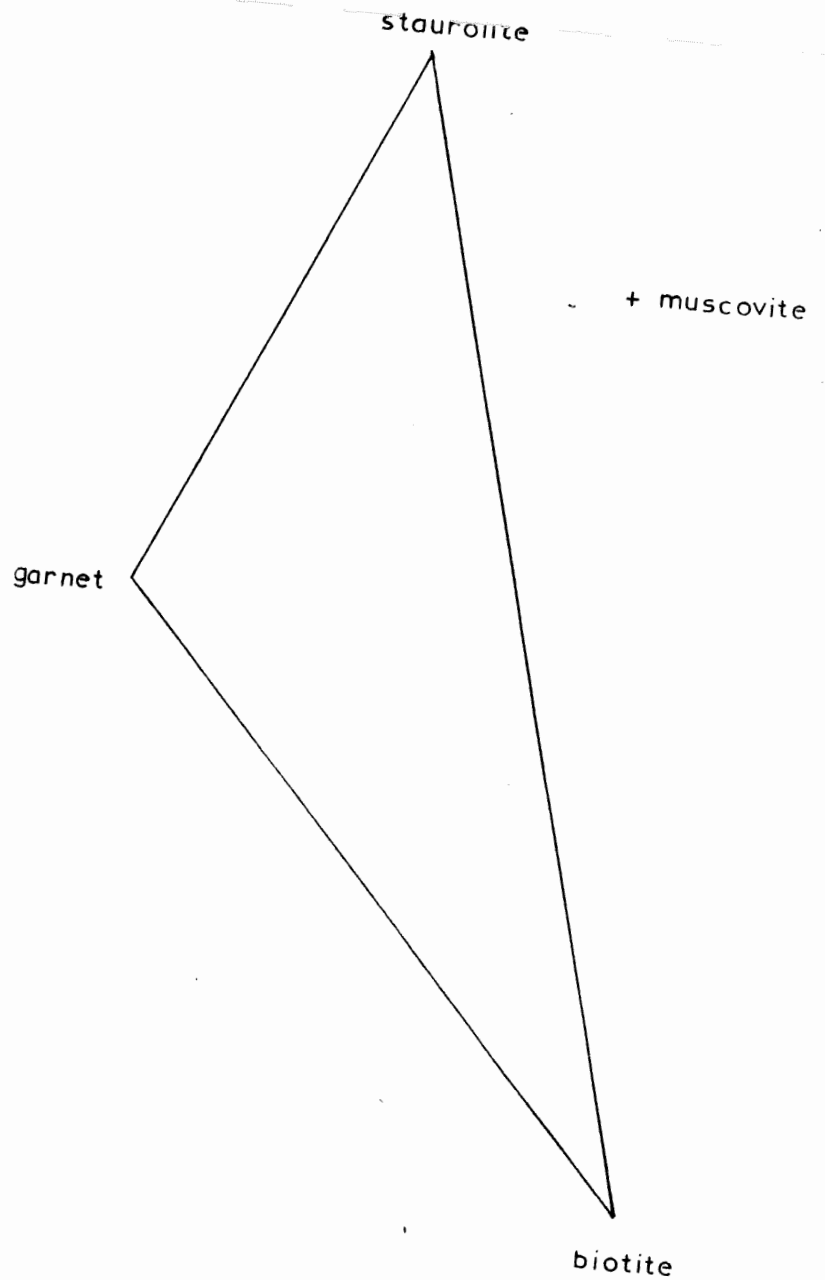

SAMPLE 81

(7) staurolite + quartz = aluminium silicate + garnet + $H_2O_{(v)}$

(Hoschek, 1969)

(8) staurolite + muscovite + quartz = aluminium silicate + biotite + garnet + $H_2O_{(v)}$ (Hoschek, 1969)

(9) staurolite + muscovite = biotite + kyanite + $H_2O_{(v)}$

(Nockolds, et al., 1979, p. 400)

(10) staurolite + chlorite + muscovite = aluminium silicate + quartz + $H_2O_{(v)}$ (Hoschek, 1969)

(11) chlorite + muscovite + quartz = kyanite + biotite + H_2O

(Carmichael, 1969)

(12) chlorite + muscovite = kyanite + phlogopite + quartz + H_2O

(Bird et al., 1973)

(13) muscovite + Na-feldspar + quartz = K-feldspar + aluminium silicate + melt (Doucet, 1983)

Reactions (10) to (12) require that kyanite is formed at the expense of chlorite. If the gneiss is part of the progressive metamorphic sequence found within the metasedimentary rocks than reactions (10) to (12) are unlikely to be the ones involved in the formation of kyanite as the staurolite-bearing phyllite does not contain significant amounts of chlorite that could be used in the reaction. The relation between the staurolite and the kyanite is difficult to assess, as only one grain of altered staurolite was observed in the kyanite-bearing gneiss and this grain was not in contact with the kyanite. Reactions (6) and (8) fall into the sillimanite stability field and because there is no significant amount of sillimanite in the rocks of French Mountain,

these reactions are unlikely to be the ones involved in the formation of the kyanite. It is therefore unresolved from this study how the kyanite formed. Doucet (1983) found that boundaries between kyanite and staurolite in the Middle River area, are gradational and determination of the reactions (if any) between these two phases was inconclusive. If reaction (13) were correct, one would expect to find significant amounts of potassic feldspar in the gneiss, which is not the case. Although potassic feldspar is present, it is not a major phase.

Approximate pressure-temperature paths for the rock of the French Mountain area is given in Figure 5.5. The pressure-temperature path is drawn as such, because reaction (1) is believed to be the reaction involved in the formation of the staurolite and either reaction (13) or (7) are possibly the most likely reactions involved in the formation of the kyanite. Chlorite is a retrograde phase in the highest grade metasedimentary rocks and so reactions involving chlorite are unlikely. In both reactions (13) and (7), significant amounts of potassic feldspar are produced. Although potassic feldspar is present in the gneiss it does not occur in significant quantities in the kyanite-bearing gneiss. The potassic feldspar may be replaced by a retrograde muscovite. The "return" path represents the rather extensive alteration of kyanite to muscovite (with very minor biotite) and the local retrograde alteration of staurolite to chlorite, garnet to chlorite and biotite to chlorite. The progressive P-T path is not well constrained with respect to the pressure, however the retrograde muscovite replacing the kyanite marks peak metamorphic conditions and the retrograde path is constrained by the minor amount of sillimanite in the staurolite-bearing phyllite.

Figure 5.5. Approximate pressure temperature paths of the rocks of the French Mountain area. The triple point for the Al_2SiO_5 system is according to Holdaway (1971). The reaction data are from the following sources: (1)(5) and (7), Hoschek (1969), (2) Bird and Fawcett, (1973); (3) and (4), Doucet, (1983); (6) Thompson, (1973).

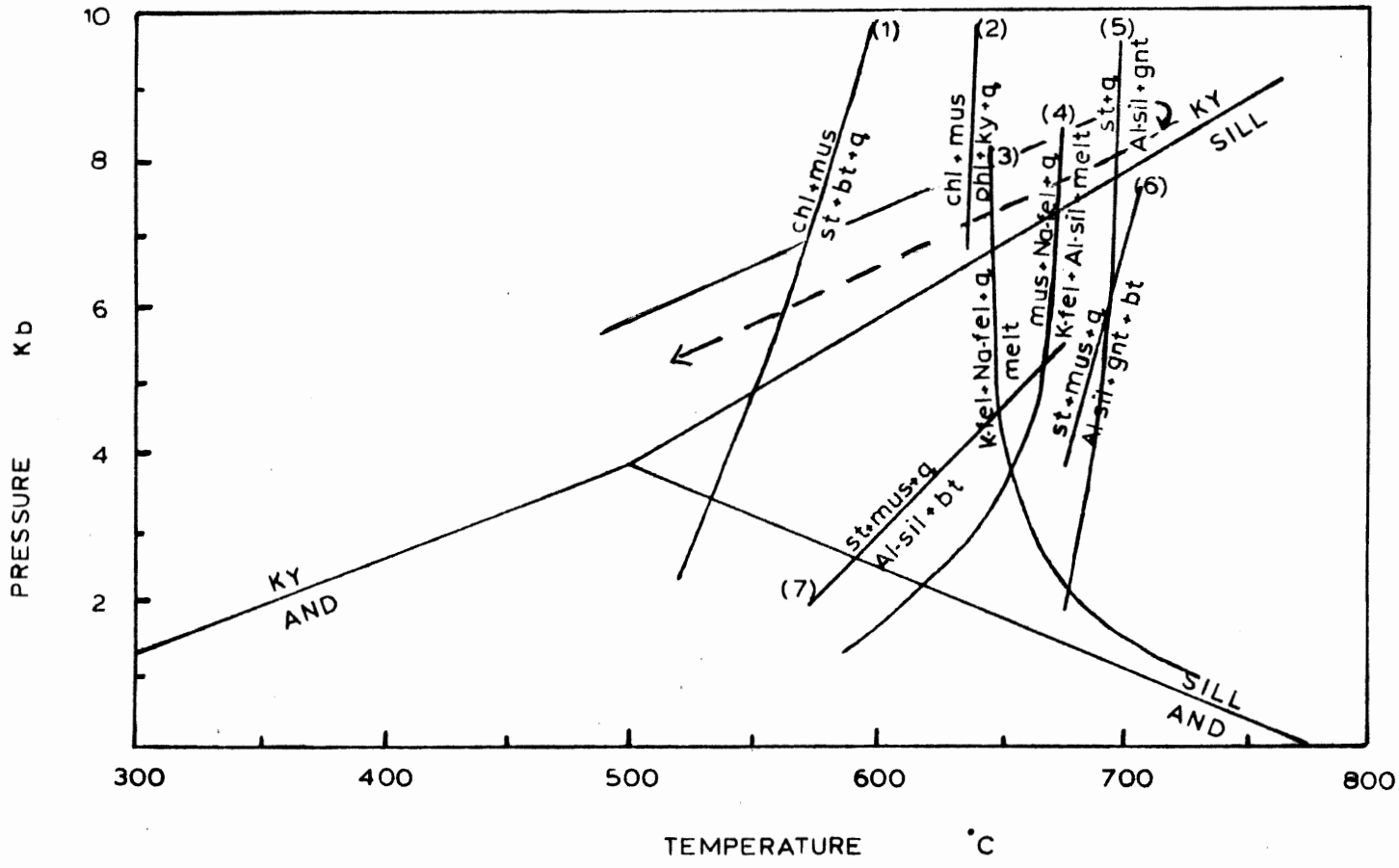

figure 5.5

Approximate pressure temperature paths of the rocks of the French Mountain area. The triple point for the Al_2SiO_5 system is according to Holdaway (1971). The reaction data are from the following sources: (1) (5) and (7), Hoschek (1969); (2) Bird and Fawcett, (1973); (3) and (4), Doucet, (1983); (6) Thompson, (1973).

Diagram after Doucet (1983)

5.5 TIMING OF METAMORPHISM

Limited age dating has been done in the French Mountain area. Muscovite from pegmatites near the head of Fishing Cove Trail yield Acadian ages (395 million years) (VanBreeman, pers. comm., 1984). An acid dyke located south of the mapped area at Grande Falaise has been interpreted to feed the basal volcanics of the Jumping Brook Complex (Currie, in press). This dyke was sampled for zircons and the data from the zircon analysis could be interpreted to give an age of 439 ± 7 million years (late Ordovician) or 500 million years (late Precambrian) because of the close proximity of the data points on the concordia diagram (Currie, in press). A potassium-argon age on the biotite from this dyke yielded an age of 363 ± 9 million years (Currie, in press). Currie concludes that the Jumping Brook Complex is of Ordovician age. Although the zircon age represents the age of intrusion evidence linking this dyke to the volcanic rocks of the Jumping Brook Complex is tenuous (Jamieson, in press). Currie documented a dyke of the Corney Brook Complex being truncated by the schists of the Jumping Brook Complex in the French Mountain area. The Corney Brook pluton has yielded a $^{87}Sr/^{86}Sr$ age of 550 ± 60 million years. Currie (in press) has proposed that this pluton intrudes the Pleasant Bay Complex but is younger than the Jumping Brook Complex. The date was confirmed; as a Cambrian age was obtained by Barr (pers. comm. 1984). The fact that the pluton is undeformed with no fabric suggests that it is more likely to post-date the Jumping Brook Complex which is highly foliated.

5.6 SUMMARY

The metamorphic rocks of the French Mountain area show a progressive metamorphic sequence with index minerals from chlorite to kyanite. Metamorphism is believed to have begun in the early stages of deformation as indicated by the biotite which is interpreted to be early syn-tectonic to the pervasive schistosity. Metamorphism continued into the late stages of deformation or even after deformation ceased as indicated by the staurolite which is interpreted to be late syn- or post-tectonic to the pervasive schistosity of the metasedimentary rocks. The kyanite within the gneiss is interpreted to be pretectonic to the pervasive foliation of the gneiss. It is unknown if the pervasive schistosity of the metasedimentary complex was developed by the same deformational event that developed the pervasive schistosity of the gneiss complex. If the kyanite present in the gneiss belongs to the metamorphic sequence that is present in the metasedimentary complex, then the pervasive schistosity of the gneiss (Sg) would not be equal to the pervasive schistosity of the metasedimentary rocks (Sm). This is indicated by the staurolite being post-tectonic to (Sm) and kyanite being pretectonic to (Sg). Peak metamorphism was indicated by the kyanite index mineral, and according to garnet-biotite geothermometers temperatures reached approximately 630°C. Because of the lack of potassic feldspar within the leucosomes of the migmatites within the gneiss, leucosomes are believed to have formed from either introduction of a fluid from outside the rock, or as a result of metamorphic segregation.

CHAPTER 6

DISCUSSION AND CONCLUSIONS

6.1 INTRODUCTION

The rocks of the French Mountain area, have been subdivided in this study into two units, distinguished by metamorphic grade: the Metasedimentary Complex and the Gneiss Complex. Mineralogically, except for the presence of key index minerals, the two units are the same. The Metasedimentary Complex consists of interlayered psammite, semi-pelite and phyllite. The gneiss also consists of varying amounts of micaceous minerals, quartz and feldspar, although some of this variation may be a reflection of metamorphic segregation.

6.2 FIELD RELATIONS, STRATIGRAPHY AND GEOLOGICAL HISTORY

The alternating horizons of psammite, phyllite and semi-pelite within the Metasedimentary Complex suggest that the original deposition of sediment involved interlayering of fine grained shale, siltstone and coarse grained sandstones. The amphibolitic horizons found throughout the sequence are generally non-foliated, however depending on the amount of biotite present in the rocks, they may be well foliated. These are interpreted as either volcanic interruptions during the deposition of the sediments or later basic intrusions that penetrated the metasediments. The rather gradational contact between the hornblende-rich psammite and amphibolite suggests that at least some of the amphibolite was probably due to periodic volcanism during the time of deposition of the sediments. The compositional layering on the centimeter scale characteristic of Unit 2 of the Metasedimentary Complex may represent original bedding or

metamorphic segregation. The fine grain size of these rocks suggest that they are not a gneiss, however no sedimentary features are preserved. Unit 1 of the Metasedimentary Complex contained graded bedding in one location, however because of local isoclinal folding and contradictory indications, "way up" directions could not be determined with confidence.

The Composite Gneiss Complex consists of three subunits: biotite-quartz-feldspar gneiss, potassic feldspar augen gneiss, and amphibolite augen gneiss. The biotite-quartz-feldspar gneiss is believed to be a paragneiss because of its similar mineralogy to the Metasedimentary Complex and the fact that local areas within the gneiss are fine grained and schistose, similar to the metasedimentary rocks. In this study the gneiss is believed to have been deposited in a similar fashion to the metasedimentary rocks. The amphibolite gneisses are believed to be local intrusions of basic dykes or periodic volcanism during deposition, and the augen gneiss is interpreted to be foliated and sheared pegmatite intrusions or segregations.

Determination of the stratigraphy is hampered by the lack of outcrop within the area. Structurally the Metasedimentary Complex is located at the bottom of the sequence and the Gneiss Complex is located at the top.

6.3 STRUCTURE

Structural elements within the Metasedimentary Complex include a pervasive schistosity, biotite mineral lineation, crenulations, minor folds and a large scale fold which folds both Units 1 and 2 of the complex. The pervasive foliation strikes northeast-southwest dipping moderately to the northwest in the west but swings northwest-southeast dipping moderately to the northeast, in the east. Minor folds and crenulations plunge shallowly to the north, while the mineral lineations generally plunge shallowly to the northeast. Rare kinks were observed, however an orientation could not be obtained.

Structural elements within the gneiss include the pervasive schistosity which strikes consistently north-south dipping steeply to the east. Minor folds, tight to isoclinal, generally plunge shallowly to moderately to the east-southeast. Poorly preserved crenulations were observed but no orientation was obtained.

The gneiss has at least three phases of deformation while the metasedimentary rocks have at least two phases. It is not known whether the pervasive schistosity of the Metasedimentary Complex was developed by the same "event" that produced the pervasive schistosity of the gneiss. The orientations of the structural elements are quite different between the two Complexes, which strongly suggests that some sort of structural break exists between the two Complexes. The steeper dip of the foliation found within the gneiss suggests that thrusting of the gneiss over the metasedimentary rocks may have occurred, but because

over a kilometer of land devoid of outcrop exists between the Metasedimentary and the Gneiss Complexes, the nature of the contact is unknown. From the data collected in this study it appears unlikely that the metasediments overlie the gneiss. Although it has been proposed that the whole sequence is overturned with the nose of the fold plunging to the west (Currie, in press), none of the data obtained within the mapped area confirmed this. If the sequence is truly overturned then the sediments may overlie the gneiss (Figure 6.1). The distinctly different orientation in the structural elements between the two complexes suggest that the two were not folded together in a manner as displayed in Figure 6.1. More likely it appears that the Gneiss was moved into its present position either during or after the folding of the Metasedimentary Complex. This view is favored because of the steeper dip of the foliation within the gneiss and the fact that the orientation of the structural elements is significantly different between the two Complexes. The question of whether the Gneiss and Metasedimentary Complexes represent a single protolithic package is not answered by the structure of the area.

6.4 METAMORPHISM

The Metasedimentary Complex shows a progressive metamorphic sequence by the presence of key metamorphic index minerals including chlorite, biotite, garnet and staurolite. The grade of metamorphism increases "downward" into the sequence. Metamorphism is interpreted to

Figure 6.1. The Jumping Brook and Pleasant Bay Complexes Overturned and Plunging to the West.

PRESENT SITUATION :

(in the French Mountain area)

The Jumping Brook Complex is isoclinally folded and the nose outcrops north of Grande Falaise. Such recumbent folds cannot be demonstrated to affect the Pleasant Bay Complex (Currie, in press).

SITUATIONS:

(folding of only the Metasedimentary Complex)

(1)

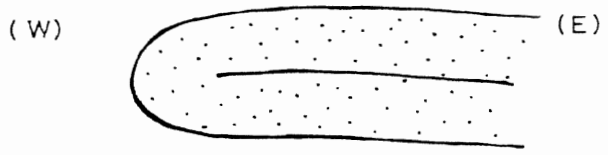

(folding of Metasedimentary and Gneiss Complexes.

(2)

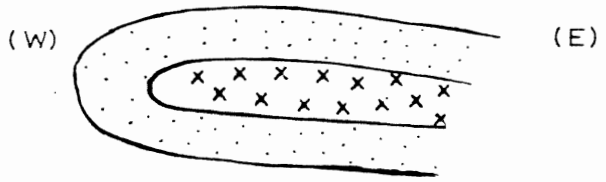

The Metasedimentary Complex is refolded along upright folds plunging to the north (Currie, in press).

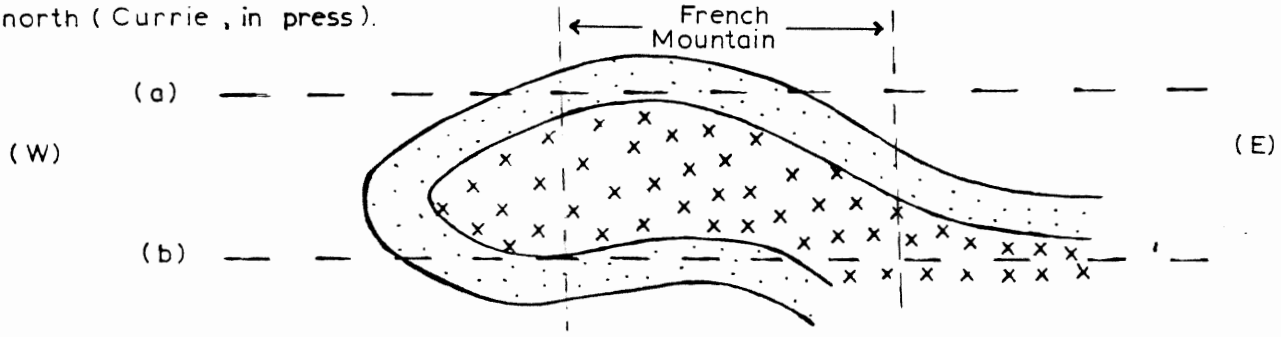

THERE ARE TWO POSSIBILITIES TO EXPLAIN THE PRESENT SITUATION :

- If the present situation represents erosion at level (a) then the gneiss is unlikely to underlie the metasedimentary rocks unless the metasedimentary rocks were 'peeled' off of the gneiss during the recumbent folding.

- If the present situation represents erosion at level (b) then the gneiss most likely underlies the metasedimentary rocks and was folded with the unit unless again the metasedimentary rocks were "peeled" off of the gneiss during the recumbent folding.

have begun during the early stages of deformation as indicated by many of the garnets which are interpreted to be syn-tectonic to the pervasive schistosity of the Metasedimentary Complex. Metamorphism continued into the later stages and possibly after deformation ceased as indicated by the presence of the late syn- to post-tectonic staurolite within Unit 2. Only limited retrograde metamorphism was observed within the rocks and was indicated by garnet, staurolite and biotite altering to chlorite along grain boundaries and fractures.

The Gneiss Complex shows a more extensive retrograde metamorphism as indicated by kyanite, interpreted to be pre-tectonic to the schistosity of the Gneiss Complex, altering extensively to muscovite. If the kyanite developed during the formation of the index minerals within the Metasedimentary Complex, then the schistosity within the gneiss (Sg) did not form at the same time as the schistosity within the metasedimentary rocks (Sm); and (Sg) would have to post date (Sm). Unfortunately it is not known whether the kyanite belongs to the metamorphic sequence indicated by the other index minerals or is the result of an earlier metamorphic "event", or whether (Sg) = (Sm).

6.5 BASEMENT - COVER RELATIONS

Data obtained within the French Mountain area do little to help in answering the question of basement-cover relations. The large area devoid of outcrop separating the two complexes is a major problem. Structural elements within the two units are significantly different

and the metamorphism-deformation relationships offer few clues. It is not known whether (Sg) = (Sm) or whether the kyanite is part of the metamorphic sequence found within the metasedimentary rocks. Although the kyanite appears to be pre-tectonic to (Sg); (Sg) may have developed during a stacking event when the gneisses were thrust from east to west over the metasediments. This is only one of many possibilities. The steep dip of the gneisses suggest that thrusting from east to west may have occurred but does not give any clues for the relative ages of the two Complexes. The mineral chemistry although very limited and therefore tenuous, suggests that perhaps the gneiss is not part of the metamorphic sequence found within the Metasedimentary Complex. Chemical trends of increasing magnesium and decreasing iron within the biotite, with increasing metamorphic grade was not followed into gneiss. The chemical trend of a higher anorthite content with increasing metamorphic grade was not followed into the gneiss; however the chemical trend of increasing iron and magnesium and decreasing calcium and manganese within the garnet with increasing metamorphism was followed into the gneiss. A detailed geochemical comparison of the rocks from the two complexes may help in proving or refuting the presence of basement and cover rocks; however a study of this kind may be fraught with sampling problems in the gneissic rocks because of metamorphic segregation. The results of this study do not solve the question of cover-basement relations within the French Mountain area, however the study does not confirm the presence of an unconformity between the two Complexes and gives an insight into the relationship between the timing of the

metamorphism and the deformation within the area. From the results of this study it appears most likely that the gneiss was thrust over the metasedimentary rocks (Figure 6.2).

6.6 REGIONAL BEARING

The Gneiss and Metasedimentary Complexes have been described as cover and basement rocks (Currie, in press); and as a single protolithic package (Craw, in press). Currie claims an unconformity separates the two Complexes while Craw proposes that a crustal stacking "event" is responsible for thrusting the gneiss over the metasedimentary rocks. Doucet (1983) studying similar rocks in the Middle River area has also proposed the stacking of crustal units in that area. The timing of such a stacking event is proposed to have occurred during the Middle Devonian Acadian Orogeny (Doucet, 1983). The Corney Brook Pluton (Cambrian) interpreted by Currie to predate the Jumping Brook Complex is believed to most likely post date the metasedimentary rocks because of its lack of a penetrative fabric. The linking of the rhyolite dyke, dated at 439 $\pm$ 7 million years (Currie, in press) to the basal volcanics of the Jumping Brook Complex is tenuous (Jamieson, in press). Macdonald and Smith (1980) studying the metasedimentary rocks and gneisses in the Cape North area found that the two were essentially conformable with no erosional or tectonic break between them.

Figure 6.2. Schematic Model where the Gneiss Complex is thrust from east to west against and possibly over the Metasedimentary Complex.

(W) (E)

DEPOSITION

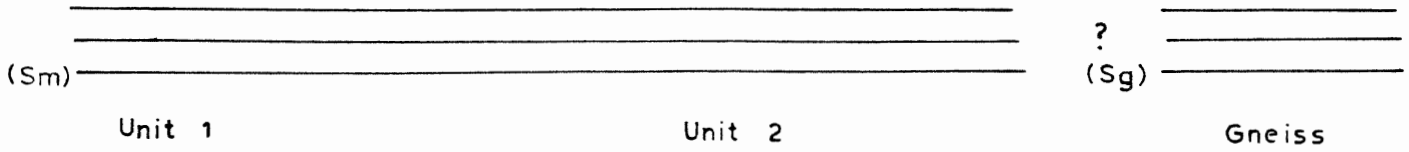

DEFORMATION

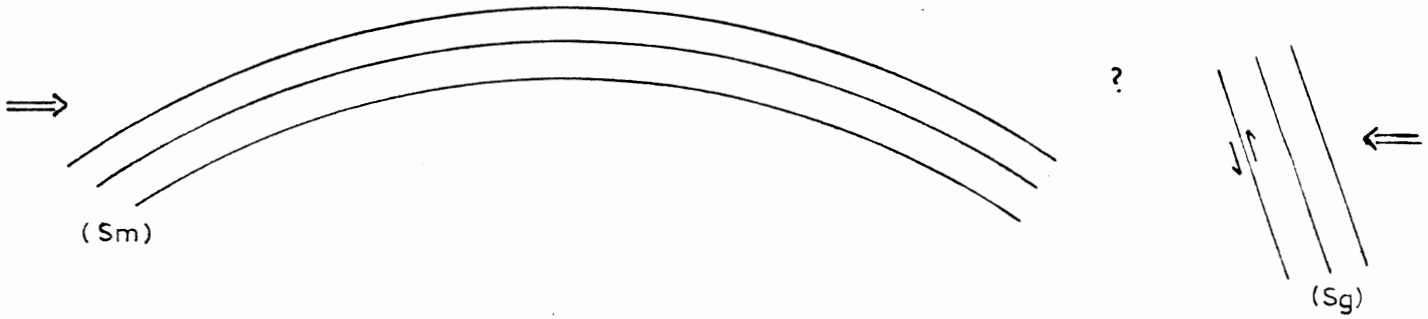

EROSION

In this model there is no inference for relations between (Sm) and (Sg).

For the French Mountain area, the thrusting model proposed by Craw (in press) for the Cheticamp River area, seems applicable. The model does not infer basement and cover rocks within the area.

REFERENCES

Albee, A.L. (1965). A petrogenetic grid for the Fe-Mg silicates of pelitic schists. Am. J. Sci., 263, 512-536.

Atherton, M.P. (1968). The variation in garnet, biotite and chlorite in medium grade pelitic rocks from the Dalradian of Scotland, with particular reference to the zonation in garnet. Contr. Mineral. Petrol., 18, 347-371.

Bates, R. L. and Jackson, J.A. (1980). Glossary of Geology, 2nd ed. American Geological Institute, Virginia, 751 pp.

Bird, G.W., Fawcett, J.J. (1973). Stability relations of Mg-chlorite-muscovite and quartz between 5 and 10 Kb water pressure. J. Petrol., 14, 415-428.

Carmichael, D.M. (1969). Intersecting Isograds in the Whetstone Lake Area, Ontario, J. Petrol., 11, 147-181.

Chatterjee, A.K. (1980). Mineralization and associated wall rock alteration in the George River Group, Cape Breton Island, Nova Scotia. Unpublished Ph.D. thesis, Dalhousie University, 197 pp.

Cooper, A.F. (1972). Progressive metamorphism of metabasic rocks from the Haast Schist Group of southern New Zealand. J. Petrol., 13, 457-492.

Cormier, R.F. (1972). Radiometric ages of granitic rocks, Cape Breton Island, Nova Scotia. Can. J. Earth Sci., 9, 1074-1086.

Craw, D. (1983). Tectonic stacking of metamorphic zones in Cheticamp River area, Cape Breton Highlands, Nova Scotia (in Press). Submitted to Canadian Journal of Earth Science.

Currie, K. L. (1982). Paleozoic supracrustal rocks near Cheticamp Nova Scotia. Maritime Sediments and Atlantic Geology, 18, 94-103.

Currie, K. L. (1983). Relations between metamorphism and magmatism near Cheticamp, Cape Breton Island. (in Press), Geological Survey of Canada Bulletin.

Deer, W.A., Howie, R.A. and Zussman, J. (1966). An introduction to the rock-forming minerals. Longman Group Limited, London, 528 pp.

Doucet, P. (1983). The Petrology and geochemistry of the Middle River Area, Cape Breton Island, Nova Scotia. Unpublished M.Sc. thesis, Dalhousie University, 339 pp.

Ferry, J. M., Spear, F.S. (1978). Experimental calibration of the partitioning of Fe and Mg between garnet and biotite. Contrib. Mineral. Petrol., 66, 113-117.

Goldman, D.S., Albee, A.L. (1977). Correlation of Mg/Fe partitioning between garnet and biotite with $^{18}O/^{16}O$ partitioning between quartz and magnetite. Am. Jour. Sci., 277, 750-767.

Holdaway, M.J. (1971). Stability of andalusite and the aluminum silicate phase diagram. Am. Jour. Sci., 271, 97-131.

Hollister, L.S. (1966). Garnet zoning: an interpretation based on the Rayleigh fractionation model. Science, 154, 1647-1651.

Hoschek, G. (1969). The stability of staurolite and chloritoid and their significance in metamorphism of pelitic rocks. Contrib. Mineral. Petrol., 22, 208-232.

Hoschek, G. (1976). Melting relations of biotite + plagioclase + quartz. Neues Jahrbuch Fur Mineralogie Montashefte, 79-83.

Jamieson, R.A. (1981). The geology of the Crowdis Mountain volcanics, southern Cape Breton Highlands. Current Research, Part A., Geological Survey of Canada Paper 81-1c, 77-81.

Jamieson, R.A. (1983). Timing of tectonism in the Cape Breton Highlands - new evidence from Rb-Sr geochronology. (In Press), submitted to the Canadian Journal of Earth Sciences.

Jamieson, R.A., Doucet, P. (1983). The Middle River-Crowdis Mountain area, southern Cape Breton Highlands. IN Current Research, Part A, Geological Survey of Canada, Paper 83-1A, 269-275.

Keppie, J.D. (1979). Geological map of the province of Nova Scotia. Nova Scotia Department of Mines and Energy.

Macdonald, A.S., Smith, P.K. (1980). Geology of Cape North area, northern Cape Breton Island, Nova Scotia. Nova Scotia Department of Mines and Energy, Paper 80-1, 60 pp.

Mason, R. (1978). Petrology of the metamorphic rocks. George Allen and Unwin Ltd., London, 254 pp.

Mehnert, K.R. (1968). Migmatites and the origin of granitic rocks. Elsevier, New York, 393 pp.

Milligan, G.C. (1970). Geology of the George River Series, Cape Breton. Nova Scotia Department of Mines, Memoir 7, 111 pp.

Miyashiro, A. (1953). Calcium-poor garnet in relation to metamorphism. Geochim. Cosmochim. Acta, 4, 179-208.

Miyashiro, A., Shido, F. (1973). Progressive compositional change of garnet in metapelite. Lithos, 6, 13-20.

Neale, E.R.W., Kennedy, M.J. (1975). Basement and cover rocks at Cape North, Cape Breton Island, Nova Scotia. Maritime Sediments, 11, 1-4.

Nockolds, S.R., Knox, R.W.O'B., Chinner, G.A. (1979). Petrology for students. Cambridge University Press, London, 435 pp.

Ragan, D.M. (1973). Structural Geology: An introduction to geometrical techniques, 2nd ed. John Wiley and Sons, Toronto, 208 pp.

Rast, N. (1958). Metamorphic history of the Schichallion Complex. Trans. Roy. Soc. Edinb., 63, 413-431.

Schoneveld, C. (1977). A study of typical inclusion patterns in strongly paracrystalline-rotated garnets. Tectonophysics, 39, 453-471.

Spry, A. (1969). Metamorphic textures. Pergamon Press, New York, 350 pp.

Sturt, B.A. (1962). The composition of garnets from pelitic schists in relation to the grade of regional metamorphism. J. Petrol., 3, 181-191.

Sturt, B.A. and Harris, A.L. (1961). The metamorphic history of the Loch Tummel area, central Perthshire, Scotland. Liverpool Manchester Geol. J., 2, 689-711.

Terry, R.D. and Chilingar, G.V. (1955). Summary of "Concerning some additional aids in studying sedimentary formations", by M.S. Shvetsov. Jour. Sed. Petrol., 25, 229-234.

Thompson, A.B. (1976). Mineral reactions in pelitic rocks: II. Calculation of some P-T-X (Fe-Mg) phase relations. Am. Jour. Sci., 276, 425-454.

Thompson, A.B. (1982). Dehydration melting of pelitic rocks and the generation of H_2O-undersaturated granitic liquids. Am. Jour. Sci., 282, 1567-1595.

Vernon, R.Hi (1978). Porphyroblast-matrix microstructural relationships in deformed metamorphic rocks. Sonderdruck aus der Geol. Rundschau Vand., 67, 288-305.

Weibe, R.A. (1972). Igneous and tectonic events in northeastern Cape Breton Island, Nova Scotia. Can. J. Earth Sci., 9, 1262-1277.

Yardley, B.W.D. (1978). Genesis of the Skagit Gneiss migmatites, Washington, and the distinction between possible mechanisms of migmatization. Geol. Soc. America Bull., 89, 941-951.

WORK SCHEDULE

Field mapping and sample collection	16 days
Cutting samples	∿ 5 days
Microprobe analyses	4 days
*Structure, Field Relations, and Lithology determination (September and October)	∿61 days
*Petrology (November)	∿25 days
*Petrology, Mineral Chemistry, Metamorphism,	
*Introduction and Conclusion and Discussion (January)	∿30 days
*Rewriting and final drafting** (February)	∿28 days

*each day consists of a minimum of 8 hours spent working on the thesis.

** most drafting was done during the writing of each chapter and therefore it is difficult to separate the time spent on drafting alone from other work done on the thesis.

SAMPLE LOCATION MAP, FRENCH MOUNTAIN AREA
CAPE BRETON HIGHLANDS, NOVA SCOTIA

SYMBOLS

- area of bedrock outcrop
- x small bedrock outcrop
- paved highway
- gravel road
- foot trail
- stream or brook
- swamp

sample number locations indicated on map

SCALE 1 : 10,000

500 0 500 1000 m

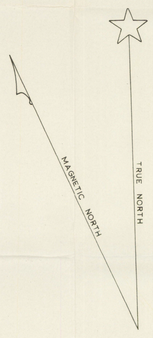

GULF OF
ST LAWRENCE

FISHING
COVE

PIGEON
COVE

FRENCH
MOUNTAIN

JUMPING BROOK

SKYLINE TRAIL

SKYLINE TRAIL

FIRE TOWER ROAD

CABOT TRAIL

FRENCH
LAKE

FLEMING COVE RIVER

MACKENZIES
MOUNTAIN

MAP 2

GEOLOGICAL MAP OF THE FRENCH MOUNTAIN AREA
CAPE BRETON HIGHLANDS, NOVA SCOTIA

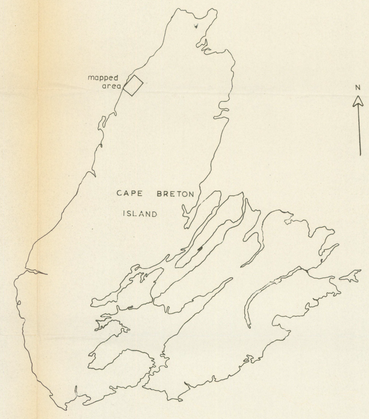

LEGEND

8 UNDIVIDED GRANITIC DYKES
- 8a granitic dykes

7 GRANITOID UNIT A
- 7a foliated
- 7b brecciated
- 7c with slickensides

6 JUMPING BROOK GRANITOID
- 6a unfoliated
- 6b foliated and sheared

5 DIORITE
- 5a unfoliated to slightly foliated

4 METASEDIMENTARY COMPLEX
- 4a muscovite-biotite phyllite showing no compositional layering on the centimeter scale
- 4b psammite
- 4c muscovite biotite phyllite showing compositional layering on the centimeter scale
- 4d hornblende rich psammite
- 4e semi pelite

3 PEGMATITE
- 3a pegmatite of unknown origin

2 AMPHIBOLITE
- 2a coarse grained unfoliated amphibolite
- 2b fine grained unfoliated amphibolite
- 2c foliated amphibolite

1 GNEISS COMPLEX
- 1a muscovite-biotite-quartzo-feldspathic gneiss
- 1b amphibolite gneiss
- 1c feldspar augen gneiss
- 1e gneisses showing "migmatitic" segregations and pegmatite pods

SYMBOLS

- area of bedrock outcrop
- small bedrock outcrop
- geological boundary
- foliation (horizontal, inclined, vertical)
- fault (normal fault with dip of fault plane, fault plane dip unknown, fault motion uknown)
- shear
- shear with motion unknown
- minor fold with plunge
- mineral lineation with plunge
- crenulation with plunge
- dyke plane orientation
- xenolith of lithology 2b in lithology 4a
- paved highway
- gravel road
- foot trail
- stream or brook
- swamp

ABBREVIATIONS

- C chlorite
- G garnet
- K kyanite
- S staurolite

STRUCTURE

EQUAL AREA NETS SHOWING STRUCTURAL ELEMENTS OF SPECIFIC AREAS SHOWN ON MAP

1 biotite mineral lineations
contours = 1, 3, 5 percent per 1 percent area
number of data values = 12

2 poles of the pervasive foliation of the metasedimentary complex
contours = 0.4, 1, 3, 4, 6, 7 percent per 1 percent area
number of data values = 76

3 minor fold axis of the metasedimentary complex
contours = 0.5, 1.5, 2, 3, 5 percent per 1 percent area
number of data values = 97

4 crenulation axis
contours = 1, 2, 3, 5, 9 percent per 1 percent area
number of data values = 52

5 poles of the pervasive foliation of the gneiss complex
contours = 2, 5, 7, 10, 12 percent per 1 percent area
number of data values = 12

6 poles of the pervasive foliation of the gneiss complex
contours = 1, 3, 6, 14, 17 percent per 1 percent area
number of data values = 20

all data collected during field mapping in the summer of 1982

SCALE 1: 10,000

500 0 500 1000 m

CROSS-SECTIONS

- 4c,d
- 1a,e
- 1b
- 1c
- 4a,b,e
- foliation plane
- inferred foliation plane
- drawn to scale

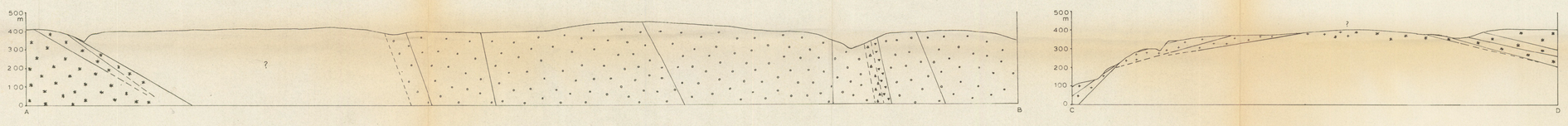

MAP 1